Durability of Steel Bridge Corrosion Protection Systems Using Environment-Based Accelerated Corrosion Testing

FINAL REPORT

Principal Investigator: Jennifer McConnell, Ph.D.

Co-Principal Investigator: Clara Chan, Ph.D.

Research Assistants: Julie Giannino and Nate Young

Other Contributors: Sally Saleem and Tian Bai

Submitted to:

American Institute of Steel Construction (AISC)

April 21, 2022

TABLE OF CONTENTS

LIST OF TABLES

LIST OF FIGURES

ACKNOWLEDGEMENTS

The contributions of the following organizations and individuals is gratefully acknowledged. Funding for this work was provided by the American Institute of Steel Construction and National Steel Bridge Alliance, with Chris Garrell serving as the project manager. In kind support was provided by High Steel Structures, LLC, who donated the specimens used in the experimental testing. High Steel, Industrial Steel Construction, AFCO and representatives from the Illinois, Kansas, New York, North Carolina, Ohio, Pennsylvania, Tennessee, and Texas transportation departments submitted data used in Chapter 2 of this report. This work was also enhanced by the thoughtful contributions of the following advisory group members: Brandon Chavel, Heather Gilmer, Ronnie Medlock, Tom Murphy, Justin Ocel, Kim Roddis, Frank Russo, and Paul Vinik.

ABSTRACT

The purpose of this study was to evaluate the performance of five of the most common corrosion protection systems: uncoated weathering steel (UWS), galvanizing, metallizing, 1-coat inorganic zinc paint, and a 3-coat organic zinc paint system, in relatively corrosive environments. The premise of this scope was that UWS is the preferred material type in most environments; but in relatively severe environments, alternative corrosion protection systems may provide benefits in terms of both corrosion protection and life cycle cost. The severely corrosive environments considered in this research are coastal environments where natural chlorides are present and environments where chlorides are present via the high use of deicing salts.

Performance was evaluated first through a statistical analysis of existing field data (Chapter 2) and subsequently through implementation of laboratory accelerated corrosion testing. The laboratory accelerated corrosion testing was customized to the goals of this research by benchmarking the laboratory results to prior field work of UWS bridges in severe environments (Chapter 3). This methodology was applied to each of the five corrosion protection systems for 80 cycles, representing 80 years in the field (Chapter 4). The results of this work were used to provide longevity estimates for each of the corrosion protection systems based on various performance benchmarks in Table 4-2. The implications of the longevity estimates show that steel can provide a long service life even in a relatively severe environment. Use of any of these corrosion protection systems can improve performance, increase service life, decrease required maintenance, and provide economical steel bridges. A more detailed summary of this work, key conclusions, and suggestions for future work are presented in Chapter 5.

Chapter 1

INTRODUCTION

1.1 Motivation

At the scoping stage of a new bridge project, a fundamental decision to be made is superstructure material: steel or concrete. A designer choosing steel then has many corrosion protection systems to choose from. This is typically a protective coating, such as paint, or uncoated weathering steel; galvanizing and metallizing are also viable corrosion protection systems. These are collectively referred to as steel corrosion protection systems in this work. These decisions are presently made largely relying on anecdotal evidence and perception, with virtually no supportive data. To make rational life-cycle cost analyses (LCCA) to support superstructure material decisions at the scoping stage, there is a need to collect and synthesize performance data related to steel bridge corrosion protection systems of weathering steel, liquid applied coatings with zinc-based primers, thermal spray coatings, and hot-dip galvanizing. Frequently, the intervals used in LCCA of steel bridges significantly underestimate the historic performance of corrosion protection systems, and by providing specific guidance on what intervals can be expected, the accuracy of LCCA of steel bridges will be improved.

There remain fundamental questions regarding the actual atmospheric corrosion loss of low carbon steels in the modern era. ASTM studies in the 1960's exposed steel and zinc to various corrosion sites throughout the US (e.g., ASTM 1968, Guftman 1968); however, modern steel chemistries contain more alloy than that era, coating technologies have improved dramatically, and environmental regulations have drastically reduced detrimental atmospheric contaminants. Therefore, it's expected

that corrosion loss rates are smaller than the literature would suggest. Additionally, superior cleaning practices are now well documented (AASHTO/NSBA 2016) and increased performance of modern coating systems now exists.

The result is that long-term corrosion performance data of modern corrosion protection systems, using modern preparation and application practices, is lacking. In addition to the challenge presented by the modernity of most corrosion protection systems, information regarding corrosion protection system use is not publicly available. The National Bridge Inventory (NBI), available to the public, requires inspectors to indicate the general type of material used (e.g., concrete or steel), but does not require indication of a corrosion protection system. Further, many owners and fabricators do not track information regarding corrosion protection systems, and those who do, don't share this information publicly. The result is that there is not currently a system in place to track the use of corrosion protection systems in bridges to be able to study long-term corrosion performance on a large scale.

1.2 Goals

The main objectives of this research were to analyze existing performance data of corrosion protection systems and to perform accelerated corrosion testing to establish a relative ranking and / or estimate of the service life of common corrosion protection systems. Through survey of state departments of transportation (DOTs), bridge owners, and bridge fabricators, a database of bridges with various corrosion protection systems could be established and linked to the NBI for analysis of overall long-term performance trends. Accelerated corrosion testing can be performed in a laboratory to overcome the shortcomings of existing performance data by simulating long-term field performance in a short amount of time in the laboratory. For best

implementation, the accelerated corrosion testing should accurately replicate field performance.

Although there is a general lack of existing data regarding long-term field performance of corrosion protection systems, there is an exception for uncoated weathering steel (UWS). A database of 10,000 UWS bridges has been collected from previous studies (McConnell et al., 2014a; McConnell et al. 2014b; McConnell et al., 2016) in specified environments. This database can be used to benchmark accelerated corrosion testing procedures to field performance. Once benchmarked to the UWS database, accelerated corrosion testing procedures can then be applied to the other corrosion protection systems to gather data on long-term performance.

The four primary goals of this research were:

1. Compile existing performance data for the different corrosion protection systems.
2. Develop realistic accelerated corrosion testing procedures that best simulate a coastal environment where atmospheric chlorides are present and a deicing environment where chlorides are present in the form of deicing salts used to melt snow on roadways during winter storm events. The procedures were evaluated based on benchmarks from field evaluations of UWS bridges that have been in service for decades in different environments.
3. Perform accelerated corrosion testing procedure on the corrosion protection systems in the simulated environments through the developed realistic laboratory accelerated corrosion testing procedures.

4. Analyze the performance of the corrosion protection systems in the simulated environments to estimate the lifespan of each corrosion protection system in the given environments.

Completing this last goal also required establishing a definition for the lifespan (number of years) of a corrosion protection system that could be assessed for the available data. For the field data, lifespan was defined as the number of years, on average, that the structure would receive a superstructure condition rating of 5 or higher (i.e., would remain in the "good" or "fair" categories of performance; based on National Bridge Inventory ratings [FHWA 1995]). For the laboratory data, various quantitative benchmarks based on percent mass loss, percent coating loss, and percent rusting were evaluated (see Table 4-2 for specifics). Therefore, the laboratory data also represents number of years of maintenance free service. Because the maintenance history of the thousands of bridges in the field database is unknown, no assumptions can be made regarding the level of maintenance required to achieve the service life estimates based on the field data analysis other than that it is the service life with typical maintenance for each corrosion protection system.

1.3 Scope

The corrosion protection systems included in this study were (with additional details on each of these provided in Appendix A):

- 1-coat inorganic zinc (IOZ) paint
- 3-coat organic zinc (OZ) paint system
- Uncoated weathering steel (Grade 50W)
- Metallizing
- Galvanizing.

Existing field performance data was compiled for the corrosion protection systems included in this study. In parallel, realistic accelerated corrosion testing procedures were developed to simulate severe environments representative of coastal environments and environments with heavy uses of deicing agents. Accelerated corrosion testing was then performed on all of the corrosion protection systems included in this study. Finally, the field and laboratory results were analyzed to estimate the longevity of each corrosion protection system in the corresponding environments (field data representing a diverse range of possible environments and laboratory data representing severe environments).

1.4 Organization

This report is organized into five chapters. Chapter 1 introduces the main concepts of this research study. Chapter 2 describes the procedure and analysis for the statistical analysis of existing long-term corrosion performance of corrosion protection systems. Chapter 3 details the methodology used for laboratory accelerated corrosion testing as well as the process for analyzing the results from laboratory testing. Chapter 4 presents the results from the accelerated corrosion testing performed on all corrosion protection systems. Finally, Chapter 5 provides a summary and suggestions for future work. Appendices are located after the conclusion for more detailed records of testing procedures, project organization, and data collected.

Chapter 2

STATISTICAL ANALYSIS OF EXISTING LONG-TERM PERFORMANCE DATA OF CORROSION PROTECTION SYSTEMS

2.1 Overview

The purpose of the statistical analysis was to compile the existing data on field performance of different steel corrosion protection systems in different environments to assess trends in their conditions. This data was collected through the cooperation of fabricators and owners who identified the corrosion protection systems of various bridges throughout the nation along with use of the National Bridge Inventory (NBI) to identify the bridges and collect superstructure performance data.

2.2 Data Considered

2.2.1 Corrosion Protection System Identification

Collection of performance data for the statistical analysis required the use of data from the NBI. The NBI is publicly available and includes records for bridges including, but not limited to, year built, year reconstructed, and superstructure condition rating (SCR), which can collectively be used to assess superstructure condition over time. Use of the NBI to analyze performance was the best available approach for the stated goals of this effort, as it includes existing national field data without the need for repeating field assessments. This was beneficial since field work is both time consuming and costly.

Identification of bridges using the different corrosion protection systems relied on the cooperation of owners and fabricators, as corrosion protection system is not an item specified in the NBI. Within the scope of this project, responses regarding the

identification of corrosion protection systems used on steel bridges in the US were solicited via a request to AASHTO Committee T-14 and were received from eight state DOTs: Illinois, Kansas, New York, North Carolina, Ohio, Pennsylvania, Tennessee, and Texas. Data was also received from three fabricators: High Steel, Industrial Steel Construction, and AFCO. In addition, responses had previously been received from 48 state highway agencies, the District of Columbia, and FHWA identifying UWS bridges in their agencies through a prior project (McConnell et al. 2014). Thus, the largest number of bridges identified were UWS bridges.

Table 2-1 shows the total number of bridges identified for each corrosion protection system using this data, and Figure 2-1 shows their geographical locations. The number of bridges in the table represent the number of bridges ≤ 50 years old that were able to be linked to the NBI database. This age limitation was included to limit the analysis to only modern corrosion protection systems, as the makeup of paint used as a corrosion protection system has changed over time, moving away from the use of lead-containing paint systems and towards zinc-rich paint systems. A further step of the analysis separated this larger group of painted bridges into smaller groups of "old" and "new," which is discussed in Section 2.3.1.3. Overall, 11,865 bridges were identified during this task.

Table 2-1. Number of Bridges Identified for Each Corrosion Protection System

Corrosion Protection System	Number of Bridges	Source
Paint	231	Owners and fabricators
Weathering Steel (UWS)	10,484	Owners, via prior McConnell et. al FHWA / LTBP study
Galvanized	1,072	Owners and fabricators
Metallized	78	Owners and fabricators

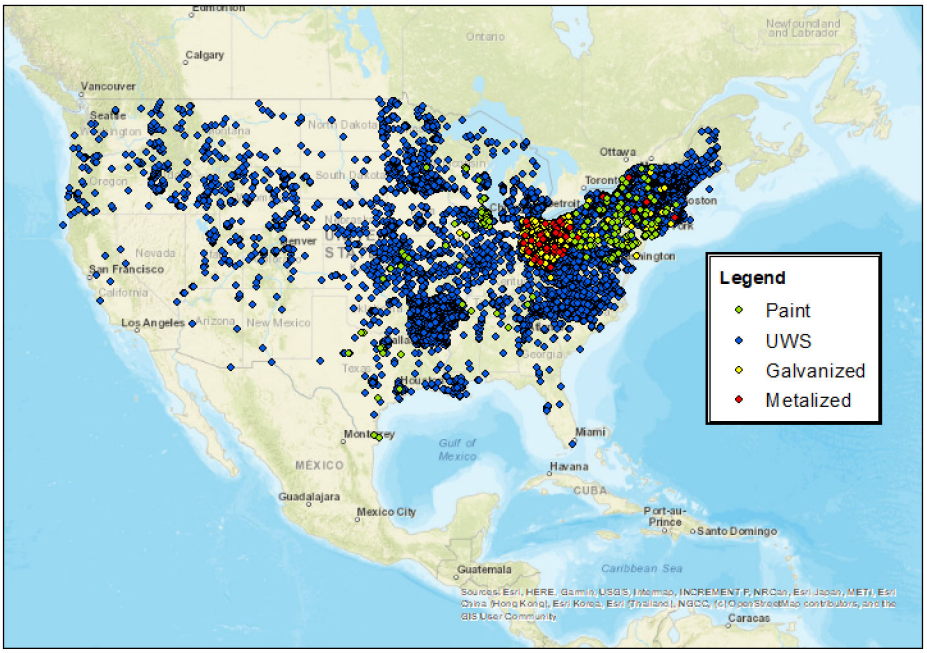

Figure 2-1. Location of Bridges Identified for Each Corrosion Protection System

2.2.2 Corrosion Protection System Performance Data

Once the corrosion protection systems were identified for the bridges described in Section 2.2.1, those bridges were located in the 2018 NBI database (the most recent year of data available at the time) to analyze performance. The owner/fabricator and NBI data were able to be linked by using the superstructure ID number of each bridge. Then, the year built (NBI item #27), superstructure condition rating (SCR, NBI item #59), and year reconstructed (NBI item #106) were identified. The year built and year reconstructed of each bridge were used to determine the bridge's age, where age was assumed to equal NBI inspection year minus the year built, or year reconstructed if applicable. It is noted that calculating age of the superstructure based on year reconstructed (where applicable) possibly under-predicts the age of the superstructure. This is an assumption to err on the conservative side in the absence of more refined data, by attributing any diminished performance to an age that may be lower than the actual age of the corrosion protection system.

The SCR was used as a metric of measuring performance with the realization that this was an imperfect approach. SCR is inherently subjective and may be influenced by factors other than corrosion. However, the use of SCR as a means to assess performance is widely used and corrosion effects are by far the most common reason for decreasing SCR. Thus, the use of SCR is advantageous for efficiently meeting the goals of this effort, as it is easily accessible through the NBI and allows the analyst to have a large database of performance data.

2.3 Data Analysis Methods and Results

2.3.1 Method 1: All Bridges, Sorted by Corrosion Protection System

2.3.1.1 One-Way ANOVA

A one-way ANOVA is a statistical test used to determine whether the variation of values within different groups are statistically different while considering only one dependent variable, which was SCR in this case. A p-value of < 0.05 is a typical threshold value used to signify that the difference in the groups is statistically significant. A one-way ANOVA was performed using the Analysis ToolPak add-in in Excel (Anaysis Toolpak, 2019). The resulting p-value was on the order of 10E-59, which is far below 0.05, indicating that the means of the groups are statistically different.

A post hoc test was then performed to determine what group(s) contributes to the differences. Which post hoc test to perform is chosen based on homogeneity of variance, which is determined by another statistical test called Levene's Test. Homogeneity of variance is an assumption that all comparison groups have the same variance. The results of this test, also performed using Analysis ToolPak, showed homogeneity of variance is not satisfied, which means the Games-Howell post hoc test should be used (One-Way ANOVA, 2018).

The Games-Howell post hoc test compares every possible pairing of groups to determine whether the means of the groups are statistically significant. This is similar to the initial one-way ANOVA, but it gives more specific results to determine which groups the differences are between. Likewise, a p-value <0.05 signifies a significant difference between the groups. The results of this test, also performed using Analysis ToolPak, are shown in Table 2-2.

Table 2-2. Games-Howell Post Hoc Test Results of the SCR Analysis

Are Differences Between Groups Statistically Significant?				
	Paint	**Weathering Steel**	**Galvanized**	**Metallized**
Paint	-	Yes	Yes	No
Weathering Steel	Yes	-	Yes	No
Galvanized	Yes	Yes	-	No
Metallized	No	No	No	-

The results of the test showed that the means of any two given groups had statistically significant differences with the exception of any group compared with the metallized bridges. One possible explanation for this is that there were far fewer metallized bridge data points than any other coating system (78, compared to the next lowest which was 231 painted bridges). Another hypothesis was that this difference resulted from the relatively young age of the metallized bridges in the dataset. 63% of the metallized bridges in the dataset were 20 years old or less, and 87% of the bridges in the dataset were 30 years old or less. Age, however, did not explain why metallized bridges showed no statistically significant difference in mean with any of the groups, as a separate post hoc test on bridges only 0-10 years old resulted in the same findings as the results using all bridges ≤ 50 years old.

The average and standard deviation were plotted to further examine the differences in performance between the different corrosion protection systems, as seen

in Figure 2-2. This plot shows that galvanized bridges had the highest average SCR, followed by metallized bridges, followed by UWS bridges, and finally followed by painted bridges. Metallized bridges had the highest standard deviation in SCR, which could contribute to the one-way ANOVA that found that all corrosion protection systems performed differently from each other except when compared to metallized. UWS and galvanized bridges had the smallest and most similar standard deviations.

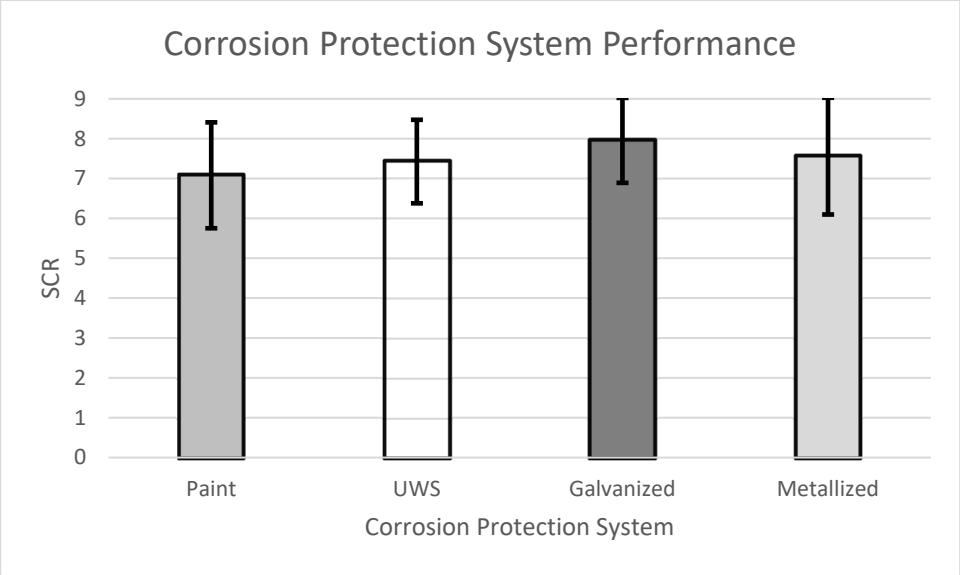

Figure 2-2. Average and Standard Deviation of Superstructure Condition Rating for Different Corrosion Protection Systems

2.3.1.2 SCR vs. Age

The data was analyzed to determine if there were any differences in SCR over time for each corrosion protection system. A scatter plot of SCR versus age was created for each individual corrosion protection system, where one point represents one bridge. This was used to create a linear regression line. Other trendline types, including logarithmic, polynomial, and power were tested as well, but it was found

that using a higher order regression did not improve the fit. Figures 2-3 – 2-6 show the data, linear regression lines, and linear regression equations for each of the corrosion protection systems; Figure 2-7 and Table 2-3 compare the four linear regression lines from the four different corrosion protection systems. NOTE: These plots should *not* be used as a design tool to extrapolate performance data, as this plot comes from a limited sample size of data, of which at least 70% of the data points for each corrosion protection system had ages of 0 to 30. This means that the performance past 30 years shown in the plot comes from an even more limited sample size. A chart usable for deterministic performance prediction would also begin with all corrosion protection systems at an SCR of 9 at age 0, which this plot does not due to the nature of linear regression and the scatter of the data used. This plot should be used to observe general trends and relative rankings in performance only.

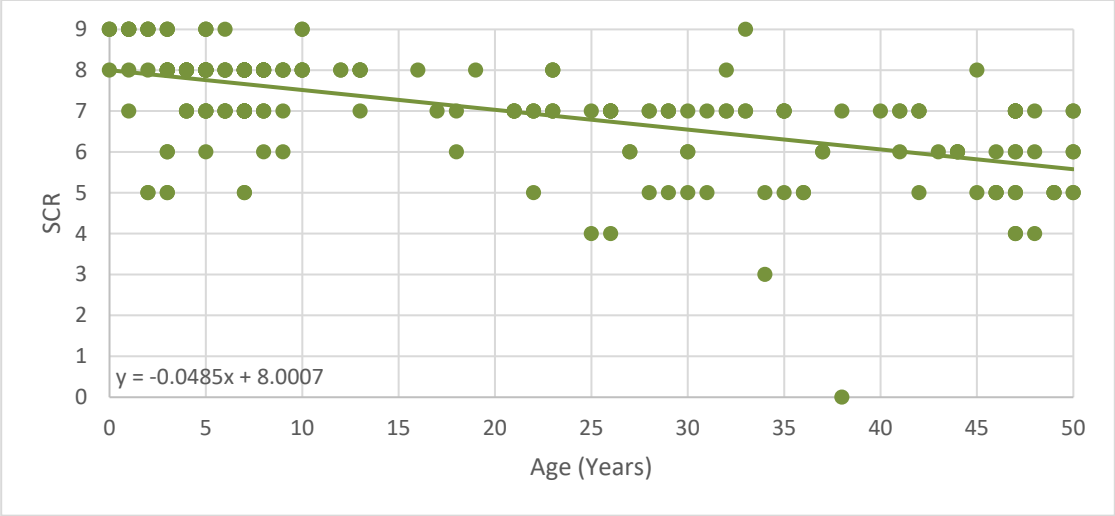

Figure 2-3. Scatter Plot and Linear Regression Line for Performance of Painted Bridges (Not for extrapolation)

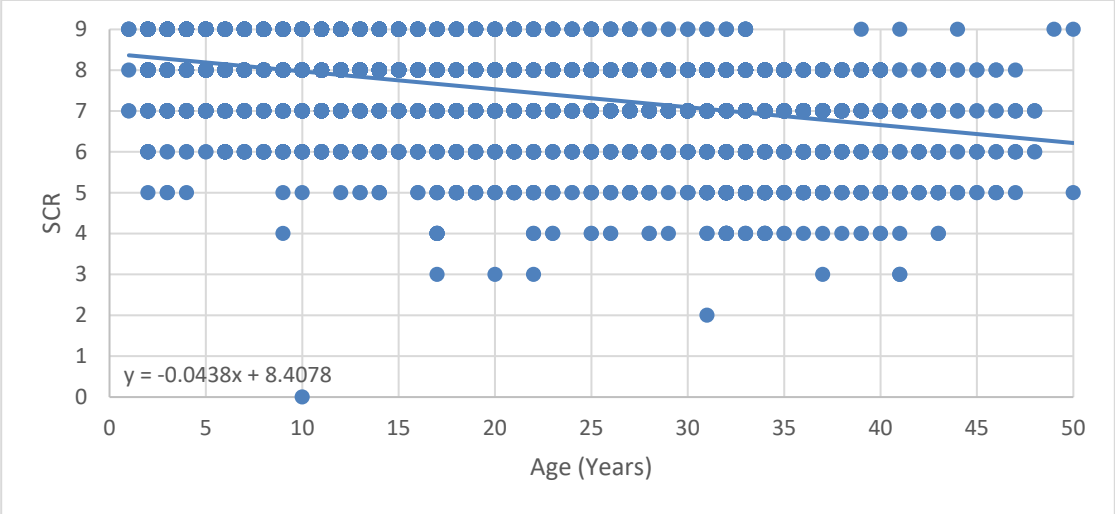

Figure 2-4. Scatter Plot and Linear Regression Line for Performance of Weathering Steel Bridges (Not for extrapolation)

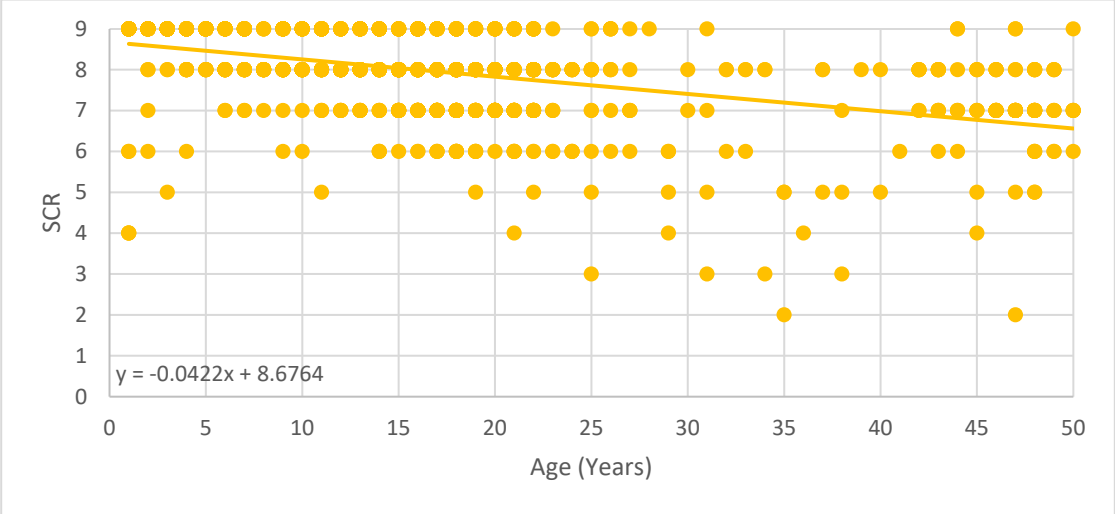

Figure 2-5. Scatter Plot and Linear Regression Line for Performance of Galvanized Bridges (Not for extrapolation)

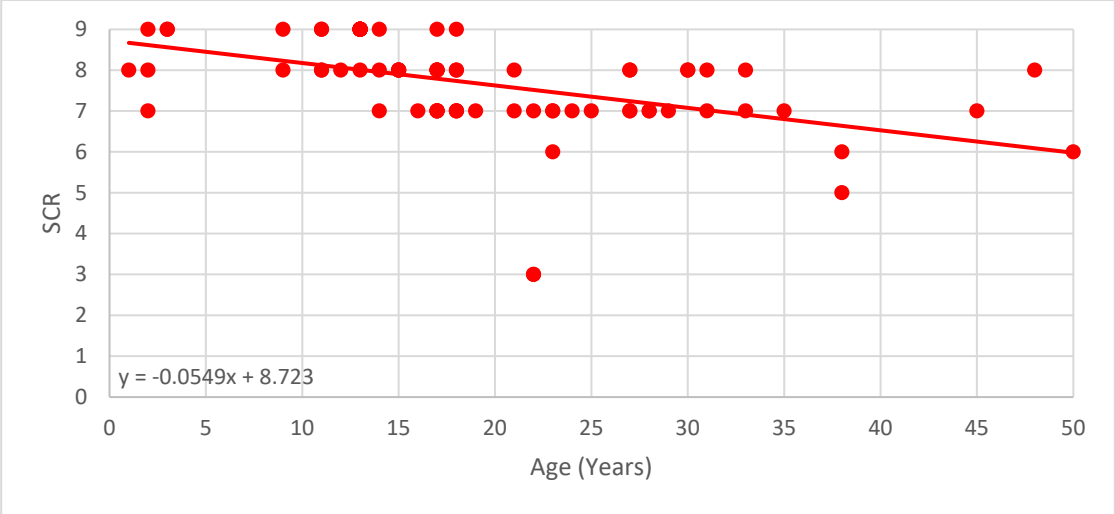

Figure 2-6. Scatter Plot and Linear Regression Line for Performance of Metallized Bridges (Not for extrapolation)

Table 2-3. Slope and Y-Intercept Values for the Linear Regression Models of All Corrosion Protection Systems of the SCR vs. Age Analysis

	Slope	**Y-Intercept**
Paint	-0.049	8.000
UWS	-0.044	8.408
Galvanized	-0.042	8.676
Metallized	-0.055	8.723

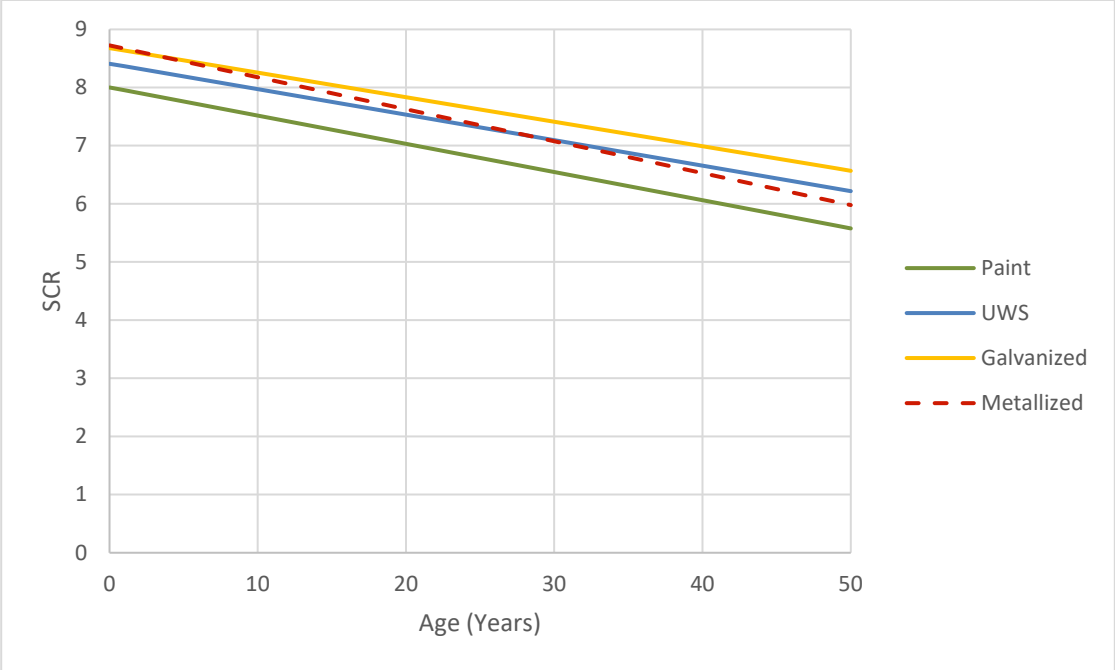

Figure 2-7. Linear Regression Lines of All Corrosion Protection Systems (Not for extrapolation)

The results can be used to determine some general trends but not to definitively determine performance of a bridge of a certain corrosion protection system at a given age. Figure 2-7 shows that the slopes of the performance of the UWS and galvanized bridges over time are remarkably similar, with less than a 5% difference in the slopes. The painted bridges also have a similar slope, that is 10% higher than the average slope of the UWS and galvanized data. The metallized bridges have the most negative slope, which is 1.13 times higher than the next highest absolute slope value (paint). This plot shows that for most age ranges considered, galvanized bridges generally have the highest SCR ratings, paint generally have lower SCR ratings, and UWS and metallized bridges fall somewhere in between. This pattern holds true except at ages

0-3, where metallized bridges have the highest SCR while the relative rankings between paint, UWS, and galvanized bridges remain the same as previously described.

One limitation of this analysis was that the y-intercept determined through linear regression did not equal an SCR of 9 as would be realistically expected for a new bridge. Figure 2-8 shows the same plot with an intercept adjustment so that all corrosion protection systems begin at an SCR rating of 9 and Table 2-4 summarizes the linear regression models shown in Figure 2-8. The results provide a similar general ranking between galvanized, UWS, and painted bridges as the original analysis without the intercept adjustment over the plotted age range. Galvanized has the highest SCR, paint has the lowest SCR, and UWS falls between the two. The biggest difference is that the plot created with the y-intercept adjustment shows UWS and metallized bridges having a slope similar to each other, with only a 6% difference in slopes. UWS and galvanized bridges also had similar slopes, with a 12% difference. All other corrosion protection systems had slopes more distinctly different from each other.

Table 2-4. Slope and Y-Intercept Values when Y-Intercept = 9.000 for the Linear Regression Models of All Corrosion Protection Systems of the SCR vs. Age Analysis

	Slope	**Y-Intercept**
Paint	-0.079	9.000
UWS	-0.062	9.000
Galvanized	-0.055	9.000
Metallized	-0.066	9.000

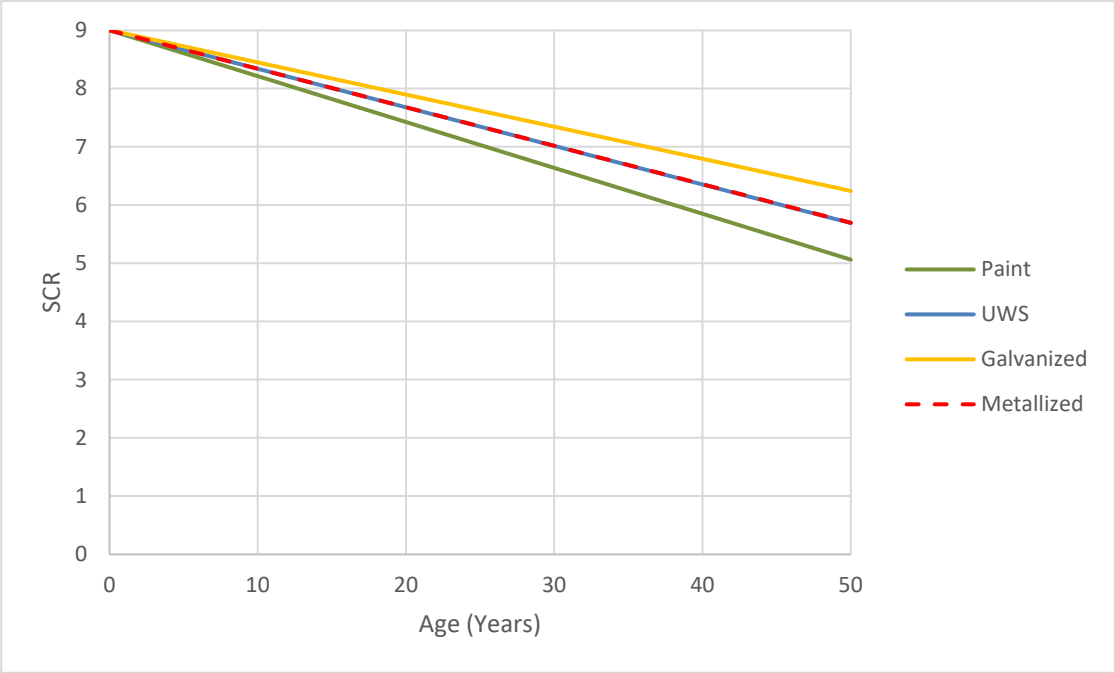

Figure 2-8. Linear Regression Lines for All Corrosion Protection Systems with Intercept Adjustment (Not for extrapolation)

2.3.1.3 Comparing Old Paint vs. New Paint

Paint was further evaluated by dividing painted bridges into two separate groups, since paint technology has changed over the years. For this analysis, paint was separated into two age categories: 0-20 years and 21-50 years. The 20-year age cutoff was determined based on stakeholder feedback to represent a general transition between current paint systems and painting best practices (e.g., surface preparation, application methods, curing conditions, etc.). Older bridges may have also contained similar paint systems and fabrication methods, but on a more variable basis. Comparison of old and new painted bridges in Figure 2-9 showed that newer bridges (0-20 years old) typically have a higher SCR vs. age trendline than that of older

bridges (21-50 years old). The solid green line in Figure 2-9 represents the trendline for all painted bridges as was used in the previous analysis.

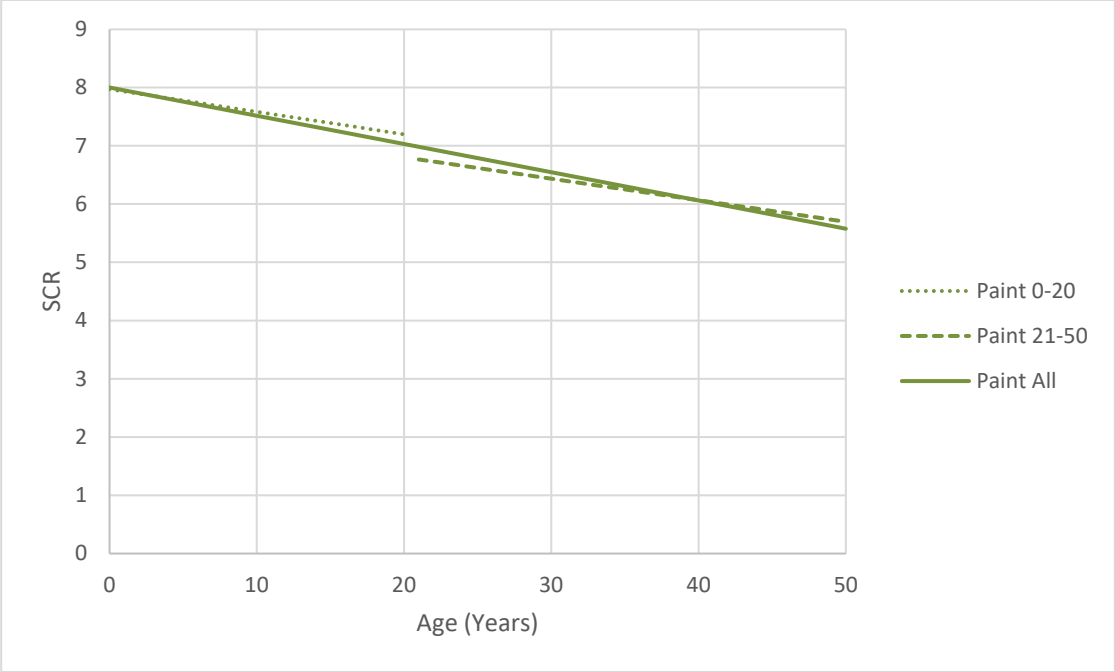

Figure 2-9. Comparison of Old and New Painted Bridge Performance (Not for extrapolation)

Comparison of performance of the corrosion protection systems when the paint is separated by age shows similar results to those seen without separating paint by age, as shown in Figure 2-10. The overall rankings of performance remain, with paint performance shown as inferior to all other corrosion performance systems. The new paint performance is, however, similar to that of metallized performance when extrapolated to an age of 50 years.

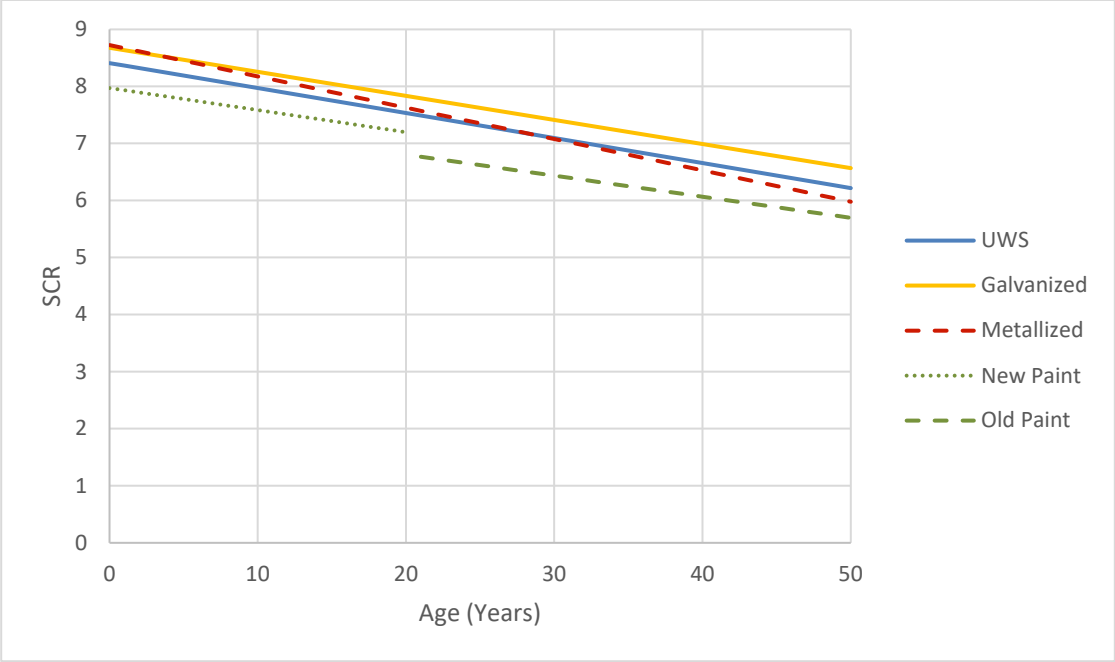

Figure 2-10. Linear Regression Lines of All Corrosion Protection Systems with Paint Separated by Age (Not for extrapolation)

2.3.2 Method 2: Temporal Analysis of Data Filtered by Environment

2.3.2.1 Bridges Selected and Filtering

Fifteen (15) bridges of each corrosion protection system (paint, UWS, galvanized, metallized) were selected for an analysis of long-term NBI data. Since the longitudinal analysis is based on fewer bridges, the dataset of bridges used were selected to resemble highway bridges in a common environment to reduce variability due to these parameters. The environment selected was one of the environments to be simulated through accelerated corrosion testing: a relatively aggressive deicing environment. The details of the quantification of what defines a relatively aggressive deicing environment are shown in Table 2-5. These quantifications were determined through a combination of data from a research project assessing the corrosion

performance of UWS in different environments (McConnell et al. 2014 and additional ongoing work), chloride concentrations and deicing data from field work (Rupp 2020), environmental data from the National Oceanic and Atmospheric Administration (NOAA 2012), and atmospheric chloride concentrations from the National Deposition Program website (NAPD 2014). The deicing environment was selected over the marine (natural-chloride) environment for this analysis due to the high volume of data received from Ohio, which matches the deicing environment. Except for the painted bridges, all of the bridges used for this dataset were from Ohio. No data on painted bridges was received from Ohio. New York and Pennsylvania bridges were used for analysis of painted bridges, as these states generally meet the criteria of a deicing environment and are geographically close to Ohio.

Table 2-5 Human-Made Chloride Environment Quantification

Environmental Characteristic	**Quantity**	**Unit**
Deicing Agent Applied Based on Survey Response (Rupp 2020)	≤ 29	Tons/Lane Mile
Average Humidity	65 - 75	Relative %
Average Annual Precipitation	20 - 40	Inches
Vertical Clearance Between Bridge and Roadway	13 - 23	Feet
Atmospheric Chloride Concentration	0.03 – 0.3	Parts Per Million

The priority for selecting bridges for the longitudinal analysis was making sure that the bridges selected were highway crossings, which are exposed to deicing agents via the roadways underneath, and furthermore that they had vertical underclearance values typical of deicing environment bridges as shown above in Table 2-5. All bridges chosen for long-term analysis met these criteria, having a vertical

underclearance between 13 and 23 feet. All bridges selected also came from states that met the criteria for the amount of deicing agent applied. The bridges selected for metallizing, galvanizing, and UWS met all identified deicing environment criteria, but the bridges selected for painted bridges did not. The data collected for painted bridges was limited, and resultantly it was not possible to find painted bridges that met all deicing environment criteria. All of the painted bridges selected met the average humidity criteria, but only 7 out of 15 met the atmospheric chloride concentration, and only 9 out of 15 met the average annual precipitation criteria. Some of the bridges included in the painted bridge dataset had atmospheric chloride values from the NOAA database that were less than 0, which is not possible. It is therefore unknown what the actual atmospheric chloride values were for those bridges. Other bridges included in the painted bridge dataset had atmospheric chloride values as high as 0.87 ppm. The precipitation values for the painted bridges included ranged from 20-50 inches.

2.3.2.2 SCR vs. Age

Once the 15 bridges were selected for each corrosion protection system, their superstructure ID numbers were used to extract their SCR over the timeframe available on the Long-Term Bridge Performance Program website (Long-term Bridge Performance, 2019). SCR records from the NBI are available beginning in 1996, so SCR's were not available for the onset of a bridge's lifespan if the bridge was constructed before 1996. As described in Section 2.2.2, when the year reconstructed was prior to 1996 (the first year in which NBI data is available) the age used in this analysis was conservatively based on the year reconstructed if reconstruction was performed, and the year built otherwise. Hence, the age of the corrosion protection

system may be longer (i.e., the corrosion protection may be better performing at a given age) than assumed.

Graphs were plotted for each selected bridge showing the performance (SCR) over time (age). An example can be found in Figure 2-11. A linear trendline was then added to quantify performance of each structure in a manner that could be easily compared. A table was created for each material type including beginning and end age of analysis, trendline slope, and trendline intercept (Tables 2-6 - 2-9). The average of both slope and intercept for each corrosion protection system were calculated and are shown at the bottom of Tables 2-6 – 2-9. One bridge (UWS bridge 4803787 (OH)) was an outlier (having a slope nearly 20 times the average for the remainder of the dataset) and was removed from the dataset. This is attributed to the fact that there was only 2 years of data for this bridge, during which the SCR changed from a 9 to an 8.

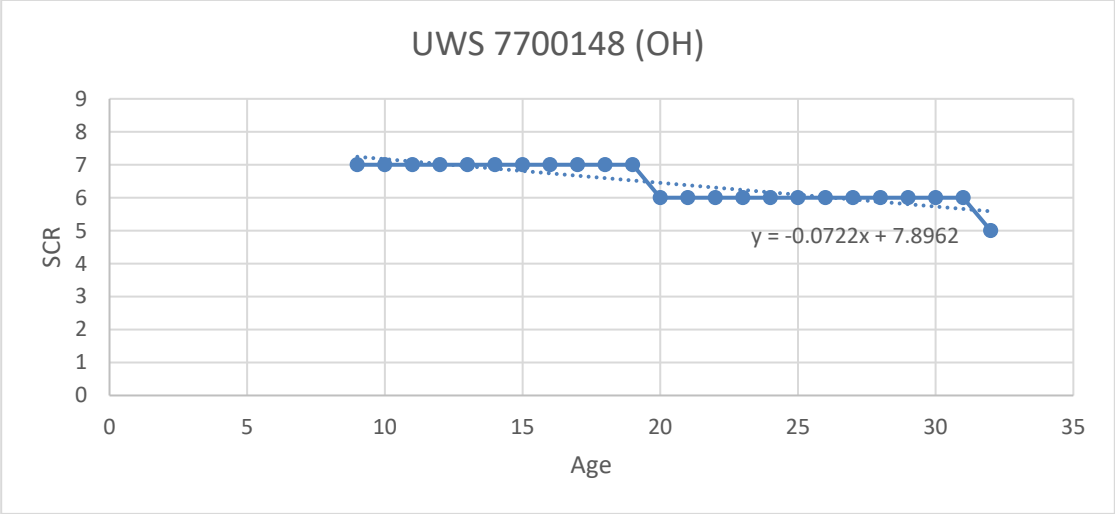

Figure 2-11. Long-Term Performance of UWS Bridge 7700148 from Ohio (Not for extrapolation)

Table 2-6. Long-Term Performance of 15 Painted Bridges

Paint				
Structure	**Beginning Age**	**End Age**	**Slope**	**Intercept**
8645 (PA)	21	28	0.000	7.000
13755 (PA)	16	23	0.000	8.000
16053 (PA)	16	23	0.000	8.000
19152 (PA)	16	23	0.000	7.000
22939 (PA)	23	30	0.000	7.000
23021 (PA)	23	30	-0.179	11.357
23056 (PA)	22	29	0.000	7.000
23059 (PA)	22	29	0.000	7.000
36788 (PA)	20	27	-0.083	8.083
38676 (PA)	22	29	0.000	7.000
44125 (PA)	5	12	0.000	8.000
1017781 (NY)	28	51	0.056	4.135
1017782 (NY)	28	51	0.019	5.161
1031450 (NY)	30	53	0.007	5.604
1054860 (NY)	28	51	0.030	5.715
Average			-0.010	7.070

Table 2-7. Long-Term Performance of 15 UWS Bridges

UWS				
Structure	**Beginning Age**	**End Age**	**Slope**	**Intercept**
700495 (OH)	3	26	-0.054	8.698
705161 (OH)	1	3	0.000	9.000
2001632 (OH)	2	9	0.000	9.000
2508923 (OH)	10	33	-0.002	8.255
2517841 (OH)	8	30	0.000	8.000
3203220 (OH)	1	8	0.000	9.000
~~4803787 (OH)*~~	~~1~~	~~2~~	~~-1.000~~	~~10.000~~
4805038 (OH)	2	10	-0.233	9.844
7604459 (OH)	1	13	-0.099	9.385
7604750 (OH)	2	13	-0.122	9.501
7700148 (OH)	9	32	-0.072	7.896
7701691 (OH)	1	13	-0.176	9.539
7702043 (OH)	17	40	0.010	6.703
7906331 (OH)	1	9	0.000	9.000
8001243 (OH)	8	31	-0.056	9.752
Average			-0.057	8.827

* Outlier: slope nearly 20 times the average for the remainder of the dataset; removed from the dataset when compiling average statistics

Table 2-8. Long-Term Performance of 15 Galvanized Bridges

Galvanized				
Structure	**Beginning Age**	**End Age**	**Slope**	**Intercept**
703036 (OH)	1	4	0.000	9.000
1814753 (OH)	25	48	-0.041	8.716
1814788 (OH)	25	48	-0.041	8.716
4100360 (OH)	1	7	0.000	9.000
6702910 (OH)	1	8	0.000	9.000
7102607 (OH)	2	16	-0.088	9.033
7600151 (OH)	1	11	0.000	9.000
7600186 (OH)	1	10	0.000	9.000
7600380 (OH)	1	10	0.000	9.000
7603754 (OH)	1	14	0.000	9.000
7603827 (OH)	1	14	0.000	9.000
7603851 (OH)	1	15	0.000	9.000
7603916 (OH)	1	12	0.000	9.000
7603967 (OH)	1	12	0.000	9.000
7704747 (OH)	1	10	0.000	8.000
Average			-0.011	8.898

Table 2-9. Long-Term Performance of 15 Metallized Bridges

Metallized				
Structure	Beginning Age	End Age	Slope	Intercept
1804715 (OH)	1	19	0.037	7.368
1804898 (OH)	1	19	-0.019	7.035
1810332 (OH)	16	19	-0.047	7.488
1811584 (OH)	1	18	0.080	6.301
1811614 (OH)	1	16	0.057	6.700
1811649 (OH)	35	58	0.000	7.000
1811673 (OH)	1	18	0.000	7.000
2103540 (OH)	8	31	0.000	8.000
2803364 (OH)	6	29	-0.038	7.920
4305345 (OH)	33	56	-0.043	8.790
7701446 (OH)	1	12	0.000	9.000
8502145 (OH)	1	14	0.000	9.000
8502269 (OH)	1	14	0.000	9.000
8502293 (OH)	1	14	0.000	9.000
8502315 (OH)	1	14	0.000	9.000
Average			-0.002	7.907

Figure 2-12 was plotted using the average slopes and intercepts calculated from Tables 2-6 – 2-9. Similar to the plots observing SCR vs. age (Figures 2-7, 2-8, and 2-10), this plot should not be used for extrapolation of performance or exact predictions of performance of a certain corrosion protection system for any given age. Instead, it should be considered to determine whether general trends exist. Overall, the trends show that galvanized bridges outperform both UWS bridges and painted bridges, similar to the results of Method 1 using all bridges sorted by corrosion protection system. For most of the age range until about 37 years, UWS performance is again between that of galvanized and paint. This plot shows that UWS bridges had the steepest negative slope. This may be a result of inspector perception of UWS. Since UWS forms a protective patina, an inspector without experience with UWS

bridges may perceive the bridge to be rusted when the patina forms, which happens early on in the life of a UWS bridge, leading to a lower SCR documented early on. This could have a drastic effect on trendline slope, especially since more than half of the UWS bridges used for the longitudinal analysis were under 20 years old. Analysis of trendlines for metallized bridges resulted in a positive slope, which is not logical for realistic situations and is most likely the result of variability of inspector perception. Galvanizing and paint both had a slightly negative slope equal to each other.

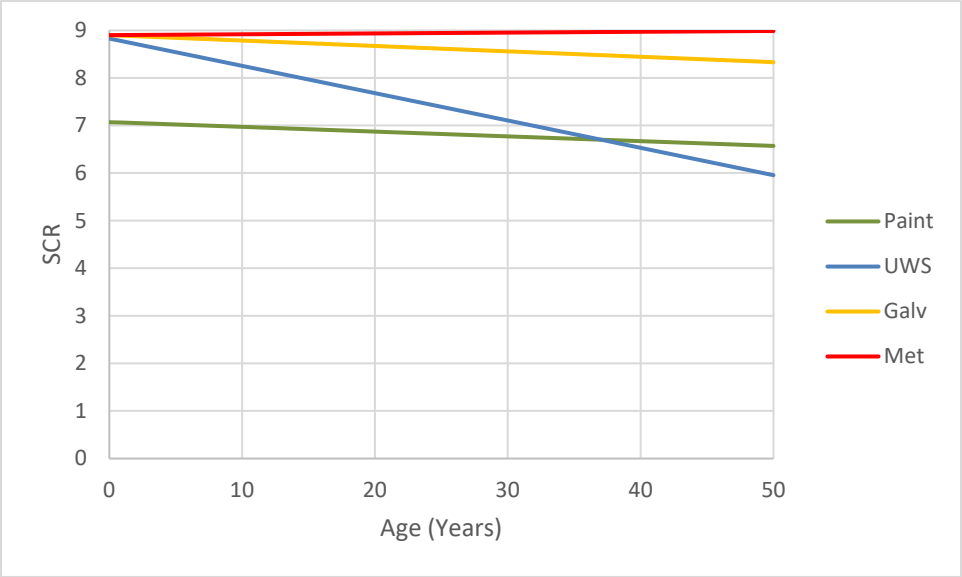

Figure 2-12. Long-Term Performance of Corrosion Protection Systems from Longitudinal Analysis of Fifteen Bridges per Corrosion Protection System (Not for extrapolation)

2.3.2.3 Longitudinal Analysis (Method 2) Limitations

Method 2 is based on only 15 bridges of each corrosion protection system, 60 bridges total; this is not a statistically significant population. Additionally, many of the slopes appear to be a result of the subjectivity and lack of standardization of the SCR.

Some bridges, such as the example UWS bridge shown in Figure 2-13a dropped one SCR at a young age in their lifespan, resulting in a more drastic slope, especially for bridges that are still relatively young and do not have a long lifespan of data to analyze. When analyzing SCR over lifespan, many bridges showed fluctuations between one SCR and another, going back and forth, which affected the slope. These fluctuations could be due to repair or rehab that occurred between inspections or due to inspector variability of perception. This can be seen in Figure 2-13b for an example metallized bridge. The result of this same type of fluctuation in Figure 2-13c for an example painted bridge counterintuitively leads to a positive trendline. Finally, many galvanized bridges, such as shown in Figure 2-13d, had only short-term data, during all of which they remained at an SCR of 9, inflating the trendline. All stated observations seem to explain the difference in slope of UWS performance compared to the other protection systems as well as the positive slope of metallized bridge performance.

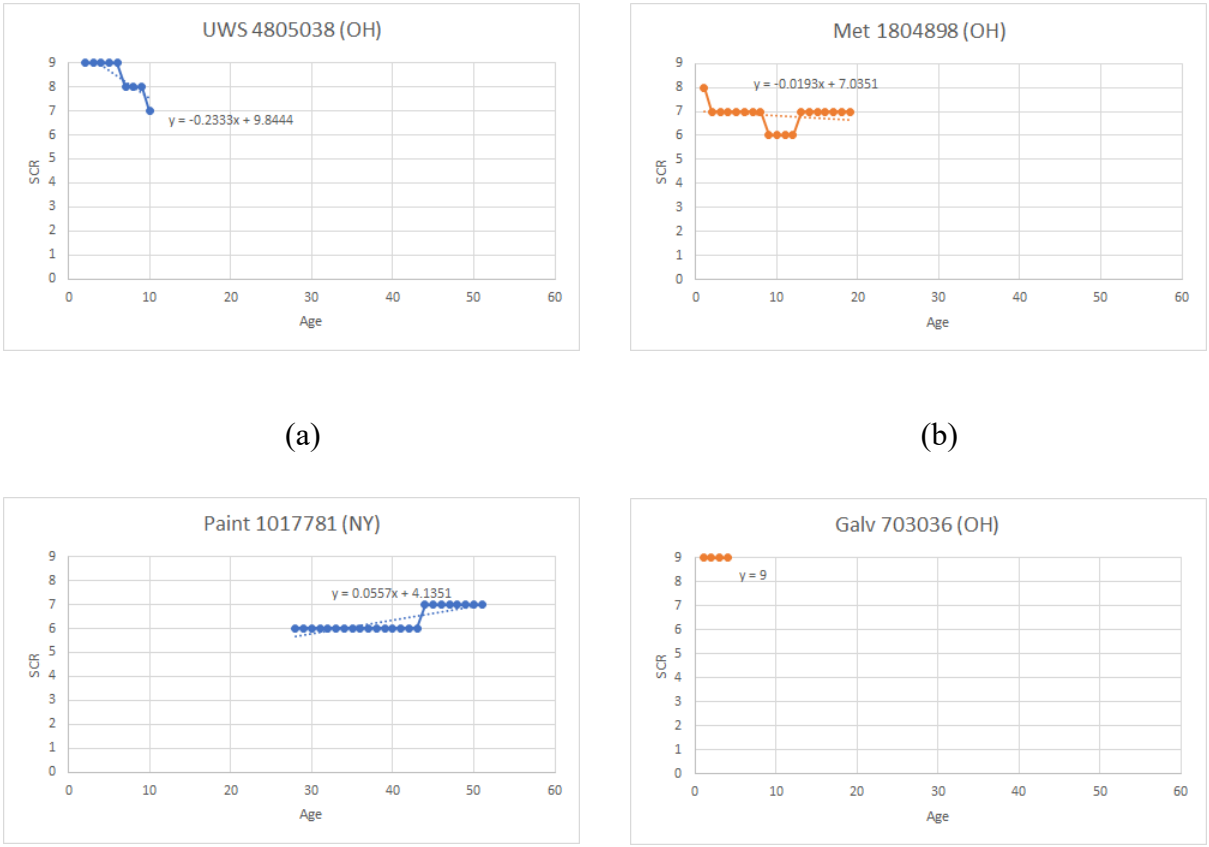

Figure 2-13. Example Longitudinal Analysis Data that Contributes to Data Interpretation Problems for a(n): a) UWS Bridge, b) Metallized Bridge, c) Painted Bridge, d) Galvanized Bridge (Not for extrapolation)

2.4 Discussion of Results

While there is a reasonable volume of existing performance data of bridges, the corrosion protection systems used on these bridges is not generally known. Determining this information is reliant on the cooperation of owners and fabricators, who have variable record keeping practices that create variability in the ease of which this information can be obtained. There are also limitations to both methods of

analysis. Both methods relied upon SCR as the performance measure. SCR is generally governed by corrosion, but this is not always the case and is therefore an imperfect measure of corrosion protection system performance. Method 1, which included the use of a larger database of bridges, analyzed corrosion performance data using a combination of statistical analysis and plots of SCR vs. age. Method 2, the longitudinal analysis, analyzed the long-term performance of fifteen bridges per corrosion protection system (paint, UWS, galvanized, metallized). The large database analysis (Method 1) was a more representative sample size but contained a large scatter of data even at a similar age and contained a small database of metallized bridges compared to the database collected for the other corrosion protection systems. The longitudinal analysis (Method 2) examined the long-term performance of individual bridges over their lifespans but was especially susceptible to variability in SCR that may have been a result of either rehabilitations or variability of inspector perception.

It is also important to note that the trendlines presented herein are based on limited data and are thus not suitable for being extrapolated to estimate performance of other bridges in different environments or situations or of different (e.g., older) ages or providing an accurate lifespan prediction. Rather, these data analysis methods can be used for observation of general relative trends. In Figures 2-7 and 2-12, both methods of analysis show slightly different results, with one commonality being that metallized bridge performance decreases the least over time and the other being that for most of the plotted age range (with exceptions in the higher end of the age range), the relative ranking of performance, from best to worst, is galvanized, then UWS, then paint. This conclusion is supported by the large sample size of the dataset that comes from the

one-way ANOVA, which showed that paint, UWS, and galvanized bridges had statistically significant difference in performance from each other.

Chapter 3

ACCELERATED CORROSION TESTING METHODOLOGY

Accelerated corrosion testing is a common means of assessing the performance of corrosion protection systems, particularly paint systems. Various standard methods exist for this purpose. While these methods are effective for certifying adequate performance of paint systems and other corrosion protection systems in some cases, they generally lack a connection to real world performance. All of these methods subject specimens to severe conditions, but how these conditions relate to real world conditions is unknown. For example, there is no known relationship between a given duration of accelerated corrosion testing and actual service life. This situation is further complicated the variability in real world performance that occurs in various environments.

For these reasons, this research set out to develop an accelerated corrosion testing method that was benchmarked to field performance. Because UWS is known to perform well in most environments, the philosophy adopted here was to evaluate the performance in environments that may be too harsh for ideal performance of UWS. Furthermore, there is an existing wealth of information on field performance for UWS bridges that have been in service for many decades. Therefore, the accelerated corrosion testing was benchmarked against the long-term field performance of UWS bridges in severe environments (representative of coastal environments and heavy uses of deicing agents). Five different iterations in methodology that ultimately resulted in a realistic accelerated corrosion testing method are described in this chapter.

3.1 Methodology Development

3.1.1 Background

The corrosion rate of metals can be described by the power law equation:

$$\Delta = At^B \qquad (1)$$

where Δ is the thickness or mass loss due to corrosion, t is time, and A and B are empirical constants obtained from curve fits of experimental data. The value of B is typically less than 1 to describe that the corrosion rate decreases with time. While alternative equations exist to overcome the simplicities of Eqn. 1, Eqn. 1 has been shown to provide a good fit to experimental data in numerous studies and can be a good approach for predicting long-term performance of steel corrosion protection systems.

Fletcher et al. (2003) provide useful corrosion data that has been carefully controlled for different materials in different US environments. Figure 3-1 shows the curve obtained by solving for constants A and B in Eqn. 1 that would fit the corrosion data on UWS coupons after 2 and 4 years of exposure at Kure Beach, NC that were reported by Fletcher et al. along with Fletcher et al.'s data for A1010 specimens. The fact that the data at 2 and 4 years is known and that the long-term corrosion behavior is extrapolated is highlighted by the filled data points at 2 and 4 years and the open data points for the remaining time periods.

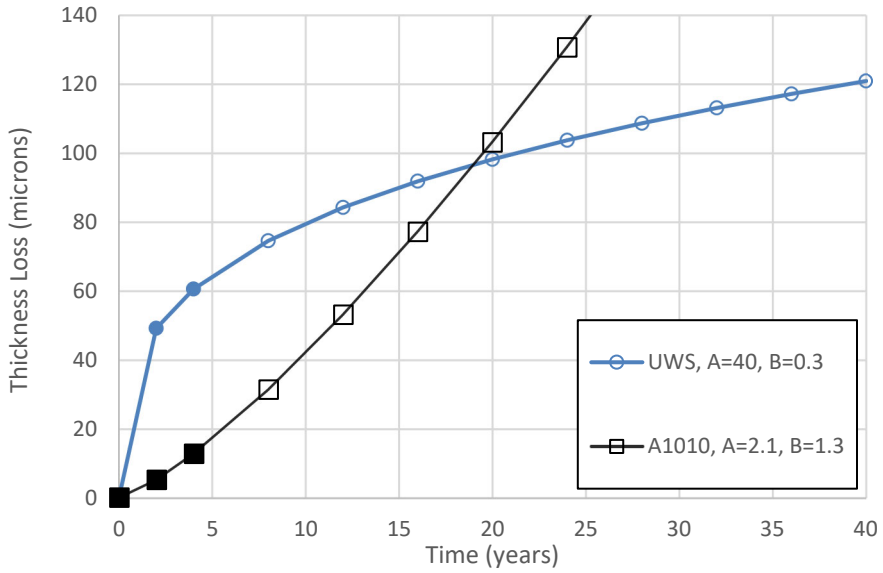

Figure 3-1. Power Law Curve Fits to Fletcher et al. (2003) UWS and A1010 Field Coupons After 4 Years of Exposure

The Eqn. 1 power law is shown to provide a reasonable approximation for the UWS data. Conversely, the A1010 specimen data does not result in an extrapolation that is consistent with expectations because B > 1, predicting an increasing corrosion rate and therefore more corrosion of A1010 than UWS after 20 years of exposure. This may be due to the fact that the A1010 specimens have not yet stabilized to a steady state of corrosion after only 4 years of exposure. Thus, longer term testing, perhaps coupled with an alternative mathematical model may correct this suspicious extrapolation.

Accelerated corrosion testing aims to reproduce the corrosion observed in natural environments through laboratory testing that exposes the specimens to more severe environments (e.g., higher humidity and / or chloride concentrations) over a shorter amount of time. The accelerated corrosion test that has been demonstrated as

being successful for several previous applications is the standard cyclic corrosion test procedure SAE J2334 (SAE 2016) and modifications thereof. This test was originally developed through the long-term, combined efforts of the North American automakers, steel producers, chemical and paint suppliers, and test laboratories. For coated and bare steel, it was shown to provide an excellent correlation with real-world behavior in automobiles driven for five years in the salt-contaminated snow belts of the US and Canada (Davidson et al. 2003). Modifications of the J2334 test have been also found to be reliable predictors of corrosion performance in bridge applications (Fletcher et al. 2003, Fletcher 2011).

Figure 3-2 summarizes the modified J2334 test cycle used by Fletcher et al. (2003), which consists of daily cycles of wetting, salt application, and drying achieved by controlled variations in humidity and temperature. This method will be referenced herein as the "standard method". Fletcher et. al showed that the test gave a good correlation for a variety of bridge steels with the corrosion in severe marine environments. This standard method modified the NaCl concentration of the salt application stage from 0.5% (used in the original SAE J2334) to 5%, which resulted in the formation of akageneite, while the original SAE J2334 test did not. Akaganeite is known to form in the field conditions where chlorides are present in sufficiently high levels, which can interrupt the formation of more protective corrosion byproducts in UWS and is likely also detrimental to other corrosion protection systems. Further modification of this testing protocol may be necessary to further improve testing such that the corrosion mechanism of accelerated corrosion testing better matches the corrosion mechanism found in the field.

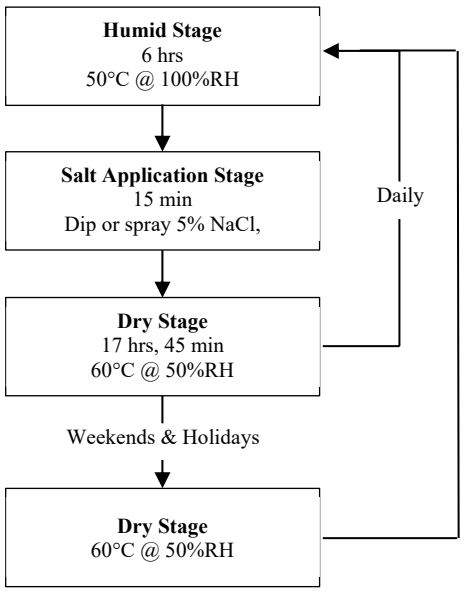

Figure 3-2. J2334 Accelerated Corrosion Test as Modified by Fletcher et al. (2003); "Standard Method" Used for Further Modifications

Figure 3-3 shows the trends in corrosion rate of UWS both from the field data previously seen in Figure 3-1 and from the data obtained through accelerated corrosion testing by Fletcher et al. (2003). The curve of the corrosion rate obtained through accelerated corrosion testing does not match that of the data obtained in the field, as it never reaches a point of stabilization and over-predicts the amount of corrosion that would actually occur. This shows the need for further modifications to the SAE J2334 testing protocol to be able to make realistic long-term predictions.

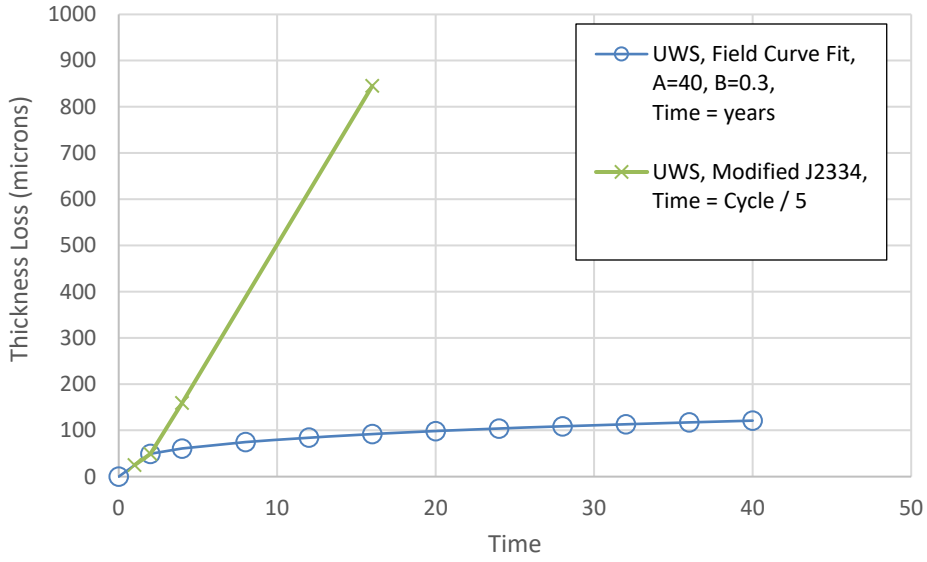

Figure 3-3. Comparison of Trends in Corrosion Rate of Field and Accelerated Corrosion Testing Specimens

3.1.2 Accelerated Corrosion Testing Methods Evaluated

3.1.2.1 Specimen Description for Trial Methods

All specimens were provided by High Steel Structures, LLC. The specimens consisted mostly of rectangular flat plates, shown in Figure 3-4a, that were 4" x 6" x 3/8" (these are later referenced as "flat plate" specimens for conciseness). Twelve flat plate specimens each of UWS and carbon steel were used for the trial methods evaluated. Additional details regarding the composition of each of these corrosion protection systems can be found in Appendix A. Additionally, there were three specimens each of UWS and carbon steel with the same dimensions as the flat plate but that had welded and bolted features, as shown in Figures 3-4b and 3-5 (although the inconsequential difference in green dye in Figure 3-4b and blue dye in Figure 3-5 is noted). Each welded section was 3" x 1.5" x 3/8" with a 3/16" fillet weld and ¼"

weld holdbacks. The bolts were ½” x 1-1/4” ASTM A3125 Grade A325-T Heavy Hex Bolts with ASTM F436 hardened washers and an A563 Grade DH Heavy Hex Nuts. All bolts were tightened to 1/6 turn.

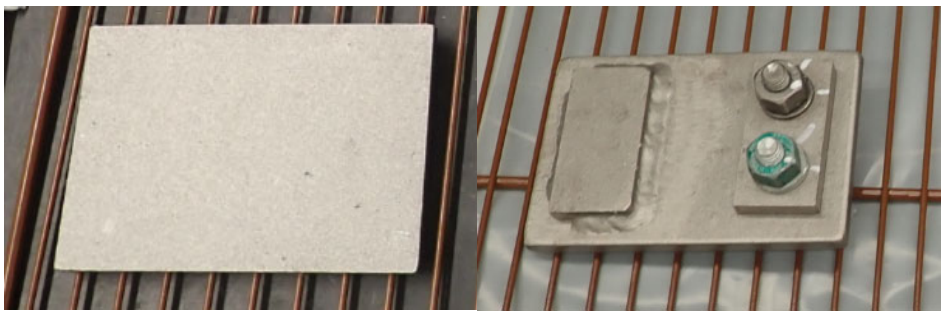

(a) (b)

Figure 3-4. a) Flat Plate b) Plate with Bolted and Welded Features

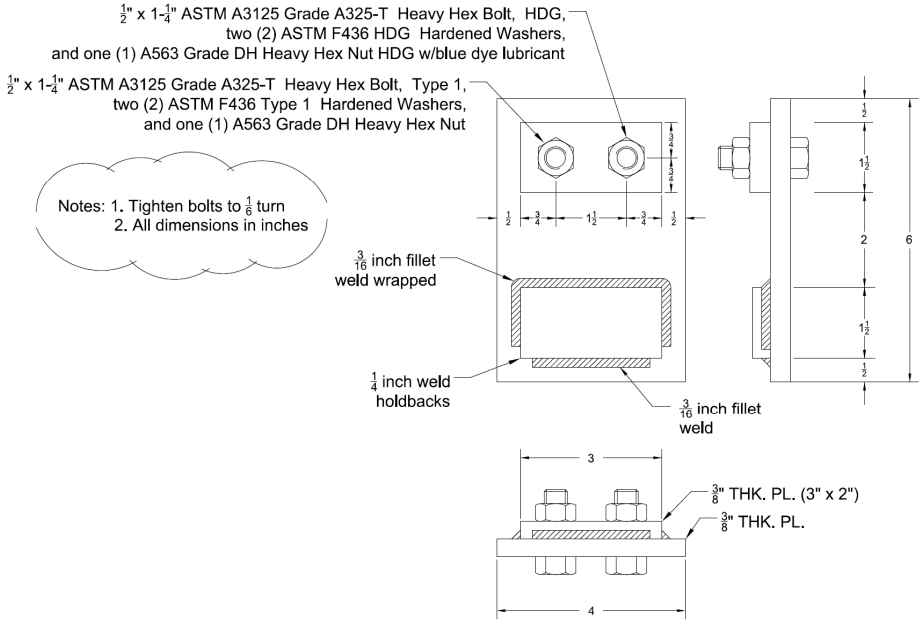

Figure 3-5. AutoCAD Drawing for Plate with Bolted and Welded Features

After 5, 10, and 20 cycles of testing, 3 of the flat plates of each material type were removed to assess mass loss and thickness loss. The chemical composition of the rust layer was also analyzed for one specimen of each steel type (UWS or carbon steel) after 5, 10, and 20 cycles of testing via x-ray diffraction (XRD) testing. The remaining specimens were retained for possible future cyclic testing, but this preliminary concept to potentially ease logistics was not necessary to implement in the final testing.

3.1.2.2 Overview of Modifications Evaluated

Five iterations of modifications to the J2334 cyclic corrosion test as modified by Fletcher et al. (2003) described in Figure 3-2, i.e., the "standard method," were performed, each varying only one variable at a time relative to the Fletcher et al. (2003) method, with the exception of the fifth and final iteration. The variables that were modified included salt concentration, duration of the humid and dry stages of testing, and temperature. A summary of the modifications is shown in Table 3-1. Each iteration was tested for a total of 20 cycles, with three unique specimens each of UWS and carbon steel sandblasted then dimensionally measured and weighed (to assess thickness and mass loss, respectively, due to corrosion) after 5, 10, and 20 cycles to assess trends in thickness and mass loss versus number of cycles. Upon conclusion of these efforts, the results of Methods 1 - 5 were evaluated to determine a methodology for use in future testing of the complete set of corrosion protection systems (UWS, two types of paint systems, metallizing, galvanizing).

Table 3-1. Accelerated Corrosion Testing Modifications, Relative to Standard Method Shown in Fig. 4-2

Method	Modification
1	Reduce salt bath concentration to 2% NaCl
2	Reduce humid stage duration to 3 hours
3	Add a rinse cycle that simulates rainwater rinsing
4	Reduce salt bath concentration to 1% NaCl
5	Reduce salt bath concentration to 2% NaCl and increase humid stage temperature to 60°C

3.1.2.3 Method 1: Reduce Salt Bath Concentration to 2%

The first attempted modification of the standard method was the reduction of the NaCl concentration in the salt bath during the salt application stage, as shown in Figure 3-6. A 5% concentration of NaCl is dictated by the standard method. However, since results show that the standard method leads to exponential increase of corrosion rate instead of exponential decrease of corrosion rate as experienced in the field, the first modification reduced that amount to a 2% NaCl concentration to attempt to lessen the rate of corrosion. The required amount of salt to satisfy this concentration was calculated and added to containers of deionized water to create the salt bath that the specimens were submerged into during the daily salt application stage. All other aspects of the daily cycles remained the same as the standard method. See Table B-1 in Appendix B for the mass of salt used in the salt baths for each method.

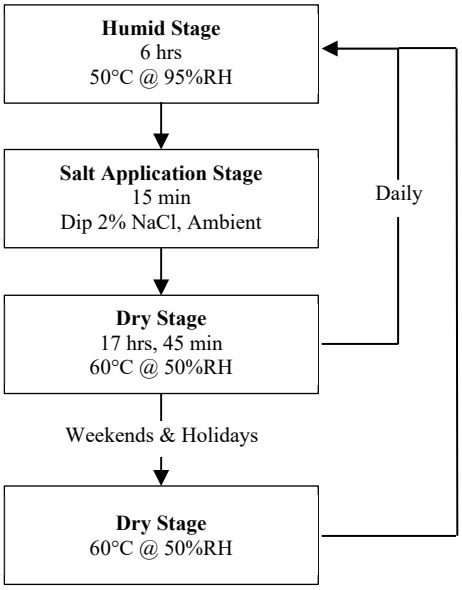

Figure 3-6 Method 1 Accelerated Corrosion Testing Protocol

3.1.2.4 Method 2: Reduce Humid Stage to 3 Hours

The second modification of the standard method was reduction of the humid stage from 6 hours to 3 hours, shown in Figure 3-7. The salt application stage remained at 15 minutes, and the dry stage was adjusted accordingly to become 20 hours and 45 minutes. The formation of rust requires atmospheric conditions where there is enough water and air. ISO 9223 (International Organization for Standardization [ISO], 2012) uses 80% relative humidity as a threshold to define corrosivity. Thus, during the humid stage when the environmental chamber is set to 95% RH, a corrosive environment is created. Therefore, the rationale of reducing the duration of the humid stage is to decrease the amount of time during which the corrosion reaction occurs, decreasing the rate of corrosion.

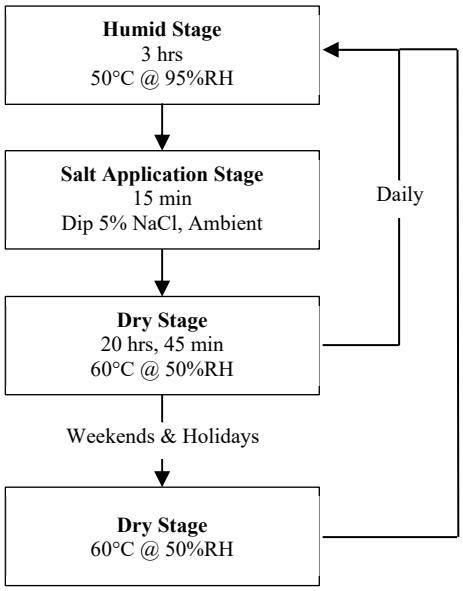

Figure 3-7. Method 2 Accelerated Corrosion Testing Protocol

3.1.2.5 Method 3: Add a Rinse Cycle

The third modification to the standard method was adding a rinse cycle to simulate more realistic field conditions, as shown in Figure 3-8. In reality, bridges are not constantly doused with chlorides. During the summer, highway overpasses are typically subject to roadway spray consisting of rainwater and other elements that may be dissolved in the rainwater. This roadway spray could provide a rinsing effect to remove corrosive elements from the steel. This rinsing effect would likely slow down the rate of corrosion.

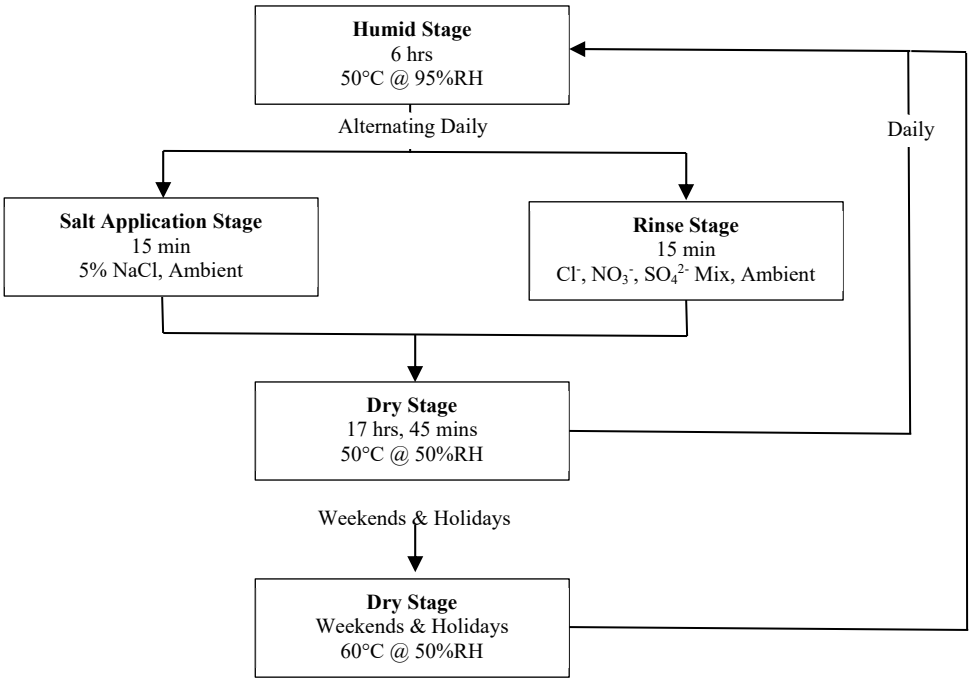

Figure 3-8. Method 3 Accelerated Corrosion Testing Protocol

To properly simulate the road spray rinse water, water was collected from the Chapman Rd. bridge crossing I-95 in Newark, Delaware. A clean oil pan was placed on the pier of the bridge and secured with tiedown straps, as shown in Figure 3-9, and was retrieved after a rainstorm. The water was then analyzed by a pH test, conductivity test, ion chromatography test, and gran titration using the methodology described in "Techniques of Water-Resources Investigations Reports" (USGS 2020). The results of these tests describing the chemistry of the water from the road spray are shown in Table 3-2.

Figure 3-9. Water Collection on the Chapman Rd. Bridge

Table 3-2. Water Chemistry of Collected Rainwater

Metric	Value	Unit
pH	6.76	NA
Conductivity	0.24	mS/cm
Chloride (Cl^-) Concentration	7	mg/L
Nitrite (NO_2^-) Concentration	1	mg/L
Nitrate (NO_3^-) Concentration	23	mg/L
Sulfate (SO_4^{2-}) Concentration	6	mg/L
Alkalinity	0.507	meq/L
	25.363	as $CaCO_3$

To recreate the field-collected water, chloride (Cl^-), nitrate (NO_3^-), and sulfate (SO_4^{2-}) were added to deionized water by adding their respective salt compounds in their measured concentrations. The calculations and quantities of each salt that was added can be found in Tables B-2 and B-3 in Appendix B. Nitrite (NO_2^-) was neglected due to its small concentration along with the fact that nitrite converts to nitrate when it interacts with oxygen. Sodium bicarbonate was added to act as a buffer to match the alkalinity of the field-collected water, which was measured from the gran titration. Hydrochloric acid was added to then lower the pH of the mixture to the measured pH of the roadway spray within a 0.5 tolerance. The ions and buffer were calculated, measured, and precisely added to the bins of deionized water. The hydrochloric acid, however, required a guess and test method. This means that small quantities of hydrochloric acid were incrementally mixed into the solution until the pH was within 0.5 of the field-measured pH of 6.76, with values hovering around neutral.

Based on thickness loss data measured from Methods 1 and 2 along with field data taken from (Rupp 2020), it was determined that it was reasonable to equate two cycles in the environmental chamber to approximately one year in the field for the Method 3 trial. Since typically a bridge would experience a higher concentration of chlorides in the winter due to deicing salts and then rinse water from road spray in the summer, it was decided that the specimens should alternate between being submerged in the salt-water bath and the rinse water bath such that they would be in the salt water one day and the rinse water the next. In this way, each set of two cycles could be generally thought of as representing the winter and summer seasons of one year in the field.

3.1.2.6 Method 4: Reduce Salt Bath Concentration to 1%

The fourth modification to the standard method was further decreasing the salt concentration to 1% NaCl during the salt application stage, as shown in Figure 3-10. The results from Method 1 showed an overall improvement in the rate of corrosion versus time when the concentration of the salt bath was reduced from 5% NaCl to 2% NaCl. The purpose of Method 4 was to test whether a further reduction of salt concentration led to further improvement in creating a corrosion rate showing exponential decay. In Method 4, the salt concentration was further reduced to 1% NaCl during the salt application phase. See Table B-1 in Appendix B for the mass of salt used in each method.

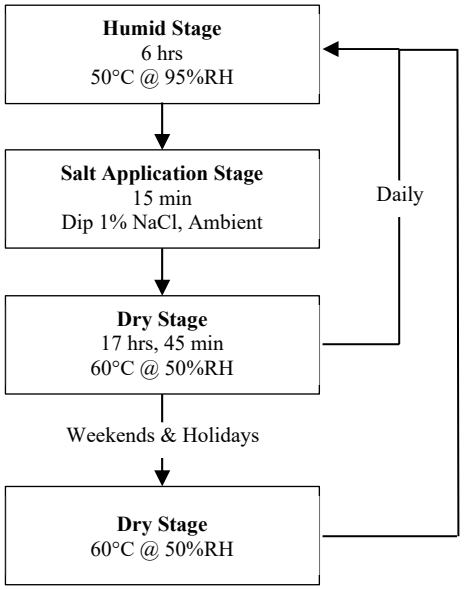

Figure 3-10. Method 4 Accelerated Corrosion Testing Protocol

3.1.2.7 Method 5: Reduce Salt Bath Concentration to 2% and Increase Humid Stage Temperature to 60° C

The results from the previous methods were analyzed to determine which modification to make for Method 5. The greatest improvement from the previous methods came from Method 3, in which the rise cycle was added. However, during this method, the corrosion was unstable, frequently resulting in full rust layers forming and then falling off of the carbon steel during the cycles. For that reason, a further modification of Method 3 was not chosen for Method 5.

The second-best results came from Method 1, in which the salt concentration of the salt application phase was reduced from 5% NaCl to 2% NaCl. For that reason, a further modification of Method 1 was chosen for Method 5. Since a further reduction from 2% NaCl to 1% NaCl in Method 4 did not improve the corrosion rate, the 2% NaCl was to be maintained, and the additional modification would be from a process other than reducing salt concentration.

Based on the results from the previous methods, it seemed as though slowing down the corrosion rate overall would not be sufficient. It is known that in realistic field conditions, the rust layer provides protection, causing a decrease in the corrosion rate with time and creating a curve of exponential decay. It was decided that speeding up the reaction may help this protection form and therefore create the desired corrosion progression. The Arrhenius Equation leads to the conclusion that a 10° C increase in temperature approximately doubles the rate of reaction. Therefore, for Method 5, in addition to reducing the salt bath concentration to 2% NaCl, the temperature during the humid stage was increased by 10° C from 50° C to 60° C, shown in Figure 3-11. Only the humid stage was changed since this is the stage in which the corrosion reaction occurs.

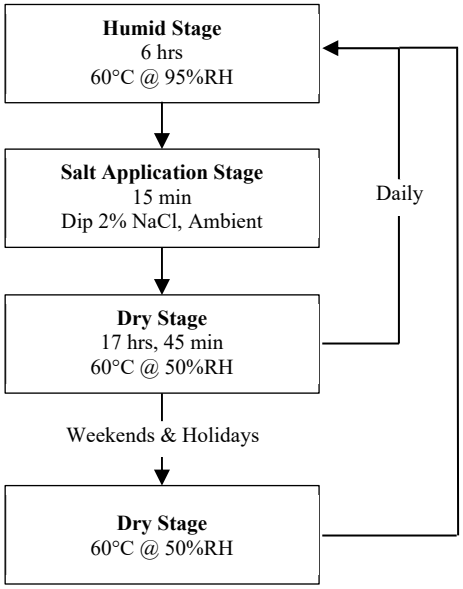

Figure 3-11. Method 5 Accelerated Corrosion Testing Protocol

3.1.2.8 Results of Modifications Evaluated

3.1.2.8.1 Mass Loss

Plots of mass and thickness loss versus number of cycles were created for each method. Both mass and thickness loss plots showed the same general trends, but mass was able to be measured with higher precision, as a single measurement can represent the entire sample, but a thickness measurement (or the average of many thickness measurements) represents only localized areas of the samples. Thus, more emphasis was placed on the mass loss when assessing trends, which are shown below in Figures 3-12a-e for UWS specimens. Figures 3-13a-e show the same data for the carbon steel specimens. Each data point in these figures represents the average of three specimens, with little variation observed between the three specimens being averaged. The R^2 values in these figures refer to the fit to a linear trendline.

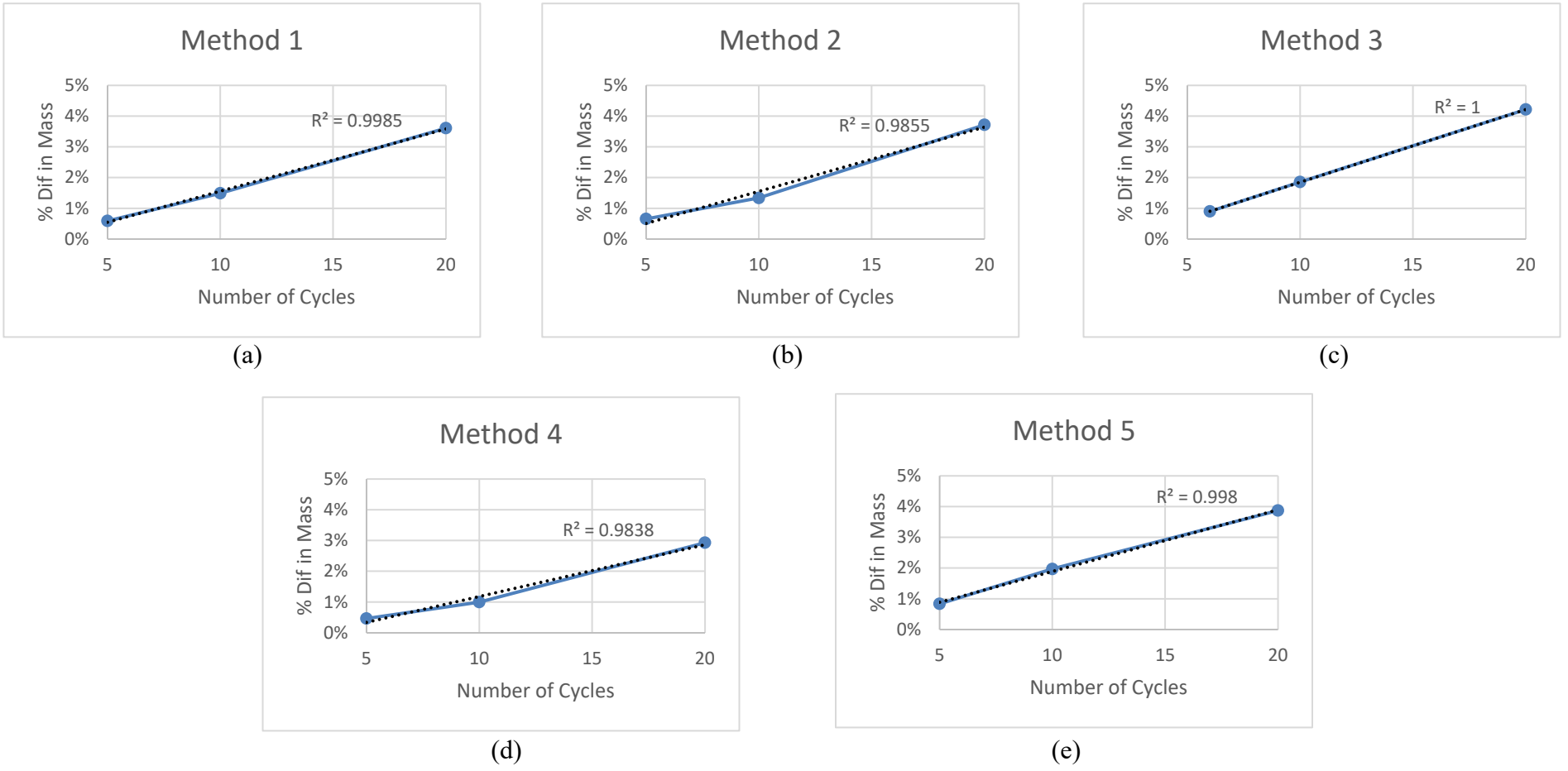

Figure 3-12. Average UWS Mass Loss for (a) Method 1 (b) Method 2 (c) Method 3 (d) Method 4 (e) Method 5

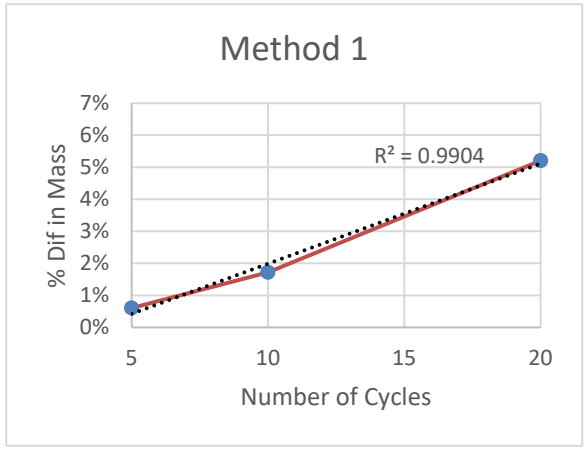

(a)

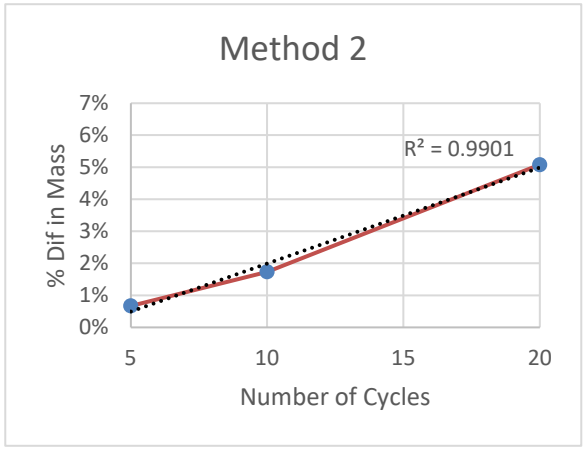

(b)

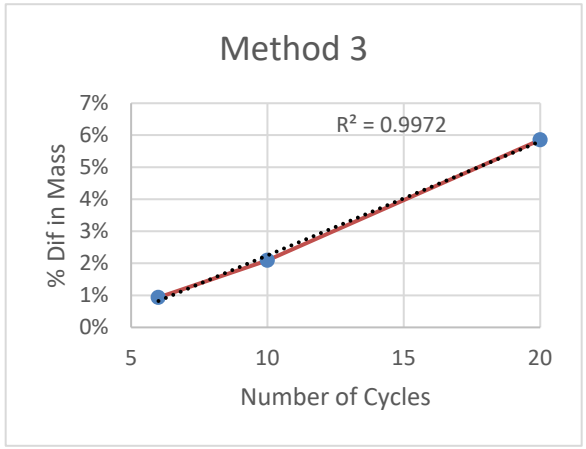

(c)

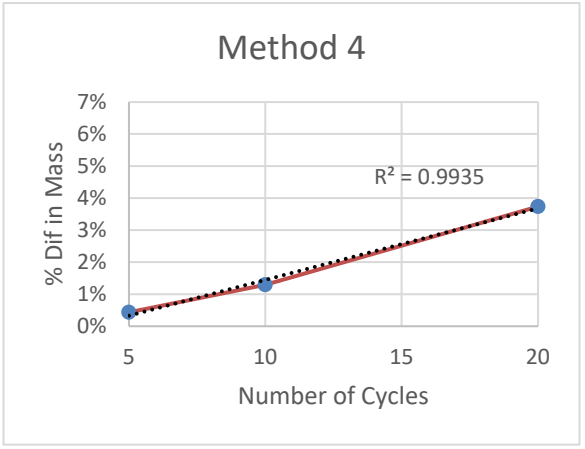

(d)

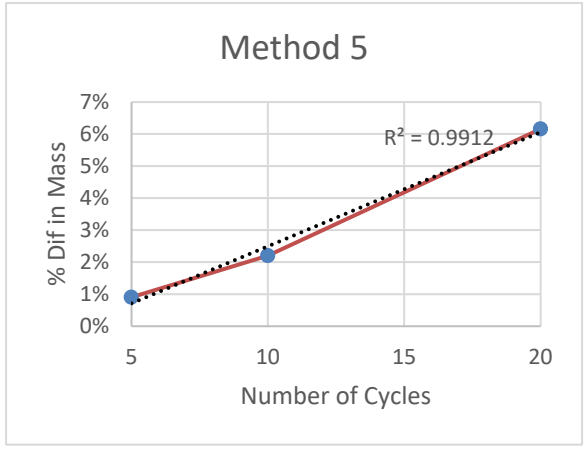

(e)

Figure 3-13. Average Carbon Steel Mass Loss for (a) Method 1 (b) Method 2 (c) Method 3 (d) Method 4 (e) Metho

3.1.2.8.2 **X-ray Diffraction (XRD) Results**

Specimens removed from the chamber after 10 cycles were also analyzed using x-ray diffraction (XRD) testing to evaluate the iron oxides that composed the rust layer created from the accelerated corrosion testing. The rust was scraped from specimens after being removed from the chamber using a putty knife. The results of the XRD analysis are summarized in Table 3-3. The percentage listed for each compound represents the percent composition of the scrape sample that was comprised of that specific iron compound. The percentages listed sum to 100% for each steel type (UWS or carbon steel) for each method.

Table 3-3. XRD Results from Cycle 10 Specimens

	Lepidocrocite		Goethite		Akageneite		Hematite		Magnetite		Ferrihydrite	
	UWS	**C**	**UWS**	**C**	**UWS**	**C**	**UWS**	**C**	**UWS**	**C**	**UWS**	**C**
Method 1	14%	15%	10%	11%	15%	11%	7%	6%	51%	45%	3%	12%
Method 2	24%	7%	11%	9%	7%	9%	0%	5%	58%	59%	0%	11%
Method 3	24%	18%	10%	6%	8%	25%	4%	4%	54%	46%	0%	0%
Method 4	15%	11%	8%	5%	23%	21%	5%	5%	49%	47%	0%	11%
Method 5	27%	40%	13%	14%	0%	0%	7%	5%	53%	41%	0%	0%

*UWS = Uncoated Weathering Steel; C = Carbon Steel

3.1.3 Selection of Final Method

3.1.3.1 Overview of Benchmarks

There were three benchmarks for evaluation of the methods: 1) rate of mass loss versus time 2) percentages of iron compounds determined from XRD values, and 3) thickness loss values compared to existing thickness loss thresholds. The rate of mass loss versus time was the primary focus, as this is the most unreasonable feature of the standard method. A linear rate of loss versus time was considered an improvement upon the standard method, but the ultimate goal was a curve showing exponential decay.

Additionally, the proportion of various iron compounds from field testing performed in complimentary work (Rupp 2020) was used as a benchmark to ensure that the corrosion mechanism was similar in the laboratory and in the field bridges. Table 3-4 shows the ranges of the different iron compounds that have been quantified from prior work along with the percentages of iron compounds found in UWS samples through laboratory testing in Method 5. The shaded rows indicate laboratory testing values that were within measured field test range for the corresponding iron oxide.

Thickness loss values were similarly compared to those from prior field work (Rupp 2020) and those from Albrecht et al. (1989). Specifically, Albrecht et al. give five qualitative "corrosivity categories" ("very low", "low," "medium," "high," or "very high") along with corresponding ranges of expected thickness losses per year. Figure 3-14 plots the upper bound of the four most severe of these ranges (with solid lines). Here it is shown that the "very high" category is quite extreme relative to the other four categories. Given that the philosophy was to focus on relatively severe environments, but ones that were not so extreme as to be unreasonable, thickness losses near the "high" range (i.e., between the "medium" and "high" lines in Figure 3-

14) were targeted. Figure 3-14 also plots average field data from prior work in deicing and coastal environments (via separate dashed lines). This information can ultimately be used to scale the accelerated corrosion testing data to realistic environments, which was finalized in the final phases of testing, discussed in Section 4.4.

Table 3-4. XRD Benchmarks and Method 5 Measured Values (UWS)

Compound	Measured Field Test Range	Measured Laboratory Test Percentage
Lepidocrocite	0 - 21%	27%
Goethite	0 - 52%	13%
Akaganeite	4 - 56%	0%
Hematite	0 - 22%	7%
Maghemite/ Magnetite	0 - 51%	53%
Ferrihydrite	0 - 34%	0%
Ferric Sulfate	0 - 19%	0%
Schwermanite	0 - 20%	0%

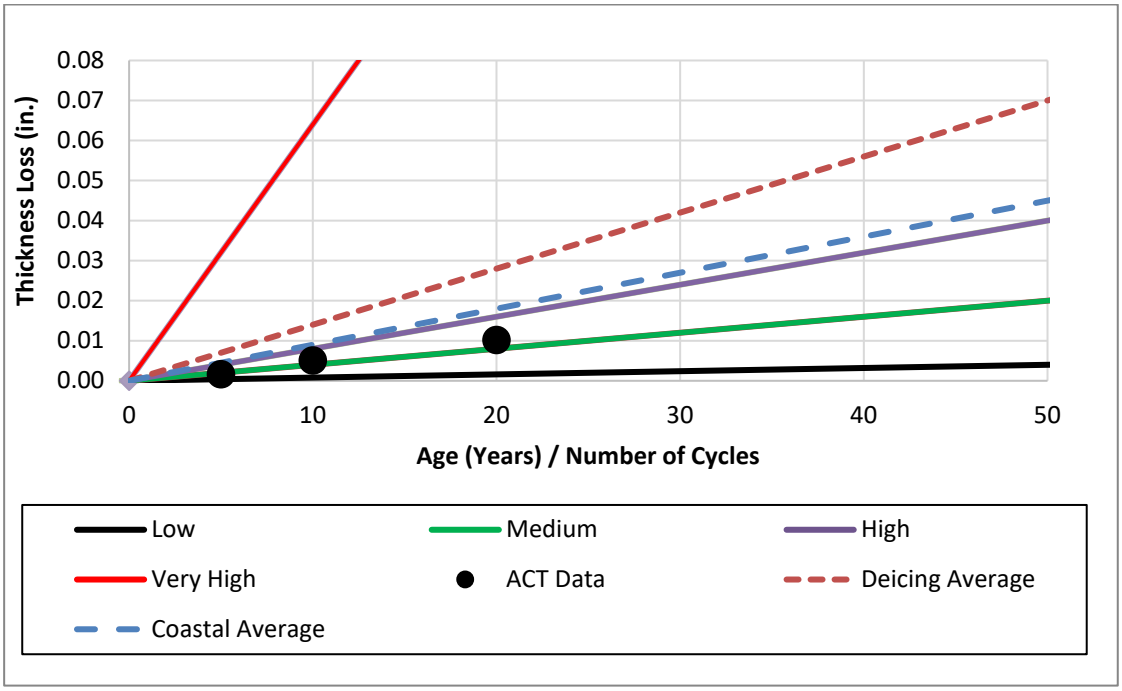

Figure 3-14. Method 5 Weathering Steel Thickness Loss Compared to Albrecht et al. Corrosivity Categories and Field Data

3.1.3.2 Rate of Loss Versus Time

All methods resulted in mass loss curves close to linear, but Methods 1, 3, and 5 had mass loss curves with R^2 values closest to 1 (0.987, 0.990, and 0.998 respectively), indicating that these mass loss versus time trends best fit a linear trendline and indicating an improvement over the standard method. But Method 5 displayed the desired decrease in corrosion rate with time, indicating laboratory results that best match field results. This was particularly encouraging considering that 20 cycles had been executed up to this point. There was confidence that the corrosion rate would continue to decrease as additional cycles are performed because of the XRD results discussed in the following section.

3.1.3.3 XRD Ranges

Evaluating Method 5 based on XRD benchmarks (Table 3-4), the XRD results of the UWS matched the ranges of deicing and coastal XRD percentages for goethite, hematite, ferrihydrite, ferric sulfate, and schwermanite. The results were also encouraging for the other three primary iron compounds. Specifically, the corrosion mechanism of UWS is such that lepidocrocite is typically one of the first iron compounds to form. This compound then often converts to goethite and / or akageneite. Thus, it is expected that as the testing is carried forward, the percentage of lepidocrocite will decrease and the percentages of goethite and / or akageneite will increase. This gives reason to believe that all three of these compounds will be within the target range once sufficient cycles have been performed to simulate the age of the bridges from which the field samples were taken. The only remaining compound is maghemite/magnetite. Not only are these compounds only 2% away from the target range, but they also form in similar environments as akageneite (Fletcher, 2011), and the laboratory measured percentage was within the range of the field akageneite values.

3.1.3.4 Thickness Loss

The Method 5 thickness loss values are plotted along with the corrosivity categories and prior field work results in Figure 3-14. In this figure, one cycle of laboratory testing equals one year of real-world corrosion. This assumption, however, can always be scaled to target different metrics. Based on this assumption, the Method 5 UWS thickness loss falls slightly within the "high" corrosivity category, which matches a relatively severe, but not extreme, environment, which is consistent with the goals of this research. Thus, the benchmarking goals for this metric were also deemed to have been satisfied.

3.1.4 Conclusion

Five methods further modifying the standard method were tested in an attempt to better match field test results. The results were evaluated based on three metrics: the rate of mass loss versus time, percentages of different iron oxides in the rust layer as determined from XRD analysis, and thickness loss values. Of the three, the greatest emphasis was placed on the shape of the mass loss curve as this is the area where prior laboratory testing is most unrealistic compared to field testing.

Most of the methods showed improvement upon the standard version of the test, but Method 5 was the only method to show a decrease in corrosion rate versus time, as desired. Method 5 consisted of reducing the salt bath concentration to 2% NaCl and increasing the temperature during the humid stage to 60°C. Method 5 XRD results also showed that the rust layer contained proportions of iron oxides that are a reasonable representation of those found in real world scenarios. This is important because it supports that the corrosion mechanism occurring in the accelerated corrosion testing is similar to field conditions, providing further confidence that corrosion rates versus time will also be grounded in reality. When compared to field data in terms of thickness loss, it was also shown that the Method 5 results have the

ability to be scaled such that both field data and existing thresholds of corrosivity categories can be not only simultaneously well represented, but well represented in a manner consistent with the philosophy of this work to represent relatively severe environments. For these reasons, the goal of creating a more realistic accelerated corrosion test to be used in further laboratory testing was best accomplished via Method 5, and Method 5 was thus selected as the environmental testing methodology to be used in later phases of this work.

3.2 Equipment and Materials

3.2.1 Specimens

The specimens used for the evaluation of Methods 1 – 5 were previously described in Section 3.1.2.1. The final phase of testing included specimens with those same dimensions and bolted and welded features but included more corrosion protection systems. The specimens used for the final phase of testing included twelve plate specimens, as shown in Figure 3-4a, each of galvanized, metallized, 1-coat IOZ paint, 3-coat OZ paint system, UWS, and, for a total of 60 flat plates. Additionally, there were three specimens of each corrosion protection system with the same dimensions as the flat plate but that had bolted and welded features (previously described in Section 3.1.2.1 and as shown in Figures 3-4b and 3-5) for a total of 15 plates with bolted and welded features.

Additional details regarding the corrosion protection systems can be found in Appendix A. The metallizing used was prescribed to be 12 mils thick of 85 zinc/15 aluminum coating, unsealed. Painted specimens did not include any stripe coating. All specimens were fabricated per typical best practices, with the exception of the metallized specimens, which did not have any edge preparation. Influences of this are discussed in sections where data from the metallized specimens is presented.

Appendix A also contains the material chemistry of all steel. It is noted that the coated specimens consisted of applying the coatings to plates that were dual certified as meeting the requirements for both Grade 50 and Grade 50W (per the typical practices of the fabricator). Given that the coatings were evaluated in terms of percent coating loss and percent rusting, it is expected that the weathering properties of the substrate material of the coating specimens would have a negligible to minor effect.

3.2.2 Humid and Dry Phase Equipment and Materials

3.2.2.1 Environmental Chamber

A Tenney C-EVO Temperature/Humidity Test Chamber, shown in Figure 3-15, was used to perform the accelerated corrosion testing. The environmental chamber has interior dimensions of 24” wide x 26” deep x 28” high. 7 racks were used to hold the specimens inside of the chamber, each of which were 24.5” x 23” x ¼” spaced at 3.5” on-center with a Heresite coating to prevent corrosion of the racks themselves. The chamber requires 230 V of power for operation. The environmental chamber is programmable such that the temperature and humidity can be controlled. The temperature of the chamber can range from -68°C to 180°C and is specified to be able to hold temperature within a ±1°C tolerance. The humidity can range from 20% RH to 95% RH when the chamber is within 20 to 85°C and is specified to be able to hold humidity within a ±5% RH tolerance. The upper bound limit of 95% RH for the humidity capabilities caused the humid stage of the test to be modified to 95% RH instead of 100% RH for this experiment as called for in the SAE J2334 and Fletcher et al. testing protocols.

Figure 3-15. Tenney Environmental Chamber

The water that is deposited into the environmental chamber must be free of corrosive materials and must have a conductivity between 10 and 20 µS/cm according to the environmental chamber's specifications. Water does not naturally occur between 10 and 20 µS/cm. Therefore, the appropriate water had to be created. Deionized water plumbed into the available laboratory facilities had a conductivity of about 2 µS/cm. To increase the conductivity of this water, sodium bicarbonate was added. Sodium bicarbonate was chosen as it is not corrosive to metals. A very small amount of sodium bicarbonate is able to quickly change the conductivity of water. Since there was a range of acceptable conductivity values, a guess and test method was used to create the appropriate water. A small amount of sodium bicarbonate, around 0.25 g, was dissolved into deionized water, and that solution was then incrementally added to the larger quantity of deionized water. The mixture was stirred, and the conductivity was measured. If the conductivity was acceptable, it was added to the environmental chamber. If not, the solution was modified by either adding more deionized water or adding more of the sodium bicarbonate solution until the conductivity was within the acceptable range.

The back of the environmental chamber contained a brass reservoir, which transported water from the filling bottle where the water is input by the user to the vaporizer where that water is turned to vapor. The brass reservoir controlled the water level and water flow through a bobber system. The procedures for maintaining the water level and bobber function are described in Section 3.3.3.

3.2.2.2 Water Filter

The environmental chamber recycles the water used within the system. Because of this process, a water filter was added to ensure all recycled water was pure and free of corrosive materials, particularly due to the presence of chlorides on the specimens that may be transferred through the system due to the humid environment. The 3M Under Sink water filter, shown in Figure 3-18, was used. This filter is designed to filter out chlorine products. The filter is 9 ¾" tall with a diameter of 2 ¼". The filter was connected to inlet and outlet tubes with an outer diameter of ¼". The filter has a capacity of 750 gallons and a service flow of 0.75 gpm. This water filter is advised to be replaced after six months of household use or whenever any problems occur. The water filter was first replaced when sediment appeared in the brass reservoir of the chamber, where water flows through to the vaporizer. This occurred after approximately 6 months of use, meaning that the six-month replacement recommendation was deemed to be generally applicable to laboratory use. After that, it was replaced every six months, as directed.

Figure 3-16. Water Filter

3.2.2.3 Painter's Plastic

During accelerated corrosion testing, the test specimens undergo wetting. The specimens become wet during the humid stage when there is 95% relative humidity in the environmental chamber as well as when they are soaked in the saltwater solution during the salt application stage. To prevent the wetted specimen on higher racks from dripping onto other specimen on a rack below them in the environmental chamber, strips of painter's plastic were attached to the bottom of the environmental chamber racks as seen in Figure 3-16. The painter's plastic was attached using zip ties and was attached in strips with one strip per row of specimen to maintain airflow within the chamber. Each strip was slightly larger than the width of the test specimen and ran the entire length of the rack to ensure the strip would effectively catch dripping water.

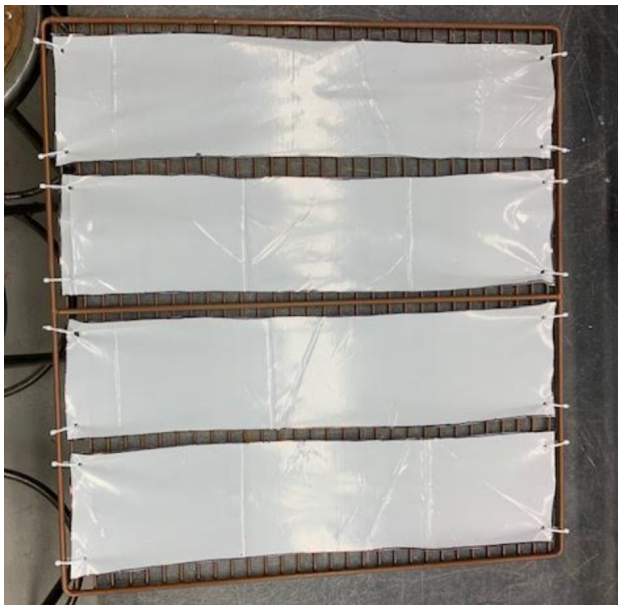

Figure 3-17. Painter's Plastic Under Racks

3.2.2.4 Nylon Spacers

The plates with bolted and welded features were such that the protrusions of the features on either side of the plate were not uniform across the surfaces, meaning that those plates would have been resting at an angle if placed directly on the racks. To avoid any unequal pooling of water that could occur, 3/8"-thick nylon spacers, equal to the thickness of the bolt heads, were placed under the bolted specimen on the side without the bolt heads, shown in Figure 3-17. With the addition of the spacers, the bolted specimens were able to lay flat on the racks in the environmental chamber (minus the deflection of the shelf due to the weight of the specimens).

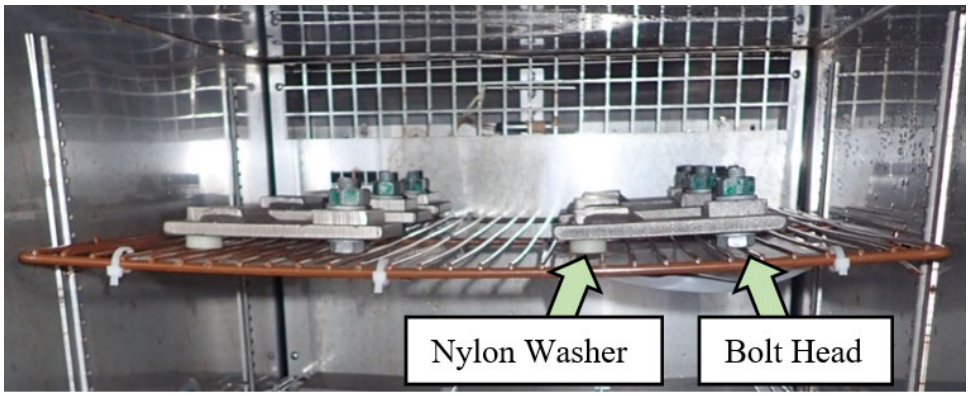

Figure 3-18. Plates with Bolted and Welded Features on Nylon Spacers

3.2.3 Salt Bath Materials

3.2.3.1 Salt Bath Containers

Four total containers were used during testing for the salt application stage. Two 27-gallon and two 55-gallon plastic "Tough Storage Bins" from Home Depot were used. For Methods 1, 2, 4, and 5, one container of each size was used. The small container was filled with 50 L of water and was used to submerge the bolted specimens, while the large container was filled with 100 L of water and was used to submerge the non-bolted specimens. For Method 3, the remaining containers were used similarly to accommodate the rinse water bath. The final phase of testing using all corrosion protection systems required all four containers as salt baths to accommodate the increased number of specimens. Once the appropriate amount of water for each container was initially measured and added to the containers, the water level was marked using duct tape for ease of measuring water quantities for future bath replacements. The containers were closed whenever they were not actively being used for a salt bath rinse to avoid evaporation and contamination from airborne debris in the adjacent laboratory areas or other accidental sources of contamination.

Figure 3-19. Salt Bath Container

3.2.3.2 Water

All water used was Type IV water as defined by ASTM D1193-06 (ASTM 2018). This water is classified as deionized water with a pH between 5 and 8 and a maximum conductivity of 5 μS/cm. This includes both the water used for the salt baths and the water that was mixed with sodium bicarbonate to be added to the environmental chamber. The pH and conductivity of the salt baths throughout testing can be found in Appendix D.

3.2.3.3 Salt

The salt added to the salt bath containers was rock salt as would be used to melt driveway snow or ice, shown in Figure 3-20. According to the accompanied safety data sheet (SDS), the rock salt used contains >99% sodium chloride by weight. No additional chemical substances were listed, although it was noted that this product may contain small quantities of naturally occurring calcium and magnesium salts. The mass quantities of salt used for each phase of testing can be found in Appendix B, Table B-1.

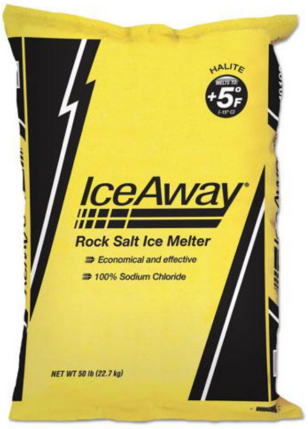

Figure 3-20. Rock Salt

3.2.3.4 Specimen Holders

During the daily testing cycles, the test specimens were soaked in the salt bath containers (described above in Section 3.2.3.1) containing the salt and water solution during the salt application stage. To allow for exposure of as much surface area of the specimens to the solution as possible and limit direct contact between the test specimens and the containers and between each other, polyvinyl chloride (PVC) specimen holders were created to hold the test specimen during the salt application stage. The large containers were used for the plate specimens, while the small containers were used for the plates with bolted and welded features. The PVC was first cut into lengths equal to the interior length of each container (39” pieces for the large containers and 23” pieces for the small containers) using a circular saw. Then, the PVC was cut in half lengthwise using a table saw to allow the specimen holders to lay flat in the containers. Finally, slits were created using the circular saw to hold the test specimen. All slots were made to be 1/8” wider than the specimens they were to hold. The slots were ½” wide x 1” deep for the 39”-long PVC pipe sections with 12 slots spaced at 3” on-center to accommodate the plate specimens, while the slots were 7/8”

wide x 1” deep for the 23”-long PVC pipe section with 3 slots spaced at 5.75” on-center to accommodate the plates with bolted and welded features. The spacings were chosen such that all spacings were equal throughout a given PVC holder for ease of cutting, resulting in the large PVC holder with 12 slots (designed to hold all 12 flat plates of a given corrosion protection system) and the small PVC holder with only 3 slots (designed to hold all the plates with bolted and welded features of a given corrosion protection system) having different spacings between the slots. The finished products are shown in Figure 3-21.

(a) (b)

Figure 3-21. PVC Specimen Holders Installed in the (a) Large (39”) Container and (b) Small (23”) Container

3.2.3.5 pH and Conductivity Meters

Oakton pH and conductivity meters, shown in Figure 3-22, were used to take pH and conductivity readings of the salt bath solutions daily. The conductivity meter

was also used to create the correct water conductivity for the water that was added to the environmental chamber, as described in Section 3.2.2.1. The pH meter can take pH readings on the full range of pH values from 0 to 14 with accuracy of 0.01. The conductivity meter can take readings from 0 to 200 milli-Siemens/centimeter. Readings can be taken in either micro-Siemens/centimeter (accurate to 0.01) or in milli-Siemens/centimeter (accurate to 0.1). The pH and conductivity readings throughout testing can be found in Appendix D.

Figure 3-22. pH (left) and Conductivity (right) Meters

3.2.4 Post Processing Equipment and Materials

3.2.4.1 Temperature- and Humidity-Controlled Room

A temperature-controlled room was used to store specimens when they were not in use. The temperature of this room was set to 70° F (21° C) and 50% relative humidity. This room was used to prevent the specimens from exposure to corrosion-causing conditions when not going through laboratory testing in the environmental chamber, both before and after testing, or otherwise being actively post processed.

3.2.4.2 Camera

An Olympus “Tough” camera, shown in Figure 3-23, was used to take pictures throughout the laboratory testing, which were later used for post processing. The camera has an effective 12 megapixel (4000 x 3000) sensor resolution and an aspect ratio of 4:3. The lens has a focal length of 4.5 to 18 millimeters and a 2x digital zoom. The focus range is 3.94”. The camera also has built-in flash that can be manually or automatically selected. Images were saved to a 128 GB memory card in the form of JPEG images, which were then transferred to the computer using a USB connector.

Figure 3-23 Olympus “Tough” Camera

3.2.4.3 Measurement Tools

Before and after testing, all specimens were massed and dimensionally measured. The mass was taken in grams using a Vibra digital mass balance that can take mass readings to the nearest hundredth of a gram. The dimensional measurements were taken using Mitutoyo digital calipers that can take readings to the millionths of an inch. This equipment is shown below in Figure 3-24.

Figure 3-24. Mass Balance (top) and Calipers (bottom)

3.2.4.4 Scraping Tools

Samples of the rust layer formed on the surface of the UWS specimens were collected for XRD analysis. This process required the use of a putty knife for scraping the rust, a paintbrush for sweeping the rust into a bag, and a Ziplock bag for collecting the scraped samples. These items are shown below in Figure 3-25. The bags of the samples were then labeled using a permanent marker.

Figure 3-25. Ziplock Bag, Putty Knife, Paintbrush, and Marker Used for Collecting and Labeling Corrosion Products Scraped from Specimens

3.2.4.5 XRD

The Bruker D8 X-ray Diffractometer (with a CuKα X-ray source), shown in Figure 3-26, was used for XRD analysis of the scraped samples described in Section 3.2.4.4, above. It is located in the Advanced Materials Characterization Laboratory at the University of Delaware. XRD is used to identify unknown crystalline materials, which in this case were iron-oxide minerals.

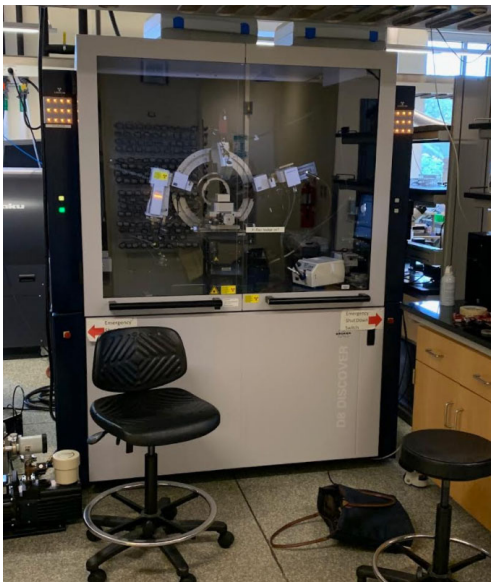

Figure 3-26. Bruker D8 X-ray Diffractometer

3.2.4.6 Blasting Equipment and Media

The Harbor Freight Benchtop Blast Cabinet, shown in Figure 3-27, was used to remove rust from the corroded specimens. The cabinet is 28” H x 18” L x 26” W. The blast cabinet came with a blast gun containing a ceramic nozzle with a 0.18” opening. The blast gun was connected to an air compressor through a 3/8” supply hose with a quick coupler. The blast gun was also connected to a siphon hose that was attached to a siphon tube which was used to transfer the abrasive from the hopper to the gun. The cabinet also came with 14” rubber gloves to protect the user’s hands and arms while working.

U.S. Minerals GRBG50 garnet abrasive was selected as the abrasive for us in the blast cabinet. This abrasive was chosen because of its hardness value of 7.5 Mohs on the Mohs scale of mineral hardness, which is relatively hard, and for the fact that the garnet is chemically inert and will not interact with the iron compounds on the specimens. The garnet has a mesh size between 80 and 90. Since the blast cabinet is a mostly closed system, the abrasive was recycled and reused throughout the blasting

process. Some abrasive escaped the chamber during the process, and additional abrasive was added as necessary.

Figure 3-27. Blast Cabinet

3.2.4.7 Galvanizing and Metallizing Cleaning Equipment and Materials

The first attempted method of cleaning the galvanized and metallized specimens was based on ASTM G1-03, Table A1.1, Designation C.9.1 (ASTM 2017), which provides procedures for cleaning zinc and zinc alloy materials (such as galvanized and metallized steel). This procedure dictates using 100 g of ammonium persulfate ($(NH_4)_2S_2O_8$) with reagent water to make 1000 mL. This procedure was used on all of the metallized and galvanized flat plate specimens removed after 10, 20, and 40 cycles using 200 g of ammonium persulfate with reagent water to make 2000 mL. However, after trial of this procedure, the specimens were not fully cleaned. As the materials for this cleaning procedure were expensive and hazardous, a different cleaning procedure was resultantly adopted.

The adopted cleaning process for galvanized and metallized specimens required the use of an ultrasonic cleaner with an Evapo-rust solution, both of which

are shown in Figure 3-28. The ultrasonic cleaner used was the Central Machinery ultrasonic cleaner from Harbor Freight, which has a volume of 2.5 L and interior dimensions large enough to accommodate one specimen at a time. This cleaner includes a digital timer with preset cycle durations of 90, 180, 280, 380, and 480 seconds that can be selected. The cleaner can work with or without heat features, which were not used for this cleaning procedure. It requires 160 watts of power to function. The cleaning process was time-consuming for cleaning 30 specimens (15 galvanized and 15 metallized), so 4 ultrasonic cleaners were used at the same time, each containing one specimen at a time, to speed up the overall cleaning process.

The cleaner was filled with a rust-removal solution, Evapo-rust, to remove the corrosion products from the specimens. Evapo-rust is safe on all surfaces, is non-toxic, and contains no acids or alkalis and was selected based on its prior successful use in work done by the American Galvanizers Association (Langill, personal communication, 2021). The directions for use suggest use at ≥ 65° F. The Evapo-rust solution was poured to a level at which the entire specimen was submerged in the solution while in the ultrasonic cleaner and the level of solution was between the minimum and maximum fill lines indicated in the ultrasonic cleaner. The Evapo-rust was replaced at the termination of a cleaning for a given specimen or at the end of a day in the lab (so that the ultrasonic cleaners could be stored dry, as recommended). In total, 20 gallons of Evapo-rust were used to clean the 30 specimens.

Figure 3-28. Ultrasonic Cleaner and Evapo-Rust Solution

3.3 Procedures

3.3.1 Preparation Procedures

3.3.1.1 Specimen Preparation

Before testing began, the specimens were cleaned, massed, and dimensionally measured. The fabrication process of steel can leave a greasy residue or other contaminants on the specimens. The grease was removed using 70% isopropyl alcohol and Wypall lab wipes. The specimens were doused and wiped until no black residue appeared on the lab wipes when wiping down the specimens. Once the specimens were properly cleaned and allowed to air dry, their masses were recorded using a mass balance. Finally, thickness measurements were taken of each specimen with accuracy to the thousandths of an inch using calipers. The locations for the thickness measurements are shown in Fig. 4-29 below. The specimens were placed in the temperature- and humidity-controlled room after preparation until testing in the

environmental chamber began to prevent any corrosion from occurring before the testing began.

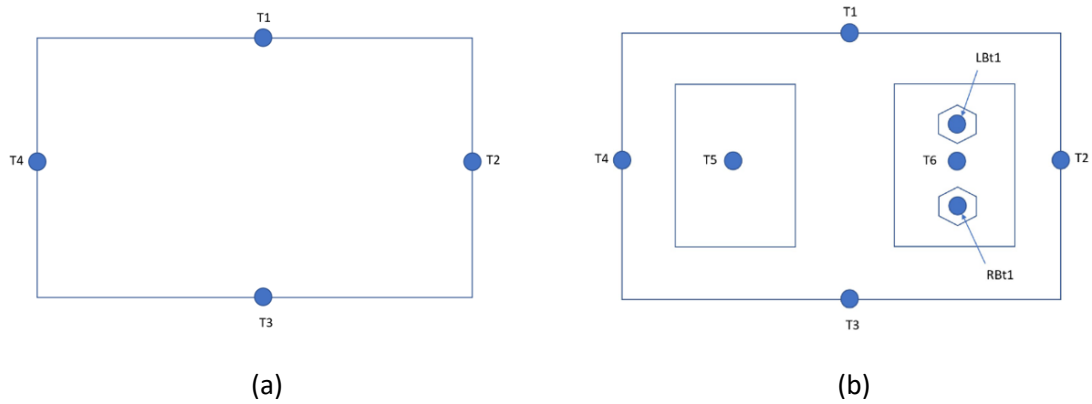

Figure 3-29. (a) Locations of Thickness Measurements for Plate Specimens (b) Locations of Thickness Measurements for Specimens with Bolted and Welded Features

3.3.2 Programming the Environmental Chamber

The chamber controls the temperature and humidity through its programming. For the final phase (and Method 5) testing protocol, the humid stage of 60° C and 95% relative humidity was 6 hours long, and the dry stage of 60° C and 50% relative humidity was 17 hours and 45 minutes. The remaining 15 minutes were the salt application stage, during which the specimens are not in the environmental chamber, but during this time the chamber transitioned to the dry stage settings. These 24-hour cycles ran daily on the weekdays, and on days when the researcher is unable to be present in the laboratory (some weekends, holidays, etc.), the environmental chamber is set to the dry stage settings of 60° C and 50% relative humidity. These temperatures and humidities were achieved using the "setpoint" and "soak" steps within the environmental chamber's programming.

The setpoint specifies the temperature and humidity the environmental chamber should target. Within the setpoint feature, there is a ramp feature where the transition time between phases is specified. The ramp time chosen to transition from the dry stage to the humid stage was 20 minutes based on the work by Groshek (2017). The ramp time chosen for the transition from the humid stage to the dry stage was 50 minutes, as this time accounts for the 15-minute salt application stage and allows for another 15-minute period for the researcher to transition the specimens from the salt baths back into the chamber before ensuring that the chamber is allowed a minimum 20-minute period to ramp up. The soak step holds a given temperature and humidity in the environmental chamber. The exact programming for each method can be found in Appendix C in Tables C-1 – C-3.

3.3.3 Humid and Dry Phase Procedures - Environmental Chamber Maintenance

Daily maintenance operations were performed for best use. Daily, the chamber was wiped down with a dry lab towel while the specimens were soaking in the salt or rinse water bath to remove extra moisture and any salt or rust particles that might be left behind in the chamber. Additionally, the water for the chamber was topped off as needed using water within the specified conductivity range. The brass reservoir in the back side of the chamber was also monitored to assure that the correct water level was maintained to allow sufficient creation of water vapor and therefore humidity. Finally, the temperature and humidity were monitored by transferring the data via USB intermittently to assure proper functioning of the environmental chamber.

3.3.4 Salt Bath Procedures

3.3.4.1 Salt Application

The salt application stage requires a NaCl (saltwater) solution for the specimen to soak in for 15 minutes during the daily cycles. This solution was prepared and replaced after every 5 cycles as called for from the SAE J2334 testing protocol (SAE 2016). The volume of water used was chosen such that all bins contained enough water to have a water level higher than the specimens when they were soaked in the bin, allowing for full submersion of the specimens. The large containers contained a mixture of 100 L of deionized water and the corresponding amount of rock salt to achieve the desired concentration, which was 2% NaCl for Method 5 and was achieved by adding 2,000 grams of NaCl. The small containers contained a mixture of 50 L of deionized water and the corresponding amount of rock salt to achieve the desired concentration, which was 2% NaCl for Method 5 and was achieved by adding 1,000 grams of NaCl. The amounts of NaCl used can be found in Appendix B, Table B-1. The mixture was stirred using a paint stirrer attached to a drill. A photo of specimens undergoing the salt application phase is shown in Figure 3-30.

The pH and conductivity of the salt bath was measured daily immediately after the soak. pH is affected by chemicals, and a change in pH can indicate a solution that is chemically changing. Typically, an increase in pH decreases the rate of corrosion. This reading was monitored for any noticeable or extreme changes. Conductivity measures water's ability to conduct electricity. This value increases with ions such as sodium. This value was measured to ensure consistency in the salinity level. The full dataset of pH and conductivity readings from laboratory testing can be found in Appendix D. Variations in salt concentrations in the salt baths explain the variations in pH and conductivity ranges from method to method. The pH and conductivity

remained relatively similar between methods with the same salt bath concentrations (Methods 1, 5, and final phase testing; Methods 2 and 3).

(a) (b)

Figure 3-30. Salt Baths (a) Large Container (Plate Specimens) (b) Small Container (Specimens with Bolted and Welded Features)

3.3.5 Rinse Application (Method 3 Only)

The rinse water bath was used for Method 3 (during the methodology development only; not the final testing). The concentrations of NaCl, $NaNO_3$, Na_2SO_4, and $NaHCO_3$ added to the baths were determined using the results of the ion chromatography and gran titration tests as discussed in Section 3.1.2.5. These salts were added to achieve the targeted ion concentrations. The amounts of each salt added to the containers along with the details of the calculations for determination of those quantities can be found in Appendix B, Tables B-2 and B-3.

The corresponding amounts of these salts were added and mixed using a paint stirrer attached to a drill. The pH is important to the rate of chemical reaction, so the pH was tested daily before the test and adjusted to be within +/-0.5 of the target 6.67 pH, hovering around a neutral pH, before the rinse bath soak. The adjustment was made through the addition of 5 M HCl diluted in deionized water using a guess and test method until the appropriate pH was achieved. A few drops of the 5M HCl solution were added at a time. The 5 M HCl solution was then mixed with the chemical bath made to simulate the rinse water. This process was done almost daily on days when the specimens were placed in the rinse baths.

3.3.6 Post-Processing Procedures

3.3.6.1 Specimen Removal

To assess the loss due to corrosion, three plate specimens of each corrosion protection system were removed from the environmental chamber after pre-determined numbers of cycles. For Methods 1-5, three UWS and three carbon steel specimens were removed after 5 cycles, then three more of each were removed after 10 cycles, then three more of each were removed again after 20 cycles, and finally the remaining specimens were removed at some point after 20 cycles. All plates with bolted and welded features were left in the chamber for the full duration of the test and were only removed at the end of the test. For the final phase of testing using all corrosion protection systems, three flat plate specimens of each corrosion protection system were removed after 10, 20, 40, and 80 cycles. Again, all plates with bolted and welded features were left in the chamber for the full duration of the test and were removed at 80 cycles.

3.3.6.2 Scrape Samples

UWS specimens were scraped using a putty knife after being removed from the environmental chamber. The resulting rust was collected in a plastic bag and stored in a temperature- and humidity-controlled room for later XRD analysis. The purpose of the XRD analysis was to evaluate the composition of iron oxides composing the rust to determine whether or not the corrosion mechanism matches that of field bridges in relatively severe environments.

3.3.6.3 Cleaning Specimens

3.3.6.3.1 UWS Specimens Cleaning through Sandblasting

The UWS steel specimens were sandblasted after being removed from the environmental chamber to remove corrosion as specified by ASTM G1-01, Section 7.4 (ASTM 2017). The specimens were placed in the blast cabinet and were blasted with the blast media. The end of blasting was determined by visual inspection when no more rust was visible and the steel specimen was a white metal, as defined by SSPC SP5 in NACE No. 1. A visual representation of this process is shown in Figure 3-31.

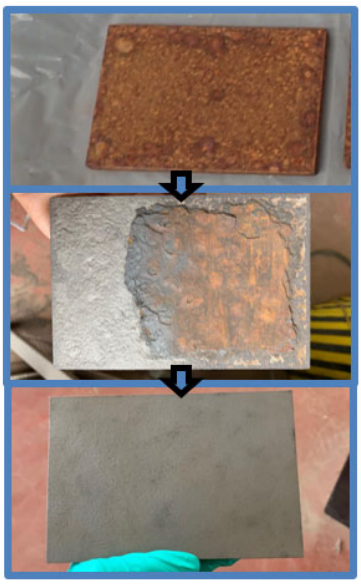

Figure 3-31. UWS Sandblasting Process: Starting Condition (top); Intermediate Condition (middle); Finished Condition (bottom)

3.3.6.3.2 Galvanized and Metallized Specimen Cleaning through Ultrasonic Cleaning

The galvanized and metallized specimens were cleaned in an ultrasonic cleaner using Evapo-rust. Photos from the cleaning process of a metallized specimen are shown in Figure 3-32. The completion point of cleaning was determined using the processes defined in ASTM G1-01 (ASTM 2017), Section 7.1.2.2, where the mass loss at equal cleaning cycles is plotted. Figure 3-33 shows sample data from this process, which shows a point, labelled “B”, where the mass loss rate decreases with increased cleaning. This point is taken as the final weight after cleaning.

All graphs of cleaning data used to determine the mass loss for galvanized and metallized specimens can be found in Appendix E. The specimens labeled “GX” or “MX” indicate either a galvanized or metallized flat plate, respectively, where X is a numerical label. A “GB-X” or “MB-X” label indicates a galvanized or metallized plate with bolted and welded features, respectively. From these, the data is divided into two

linear curve fits, as done in the ASTM G1-01 methodology. However, this standard does not specify quantified metrics for determining the transition point between the two lines. In many cases, there is no need to do this, as the transition is visually obvious. However, some cases are more ambiguous. Thus, to ensure consistency in the data analysis approach, the following criteria were developed for data interpretation of the mass loss versus cleaning cycle data: 1) the specimen is visibly free of corrosion products, 2) the final mass of the specimen is less than its initial mass, 3) the R^2 values of the trendlines are both ≥ 0.9, 4) there are at least two datapoints in line "BC," and 5) the x-value of the intersection, point "B," is greater than the x-value of the last datapoint included in line "AB" and less than the x-value of the first datapoint included in line "BC."

Separate criteria were established for specimens where two distinguishable slopes were not present, which occurred for specimen M9 even after more than 50 cleaning cycles and may occur in future cleaned specimens. These criteria were: 1) the specimen is visibly free of corrosion products, 2) the final mass of the specimen is less than its initial mass, and 3) the addition of three consecutive cleaning datapoints each respectively caused the slope of the line (calculated as the slope of a given data point relative to the first cleaning datapoint) to change by <2%. The point of completion, taken to be the final weight, in cases where these criteria were implemented was taken as the first of those three datapoints causing a <2% change to the slope of the line.

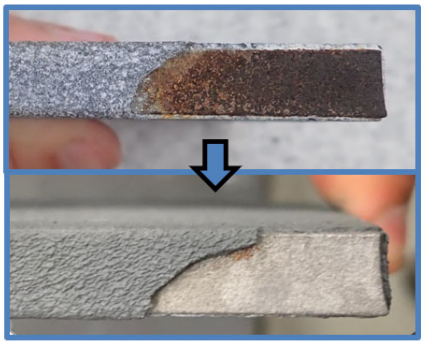

Figure 3-32. Metallized Specimen Before (top) and After (bottom) Ultrasonic Cleaning

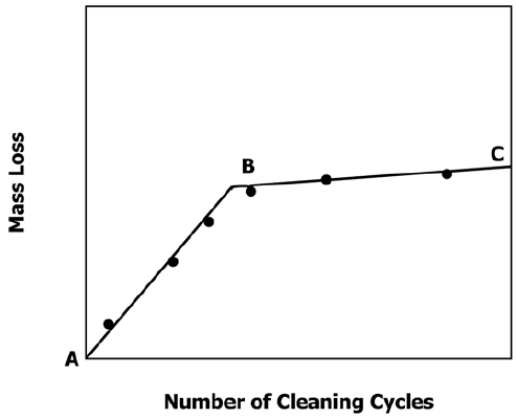

Figure 3-33. Mass Loss of Corroded Specimens Resulting from Repeated Cleaning Cycles (ASTM 2017)

Even though the specimens removed from testing at 10, 20, and 40 cycles were first cleaned using the ammonium persulfate procedure described in Section 3.2.4.7, cleaning cycle 1 in the graphs in Appendix E for these specimens indicates the cycle at which the ultrasonic cleaning procedure began. This is for consistency across all specimens and because only one cycle of the ammonium persulfate solution resulted in minimal removal of corrosion products. Some additional datapoints have been excluded from the beginning cycles of cleaning, as the slope began increasing. An

example of this trend that led to some initial datapoints being excluded for the cleaning analysis is shown in Figure 3-34 for specimen M2 (removed after 80 cycles). The increase in slope begins at cleaning cycle 7 in this example. This difference in slope may be due to replacement of the Evapo-rust solution if a specimen was cleaned over the course of multiple days. Datapoints were also removed from the initial cleaning cycles of specimens M5 and GB-1, as there was a drastic slope magnitude change that occurred in the cleaning data for these specimens. The slope of the datapoints that were removed from this cleaning data were about double the slope of the remainder of the "AB" line. Additionally, specimen G12 is missing a datapoint for cleaning cycle 2. This is because that was the first specimen cleaned, and an hour cleaning cycle was used for the first clean. After this, a half hour cleaning cycle was implemented for better insight into the cleaning process. For that reason, the G12 hour-long cleaning cycle is represented by using one datapoint over two cleaning cycles. Finally, the datapoint at cleaning cycle 21 of specimen M10 was removed because it had a smaller slope than the datapoints both before and after it, making it inconsistent with the rest of the datapoints in line "AB." This outlier, when included, led to a change in slope of line "AB" that made it impossible for the intersection point "B" to have an x-value that achieved the criteria outlined earlier in this section.

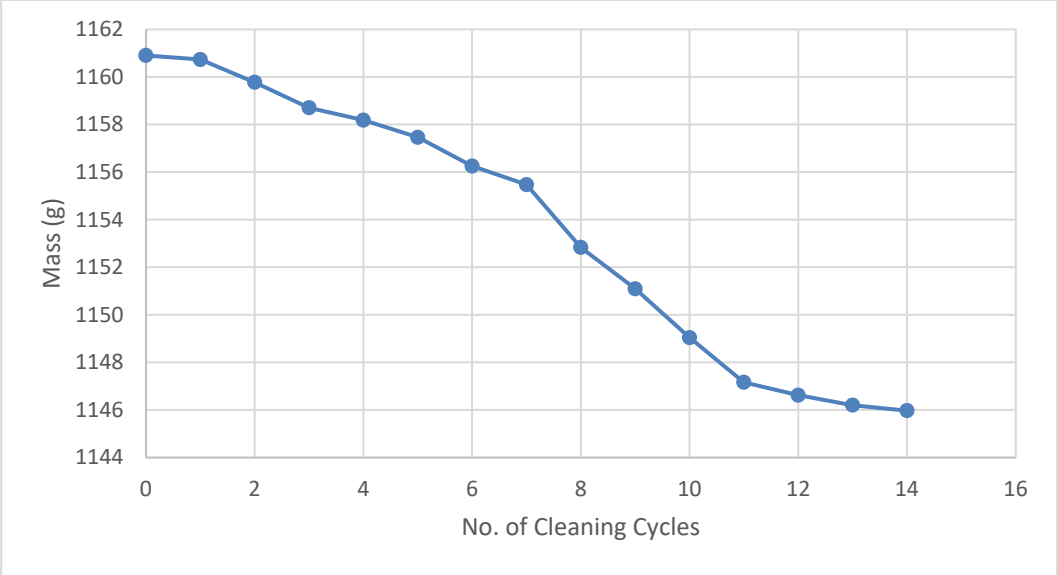

Figure 3-34. Cleaning Data for M2 (Removed After 80 Cycles) Showing an Unexpected Increase in Slope at Cycle 7, Leading to Earlier Cycles Being Excluded From Data Analysis

Mass loss of the metallized and galvanized specimens was further considered in terms of mass of coating loss and mass of steel loss. Since there was no exposed bare steel on the galvanized specimens, the mass loss of these specimens was determined to be coating loss, which was not visible to the eye. The metallized specimens, on the other hand, had visible coating loss. A value equating the mass of coating loss was determined through the use of MicroStation (Bentley 2021). Photos of all 6 sides of each metallized specimen were imported into MicroStation and appropriately scaled such that the dimensions of the specimen in the photo matched the real dimensions of the 4” x 6” x 3/8” specimens. Then, the areas where the coating was lost were traced, and those areas were calculated. This process is illustrated in Figure 3-35.

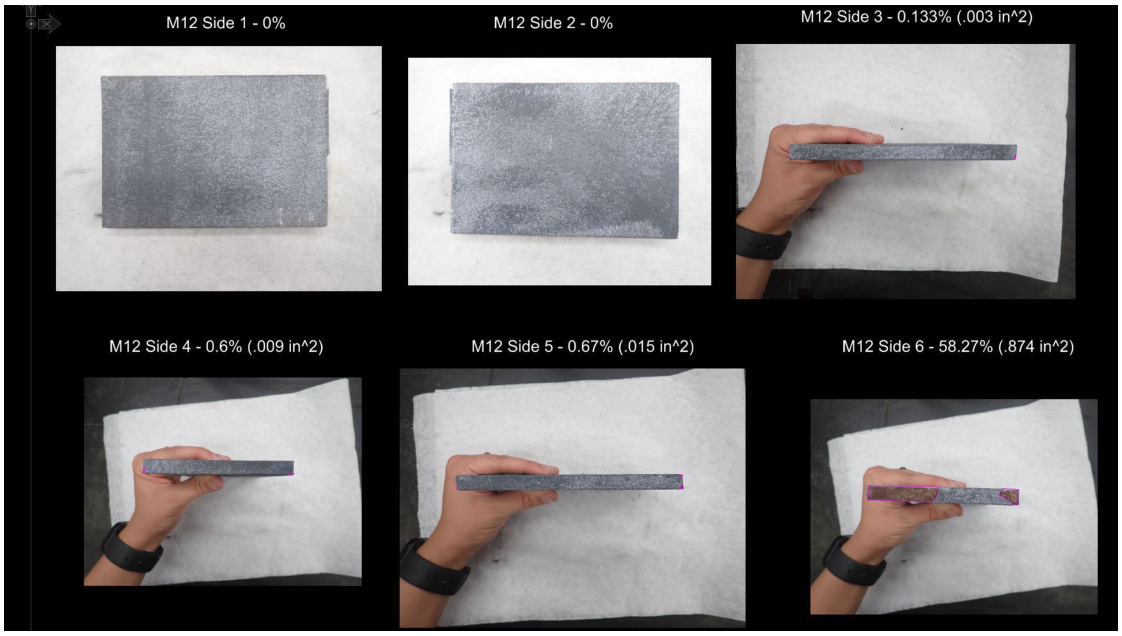

Figure 3-35. Process for Determining Metallized Coating Loss in MicroStation

During cleaning, a piece of coating fell off. From this piece, the mass per area in grams/in^2 was able to be calculated using a mass balance and MicroStation. It was found that the coating weighs 2.308 g/in^2. Using this area density and the total area of coating loss for each specimen calculated in MicroStation, the total mass of coating loss was able to be calculated. The coating loss value was used to determine how much of the overall mass loss was coating loss versus how much was bare steel loss. For the specimens removed after 80 cycles, the coating loss was not binary and instead occurred in multiple thickness layers. The MicroStation procedure described was attempted to estimate coating loss but overestimated the loss because some locations of loss were partial thickness loss of unknown thickness. Consequently, the estimated coating loss value turned out to be greater than the overall mass loss of the specimen. For that reason, the total mass loss values only were used for the 80 cycle specimens.

3.3.6.4 Re-measuring Specimens

The UWS, galvanized, and metallized specimens were weighed and dimensionally measured again after they were finished being cleaned and the rust was removed. The finalized measurements were taken in the same locations on the specimen as the initial measurements to be able to make direct comparisons of thickness. The goal was to determine how much of the base metal had been lost.

3.3.6.5 Paint Evaluation using Image Recognition Algorithms

The evaluation of the painted specimens was based on the standards set forth in ASTM D610-08: Standard Practice for Evaluating Degree of Rusting on Painted Steel Surfaces (ASTM 2019). ASTM D610-08 provides standard photos for 11 rust grades (listed in Table 3-5) along with the percent of rusting for each grade. Determining the percent surface rusted from a purely visual assessment is both subjective and difficult. So, after testing, photos were taken of the front and back of each painted specimen and were analyzed using image recognition algorithms.

3-5. Scale of Rust Ratings from ASTM D610-08 (ASTM 2019)

Rust Grade	Percent of Surface Rusted
10	Less than or equal to 0.01 percent
9	Greater than 0.01 percent and up to 0.03 percent
8	Greater than 0.03 percent and up to 0.1 percent
7	Greater than 0.1 percent and up to 0.3 percent
6	Greater than 0.3 percent and up to 1.0 percent
5	Greater than 1.0 percent and up to 3.0 percent
4	Greater than 3.0 percent and up to 10.0 percent
3	Greater than 10.0 percent and up to 16.0 percent
2	Greater than 16.0 percent and up to 33.0 percent
1	Greater than 33.0 percent and up to 50.0 percent
0	Greater than 50.0 percent

The first image recognition approach that was used was based on modifying an existing Matlab (MathWorks 2021) script from prior work that determined the size of rust particles on UWS. This script converts each pixel of an image to either black or white depending on a user-defined threshold (see Figure 3-36). For the painted specimens with minimal deterioration, thresholds were established that successfully segregated the pixels with coating loss into one group and the pixels with intact paint into a second group. The pixels representing coating loss were converted to black pixels and the remaining pixels were converted to white pixels. Then the percentage of the image with black pixels was calculated to determine the percent rusting of the specimens. The total percent of coating loss was calculated using the average of the two 4" x 6" surfaces. The evaluation found the coating loss of only the 4" x 6" surfaces, not the edge surfaces. From the evaluation of the data from the two 4" x 6" surfaces of the bolted and welded specimens, it was found that the side experiencing the maximum coating loss (generally the side facing up and having the projecting plates) on average exhibited 30% more coating loss than the average values reported herein. For the flat plate specimens, the side facing up was randomized; so, an average value for these specimens is the most informative value.

This Matlab script was validated by calculating the percent of rusting on the photos contained in ASTM D610-08. This binary process was found to work well on images that were in a binary state of either having rust or intact paint. These were the specimens subjected to 10 and 20 cycles of testing.

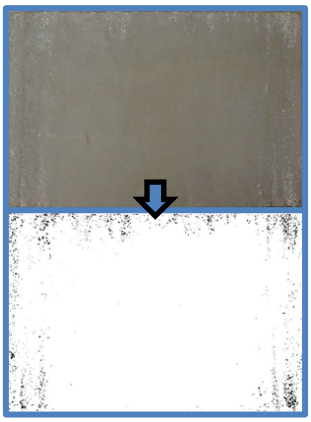

Figure 3-36. Painted Specimen Processed through Matlab Code: Photo of Specimen (top) and Corresponding Matlab Output (bottom)

Specimens that were subjected to 40 and 80 cycles of data often had a combination of intact paint, coating loss, and rusting. The binary Matlab script was not successful at consistently classifying the areas with coating loss into either category of intact paint or rusting. So, a more advanced image recognition algorithm was created in Python (2009) via Jupyter Notebook (Kluyver et al. 2016) using clustering techniques. Clustering is an unsupervised machine learning technique used to divide data into several groups. The k-means clustering method used in this report work to identify the damage in the painted steel specimens and distinguish between intact paint, coating loss, and rusting based on the colors of the specimen.

This analysis was based on the work done by Garbade (2018), Géron (2019), and Real Python (2019). Specifically, the K-means clustering algorithm from sklearn's cluster sub-package in "Python 3.7.10 Jupyter Notebook" was used to classify the colors of each pixel into similarly colored groups. The concept of this method is that the data within each group are more similar to one another than to data in other groups. The basic objective is to group the data so that the variation of the data within each cluster is minimized and between clusters is maximized. Mathematically, this is

achieved by minimizing the sum of the Euclidean distances between each data pair within a cluster, divided by the total amount of data in the cluster.

Figure 3-37 shows an example of the results of cluster analysis assuming three groups of data exist. In this two-dimensional example, each data point is described by two variables, which are plotted on x- and y-axes in Figure 3-37. The original data are shown in top left of Figure 3-37. Each data is randomly assigned to a cluster in the top center plot in Figure 3-37, where different groups are represented by different colors. In the top right of Figure 3-37, the cluster centroids are computed and shown as larger colored circles. Then, each datapoint is assigned to the nearest centroid, as shown in bottom left of Figure 3-37. Next, the cluster centroids are calculated again according to the new assignment in the bottom center graph of Figure 3-37. This process is repeated until the assignments of each datapoint no longer changes (as depicted by the bottom right plot in Figure 3-37), which means the within-cluster variation is minimized and the optimal solution has been reached.

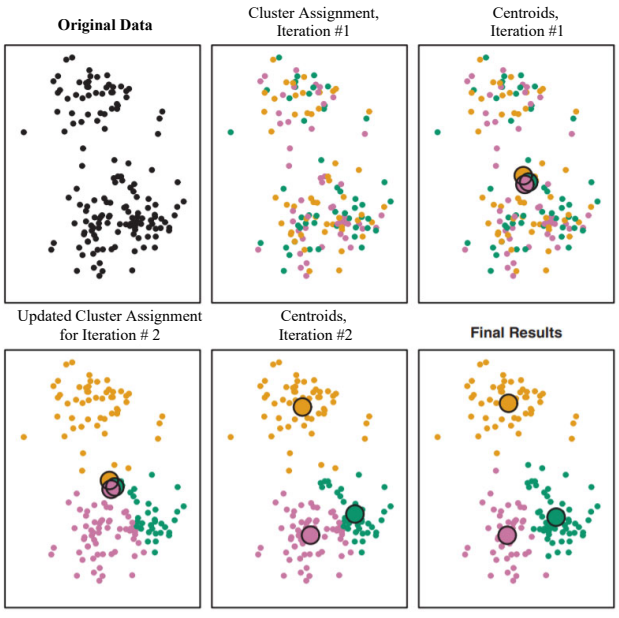

Figure 3-37. Example Clustering Analysis Results (James et al., 2017)

When applying the cluster method to the photographs of images, the algorithm starts with a random assignment of the color of each pixel to a group, then performs iterative analysis to optimize the assignment of each pixel to a group of similarly colored pixels. To identify the damage in the painted steel specimens the algorithm was used on several images separately to identify the colors that best represented the coating loss and rust. It was found that the image of Specimen 3PB-1 (shown in Figure 3-37) from the bolted group contained all of the dominant colors appearing in all of the specimens. Thus, the centroid colors (shown in Figure 3-38) were determined based on this image.

Each image was then segmented by clustering each pixel in the image based on the colors determined previously. Each pixel was then replaced by the mean color of its cluster. The difference between an original image and its segmented counterpart is shown in Figure 3-39. The percentage of each color per specimen was then calculated. The 10 colors output from the algorithm were then classified into three groups based on visual observation as follows (with reference to the color labels shown in Figure 3-38): colors 2, 6, and 8 were classified as rust; colors 4 and 9 were classified as coating loss, the remaining colors were classified as intact paint. The percentages of the pixels in these three groups were used to determine the percent paint loss and percent rust for each painted specimen.

Figure 3-37. Image of Specimen 3PB-1 in the Bolted Group

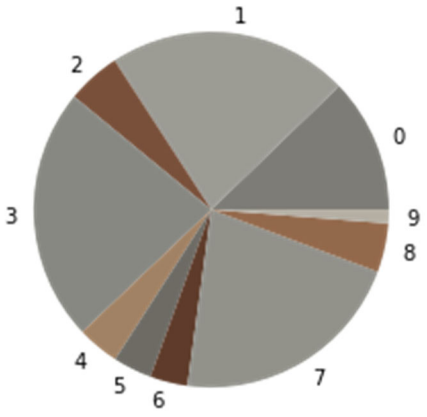

Figure 3-38. Pie Chart Representation of Colors from Photograph in Figure 3-37.

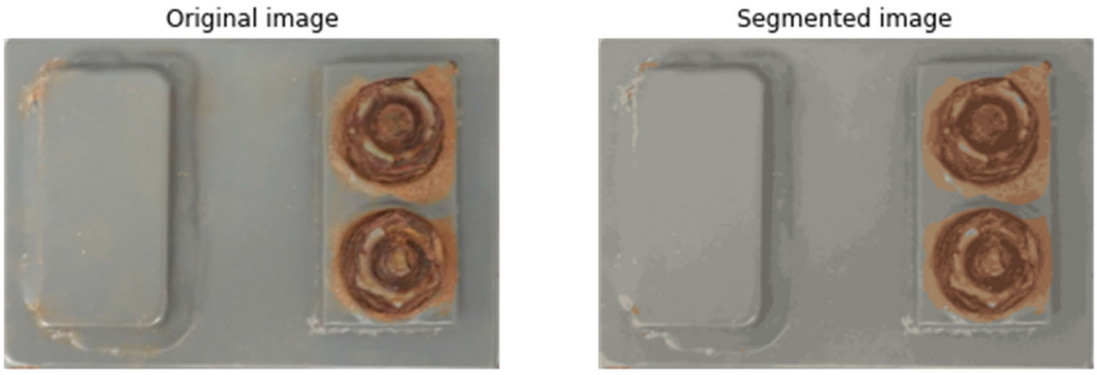

Figure 3-39. The Original Image (Left) and the Segmented Image with 10 Colors (Right)

3.3.6.6 XRD Analysis

The scrape samples described above in Section 3.3.6.2 were analyzed using XRD to determine the proportions of specific iron compounds comprising the outer layer of the UWS specimens after accelerated corrosion testing. Because specific iron compounds form in different environments, this data informs how well the accelerated corrosion testing mimics real-world conditions. In addition, different iron compounds provide different corrosion protection abilities. So, knowing the percentages of the specific iron compounds formed can also inform the extent to which a barrier protection layer is forming.

The scrape samples were first further ground into a powder consistency if not already powder-like using a mortar and pestle, as the Bruker XRD machine is for powder analysis. The sample was then placed on a slide and in line of the scanning beams. The X-ray was set to scan from 2Theta values of 5° to 75° at an increment of 0.05°. Each step was set to last 2 seconds. This scan was done continuously for at least 8 hours at a time. The purpose of the scan's long duration was to continuously scan over the same range to reduce the noise in the data.

Once the scan was finished, the remaining background noise was subtracted using DIFFRAC.EVA (Bruker 2021) software. The scan was then exported as a .xy file for analysis. The data was then analyzed using procedures from "Quantification of Suitable Environments for Unpainted Weathering Steel Bridges" (Bai 2022) to determine the percent composition of iron oxides. The iron oxides evaluated were lepidocrocite, goethite, akageneite, hematite, magnetite/maghemite, ferrihydrite, ferric sulfate, and schwermanite.

3.3.6.7 XRF Analysis

M11 and G11 were selected to be tested using XRF to confirm the chemical make up of the metalized and galvanized steel samples, respectively. A corner of each representative sample was cut in order to be analyzed. These corner pieces were then placed with the cross section face down in the XRF machine. This ensured that the chemical composition of the interior of the sample was determined. The XRF machine was then filled with Helium and the analysis performed. The results of said analysis can be seen in Tables A-4 and A-5, respectively.

Chapter 4

ACCELERATED CORROSION TESTING RESULTS

4.1 Introduction

This chapter contains the results from laboratory accelerated corrosion testing performed on galvanized, metallized, painted (1-coat IOZ and 3-coat OZ), and uncoated weathering steel in the laboratory using an environmental chamber and the methodology described in Section 3.3. Both qualitative and quantitative results are included, in Section 4.2 and 4.3, respectively. The qualitative results detail the change in appearance of the specimens throughout the cycling process, while the quantitative results detail mass loss of all specimens, XRD results from the UWS specimens, and thickness loss of UWS specimens. Mass loss is emphasized over thickness loss because mass loss represents the totality of the specimen. This is compared to the thickness of the specimens being a localized measurement that is spatially variable both before and after testing, leading to variation in results based on the location of thickness measurements. However, thickness loss is included for the UWS specimens due to the use of this data to establish a scaling relationship between these laboratory results and field performance in Section 4.4. In Section 4.5, longevity estimates are reported for each corrosion protection system in a relatively severe environment.

4.2 Qualitative Results

4.2.1 Overview

The specimens were inspected visually on a daily basis through the environmental chamber's viewing window and when the specimens were transferred between the environmental chamber and the salt baths for the salt application stage. A visual difference in the appearance of specimens over time was observed for all of the

corrosion protection systems. Figure 4-1 below shows the progression of the appearance of all specimens removed after 10 cycles, 20 cycles, and 80 cycles. The figure shows the corrosion protection systems in the order of galvanized, metallized, 1-coat IOZ paint, 3-coat IOZ paint system, and UWS from top to bottom of each image. Discussion of the observations from these photos is given in the subsequent sections. It is noted that all photos indicate visual condition at the conclusion of the accelerated corrosion testing and prior to any cleaning processes unless noted otherwise.

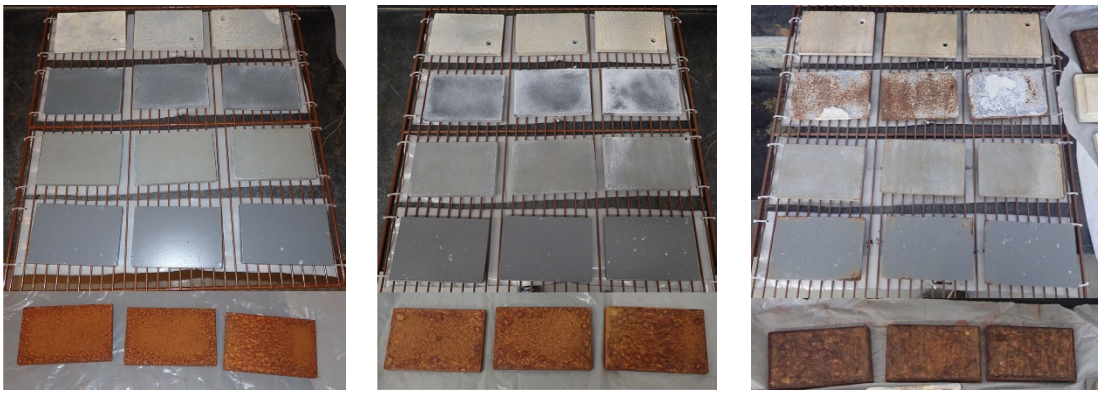

(a) (b) (c)

Figure 4-1. Specimens Removed After (a) 10 Cycles, (b) 20 Cycles, and (c) 80 Cycles

Plates with bolted and welded features were included in this research because of the potential concern that water could collect around bolts and/or welds, increasing the severity of the corrosion. However, greater severity of corrosion on the plates with bolted and welded features was not observed in this research. The methodology used for the testing in this research laid the plates flat in the chamber, which caused the ponding conditions to be the same for both the flat plates and the specimens with bolted and welded features.

4.2.2 Galvanized Specimens

4.2.2.1 Flat Plates

Figure 4-2 shows the visual progression of the galvanized specimens through 80 cycles of accelerated corrosion testing. The galvanized specimens visually changed the least out of all of the corrosion protection systems throughout the 80 cycles of accelerated corrosion testing. There was a slight darkening in color, which could indicate formation of a zinc oxide patina. Lines from where the specimens were sitting on the rack in the environmental chamber also became visible as cycling progressed. There was, however, no coating loss observed. Based on this observation, there was no exposed bare steel even after 80 cycles, meaning that any thickness or mass loss measured was coating loss only.

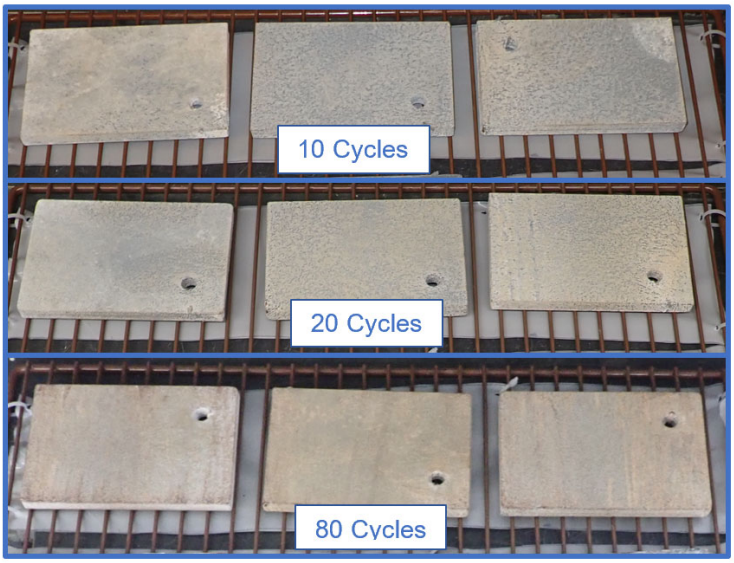

Figure 4-2. Visual Progression of Galvanized Flat Plates at 10, 20, and 80 Cycles of Accelerated Corrosion Testing

4.2.2.2 Plates with Bolted and Welded Features

The galvanized plates with bolted and welded features, shown in Figure 4-3, looked similar to the galvanized flat plates after 80 cycles of corrosion testing. The plates with bolted and welded features also experienced a slight change in color, gaining a yellow tint. The plates with bolted and welded features did, contrary to the flat plates, have noticeable rust, but this was only present around the bolts. The bolts on the right side of the specimens in Figure 4-3 rusted more than those on the left of the specimens. This is attributed to the fact that two different bolt types were used.

Figure 4-3. Galvanized Plates with Bolted and Welded Features After 80 Cycles of Accelerated Corrosion Testing

4.2.3 Metallized Specimens

4.2.3.1 Flat Plates

Figure 4-4 shows the progression of the metallized specimens through 80 cycles of accelerated corrosion testing. The metallized specimens changed drastically in visual appearance throughout the accelerated corrosion testing cycles. The coating changed colors from a gray color to a white color, and much of the coating visibly deteriorated by Cycle 80. As early as the seventh cycle, the metallized coating was detached from the steel around the edges, as shown in Figure 4-5. This was a common mechanism of deterioration of the metallized specimens and always occurred at the

specimen edges for the specimens that experienced coating loss. After this result occurred, inquiries into the fabrication of these specimens revealed that these specimens did not receive any edge preparation This is the likely explanation for the premature failure at the edges of these specimens.

At around cycle 55, the coating deterioration began to extend to the 4” x 6” faces of the metallized specimens as well and led to detachment of all or partial thickness of the metallized coating, as seen in Figure 4-6. The 4” x 6” faces typically did not lose the full thickness of the coating in places where coating was lost but instead maintained a much thinner layer of the coating. This can be seen in Figure 4-6, where the lighter colored portion of the specimen is the full thickness of the original metallized coating and the darker gray portion is a thinner layer of the coating after some portion of the thickness has been lost. The specimens that underwent 80 cycles of testing lost more than half of the metallized coating (full thickness) around the edges of the plates and experienced coating thickness loss that varied in thickness on the faces of the plates. These specimens had little to no full-thickness coating remaining on the faces of the plates.

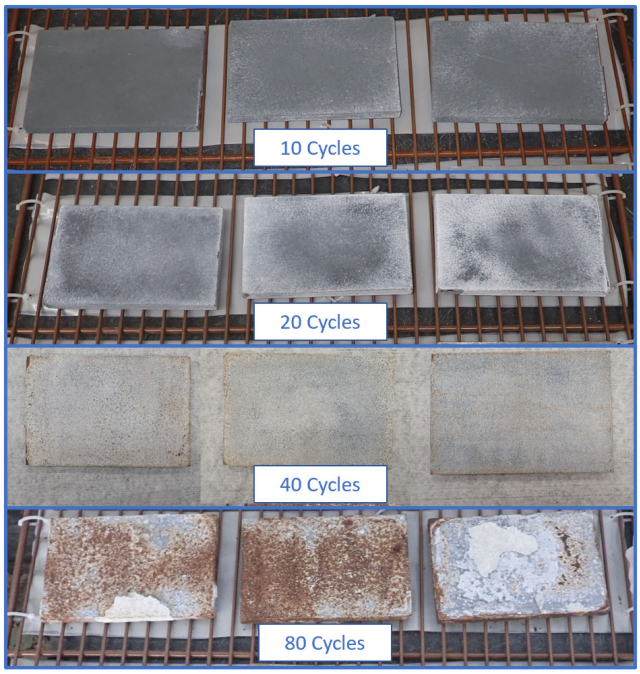

Figure 4-4. Visual Progression of Metallized Specimens at 10, 20, 40, and 80 Cycles of Accelerated Corrosion Testing

Figure 4-5. Metallized Coating Pulling Away on the Edge After 7 Cycles of Accelerated Corrosion Testing

Figure 4-6. Metallized Coating Deterioration on 4” x 6” Face of Specimen After 55 Cycles of Accelerated Corrosion Testing

4.2.3.2 Plates with Bolted and Welded Features

The metallized plates with bolted and welded features, shown in Figure 4-7, also showed a change in color, becoming whiter with increased cycling. The plates with bolted and welded features also experienced metallized coating loss but to a lesser extent than the flat plates. The plates with bolted and welded features still retained most of their full-thickness coating even after 80 cycles of testing.

Figure 4-7. Metallized Plates with Bolted and Welded Features After 80 Cycles of Accelerated Corrosion Testing

4.2.4 1-Coat IOZ Paint Specimens

4.2.4.1 Flat Plates

Figure 4-8 shows the progression of the 1-coat IOZ specimens through 80 cycles of accelerated corrosion testing. The 1-coat IOZ paint gradually had white spotting that appeared. The specimens overall faded to a lighter color during the 80 cycles. They also had a variable amount of orange-brown discoloration, especially on and near the edges of the specimens, as shown in Figure 4-8 and sometimes more generally distributed as shown in Fig 5-9. This discoloration appears to be areas where coating, but not steel, was lost on the surface. It was observed only in specimens that underwent 80 cycles of testing. The Matlab program used for the analysis of the painted specimens (discussed in Section 3.3.6.5) was not accurately able to analyze this discoloration, and the data for the Cycle 80 1-coat IOZ specimens is resultantly not included in 5.3.2.3. There was visible corrosion at the corners of these specimens as well, which can be seen in Figure 4-10.

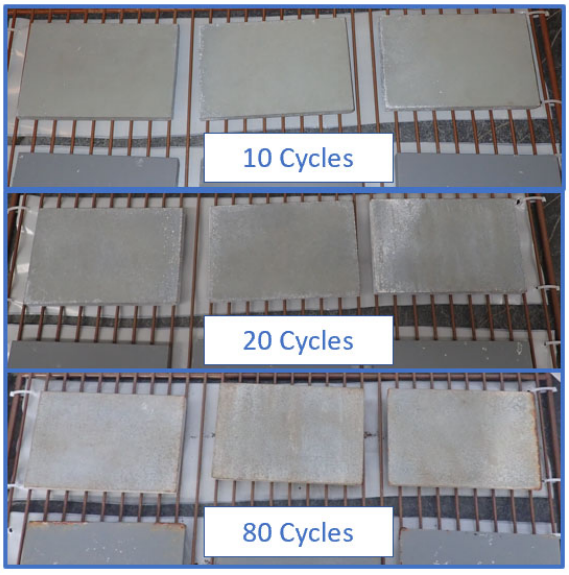

Figure 4-8. Progression of 1-Coat IOZ Specimens at 10, 20, and 80 Cycles of Accelerated Corrosion Testing

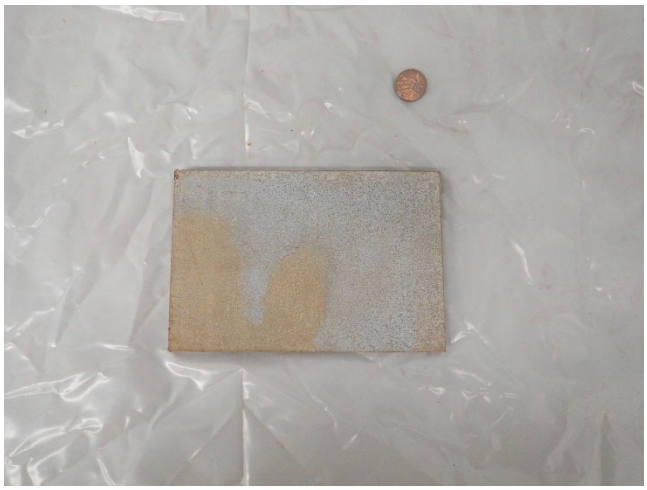

Figure 4-9. 1-Coat IOZ Specimen Discoloration After 80 Cycles of Accelerated Corrosion Testing

Figure 4-10. 1-Coat IOZ Specimen with Corrosion at the Corner After 80 Cycles of Accelerated Corrosion Testing

4.2.4.2 Plates with Bolted and Welded Features

The 1-coat IOZ plates with bolted and welded features, shown in Figure 4-11, looked similar to the 1-coat IOZ flat plates after 80 cycles of testing. They experienced white spotting and corrosion at corners and edges. The crevice between where the bolt

and the attached plate meet typically experienced additional corrosion on the plates with bolted and welded features.

Figure 4-11. 1-Coat IOZ Plates with Bolted and Welded Features After 80 Cycles of Accelerated Corrosion Testing

4.2.5 3-Coat OZ Paint System Specimens

4.2.5.1 Flat Plates

Figure 4-12 shows the progression of the 3-coat OZ specimens through 80 cycles of accelerated corrosion testing. The 3-coat OZ painted specimens also experienced coating degradation and corrosion at the edges and especially at the corners, shown in Figure 4-13. The edge and corner defects began to develop at around Cycle 20 and gradually intensified through the remaining 60 cycles after that. The 4” x 6” faces excluding the edges, however, were in good condition with only minor coating loss and corrosion. Note that the white spotting that can be seen on the three-coat painted specimens in Figure 4-12 is salt that was easily wiped off at the end of testing prior to the image processing used for analysis, not an imperfection in the coating itself. Also, the perception of a color change of the specimens from cycle to cycle in Figure 4-12 is due to lighting where the photo was taken, not an actual darkening and then lightening of the specimens.

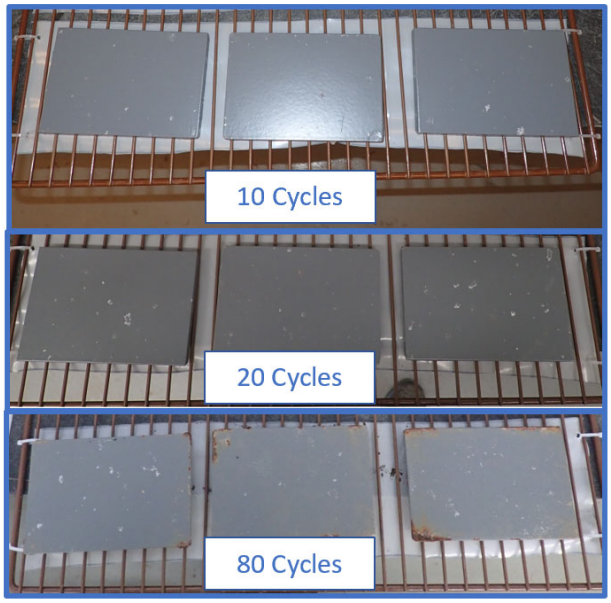

Figure 4-12. Progression of 3-Coat OZ Specimens at 10, 20, and 80 Cycles of Accelerated Corrosion Testing

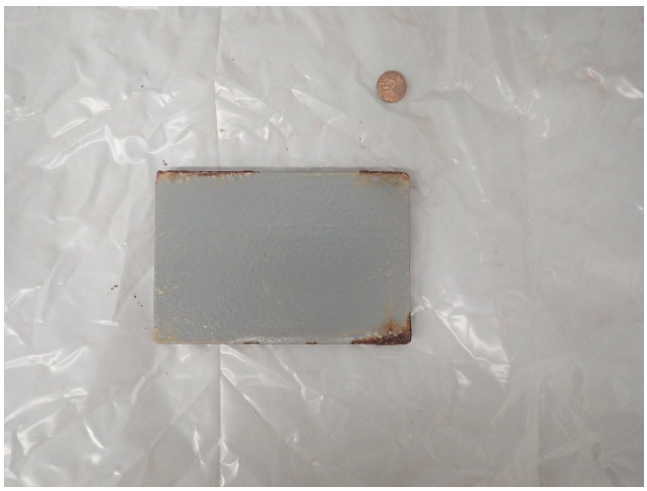

Figure 4-13. 3-Coat OZ Specimen with Corrosion at the Corners After 80 Cycles of Accelerated Corrosion Testing

4.2.5.2 Plates with Bolted and Welded Features

The 3-coat OZ plates with bolted and welded features, shown in Figure 4-14, looked similar to the 3-coat OZ flat plates after 80 cycles of testing. They experienced

coating degradation and corrosion at corners and edges. The bolts, however, were where the bulk of the corrosion occurred for the plates with the bolted and welded features.

Figure 4-14. 3-Coat OZ Plates with Bolted and Welded Features After 80 Cycles of Accelerated Corrosion Testing

4.2.6 UWS Specimens

4.2.6.1 Flat Plates

Figure 4-15 shows the progression of the UWS specimens through 80 cycles of accelerated corrosion testing, where it can be seen that the steel became darker brown with increased cycles, which is also generally considered to be indicative of a good performing patina. The UWS specimens, originally a silver color (SSPC SP5) at the start of testing, became an orange-brown color within only one cycle of accelerated corrosion testing, indicating the oxidation of the iron. Since UWS requires such oxidation to provide a protective layer, the observation of this color change within only one cycle indicates that the patina development was able to initiate rather quickly. The layer formed was a strong and solid patina layer that was increasingly difficult to remove with hand tools, such as a putty knife, as the cycles progressed. Extreme effort was required to scrape off any of the rust layer after Cycle 80.

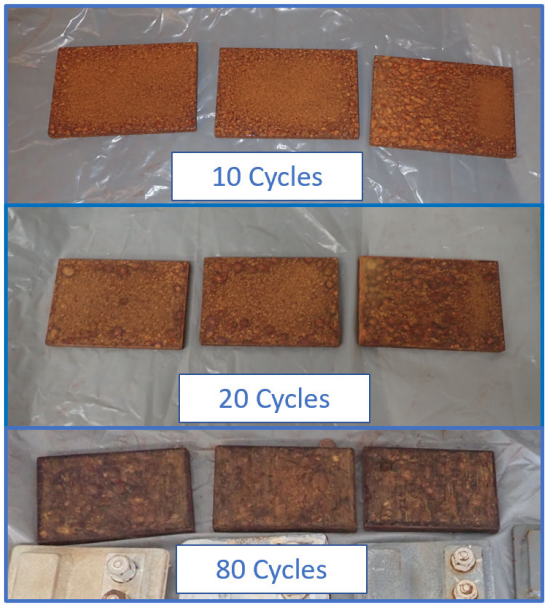

Figure 4-15. Progression of UWS Specimens at 10, 20, and 80 Cycles of Accelerated Corrosion Testing

4.2.6.2 Plates with Bolted and Welded Features

The UWS plates with bolted and welded features, shown in Figure 4-16, looked similar to the UWS flat plates after 80 cycles of testing. They became an orange-brown color within one cycle of testing. The patina layer formed was strong and solid and was resultantly difficult to remove with hand tools.

Figure 4-16. UWS Plates with Bolted and Welded Features After 80 Cycles of Accelerated Corrosion Testing

4.3 Quantitative Results

4.3.1 Overview

The quantitative results obtained from accelerated corrosion testing included mass loss, thickness loss, and XRD results. The mass and thickness loss were measured for every corrosion protection system except for the painted specimens, but the mass loss was emphasized over the thickness loss since mass loss measurements better represent the entirety of the specimens. The galvanized, metallized, and UWS specimens were cleaned of corrosion products as described in Section 3.3.6.3 before being measured for mass and thickness loss, and the final mass of each specimen after cleaning was compared to its original mass before testing to compute a percentage of mass loss. The painted specimens were analyzed to determine the percentage of surface area rusted using the procedures in ASTM D610-08 (ASTM 2019) as described in Section 3.3.6.5. Scrape samples of UWS specimens were taken before cleaning at 10, 20, 40, and 80 cycles and were used for XRD analysis to be compared to benchmarks from field data, as previously described in Section 3.3.6.6.

4.3.2 Corrosion Losses

In this section mass loss data is presented for the galvanized, metalized, and UWS specimens, according to the methodology presented in Sections 3.3.6.3 and 3.3.6.4. Because mass loss of painted specimens was not a useful metric, percent rusting of these specimens is presented, according to the methodology presented in Section 3.3.6.5.

4.3.2.1 Galvanized Specimens

4.3.2.1.1 Flat Plates

Since there was no observed coating loss for the galvanized specimens, any mass loss found after cleaning was determined to be from coating loss only. This means that the mass loss of bare steel for all specimens was equal to 0 grams (and 0%). The mass of coating loss found for each galvanized specimen was low, as shown in Figure 4-17. The average coating loss as a percent loss of the original masses of the specimens was 0.25% at 10 cycles, 0.33% at 20 cycles, 0.47% at 40 cycles, and 0.70% at 80 cycles. Figure 4-17 shows the bare steel mass loss, the coating mass loss, and the average values of the coating loss of the galvanized specimens. This graph also shows a decreasing rate of mass loss with time.

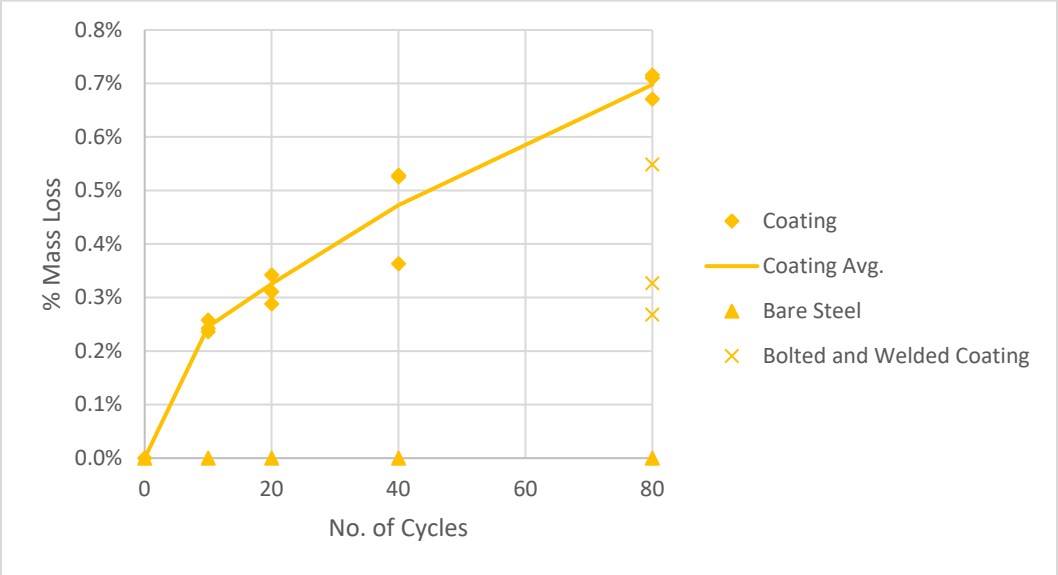

Figure 4-17. Galvanized Mass Loss Due to Accelerated Corrosion Testing

4.3.2.1.2 Plates with Bolted and Welded Features

Similar to the flat plates, none of the galvanized plates with bolted and welded features experienced visible coating loss on the steel plates, meaning that no bare steel was exposed, except for on the bolts. Because of this, all mass loss of bare steel for the plates with bolted and welded features was equal to 0 grams. Figure 4-17 shows the coating loss of these specimens, indicated by the "x" points, found from the cleaning procedure described in Section 3.3.6.3.2. The figure shows that the coating loss as a percentage of the total mass of the plates with bolted and welded features was lower than the coating loss of the flat plates. However, even when the plates with bolted and welded features were determined to be finished cleaning based on the ASTM procedures, visible rust was still present on the bolts. Therefore, further cleaning or different cleaning procedures are required for more accurate coating loss results for the galvanized plates with bolted and welded features.

4.3.2.2 Metallized Specimens

4.3.2.2.1 Flat Plates

The metallized specimens experienced both coating and bare steel loss, which produced the total mass loss shown in Figure 4-18. The relative contributions of coating mass loss and steel mass loss was determined as described in Section 3.3.6.3.2. This method was piloted for six of the nine specimens subjected to 10 to 40 cycles shown in Figure 4-19, for which reasonable results were obtained. For these specimens the coating loss was 0 to 0.23% of the original mass. This represented a wide range relative to the total mass loss, varying between 0 and 70%. This method was also piloted for specimens subjected to 80 cycles, but produced unreasonable coating mass losses that exceeded the total mass losses (for reasons explained in Section 3.3.6.3.2). Because of the lack of reliability in determining the coating mass

loss, the total mass loss is presented as a conservative indicator of corrosion losses. In other words, the steel mass loss is less than the total mass losses reported.

Figure 4-18 shows that the metallized specimens experienced relatively little corrosion for the first 40 cycles and then a significant increase in corrosion at 80 cycles. The average total mass loss as a percent loss of the original masses of the specimens was 0.5% at 10 cycles, 0.4% at 20 cycles, 0.4% at 40 cycles, and 5.2% at 80 cycles. This data fails to produce a consistently increasing relationship, which may be attributed to the unequal levels of coating loss between specimens removed at the same cycle and the omission of proper edge preparation in the fabrication of these specimens (see Section 3.2.1).

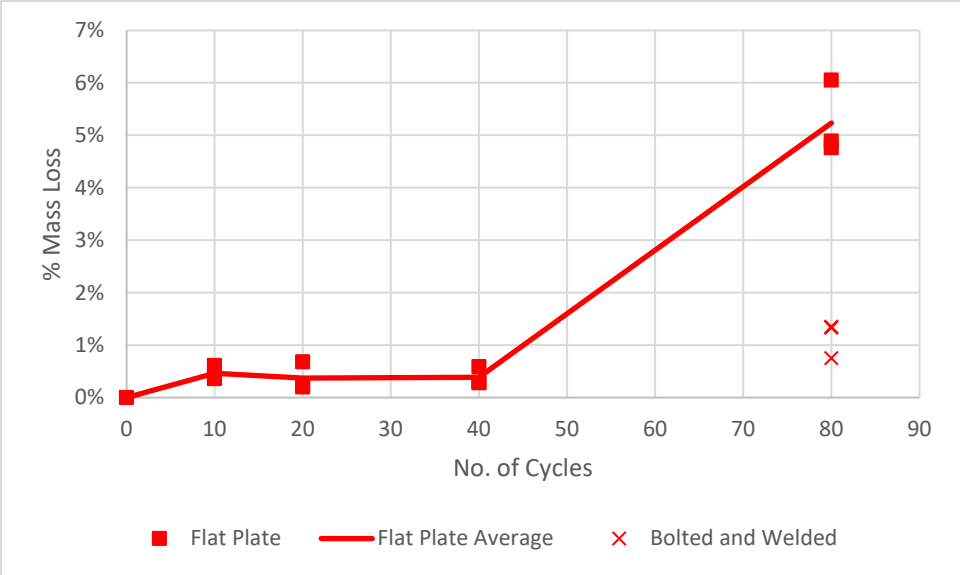

Figure 4-18. Metallized Total Mass Loss Due to Accelerated Corrosion Testing

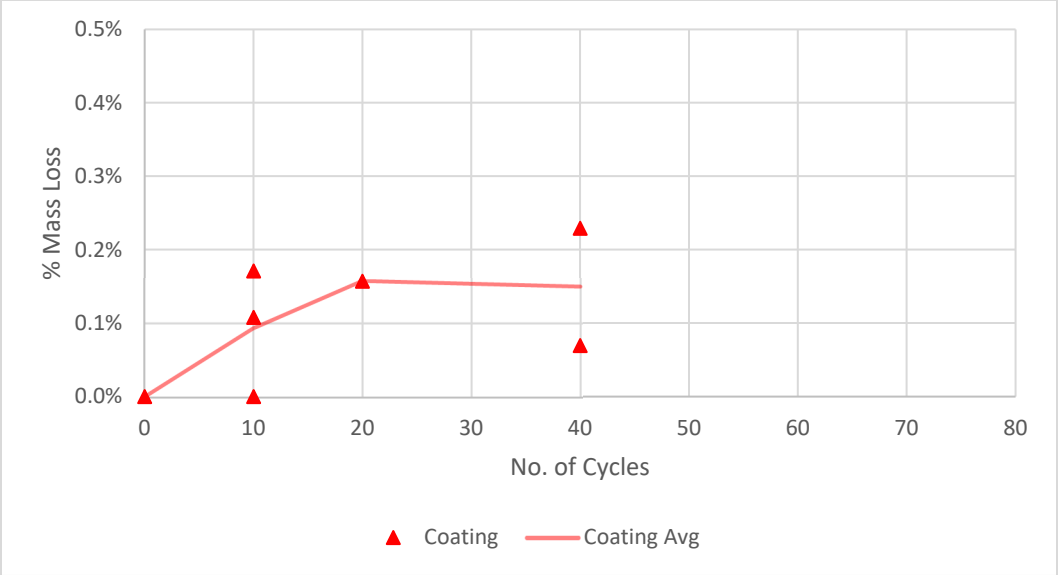

Figure 4-19. Metallized Coating Mass Loss Due to Accelerated Corrosion Testing, Selected Specimens, Cycles 10 through 40

4.3.2.2.2 **Plates with Bolted and Welded Features**

Data for metallized plates with bolted and welded features resulted in significantly less corrosion than the flat plates. This is shown in Figure 4-18, where it is shown that the flat plates experienced about five times the corrosion of the plates with bolted and welded features in terms of percent mass loss. If the greater mass of the plates with bolted and welded features is considered and total mass loss is compared (as opposed to a percentage), the flat plates still experience more mass loss, although by a smaller margin of about three times as much mass loss as the plates with bolted and welded features. This is consistent with the visual observations discussed in Section 4.2.3, where less coating loss (and hence more corrosion protection) of the plates with bolted and welded features is shown.

4.3.2.3 1-Coat IOZ Paint Specimens

4.3.2.3.1 Flat Plates

The results for the painted specimens are in terms of percent coating loss and percent rusting, as shown in Figure 4-20. These metrics cannot be directly compared to mass loss, but similarly measure the effectiveness of the corrosion protection. The process for determining these values is described in Section 3.3.6.5. The average percent coating loss of the included specimens was 1.2% at 10 cycles, 2.4% at 20 cycles, 11.4% at 40 cycles, and 24.5% at 80 cycles. These values can be viewed relative to typical owner thresholds for remedial action at 10 to 20 percent coating failure. However, the percent of the surface area that is rusted is much lower, with a maximum value of 0.6% at 80 cycles of testing.

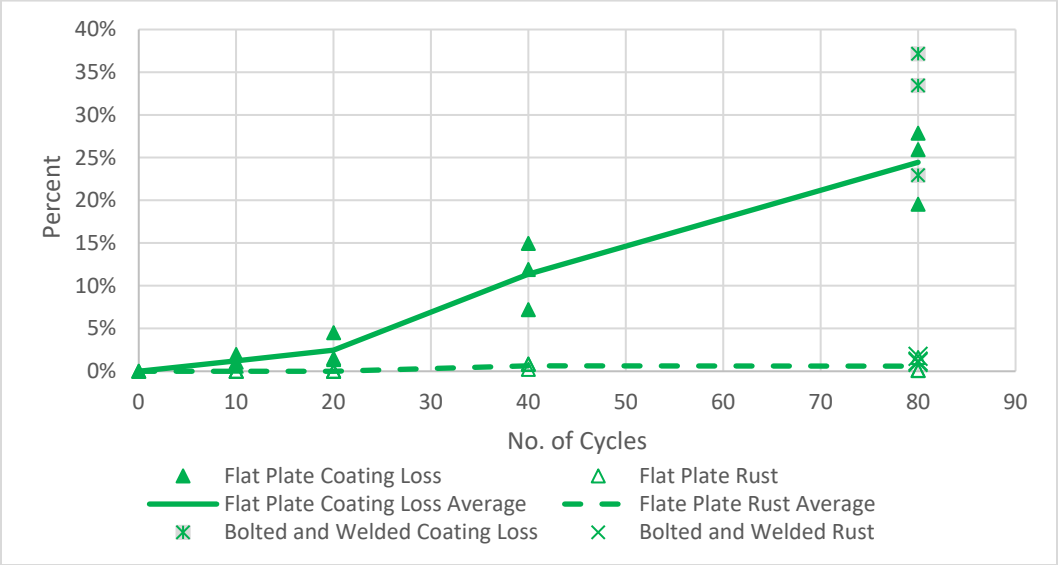

Figure 4-20. 1-Coat IOZ Percent Coating Loss Due to Accelerated Corrosion Testing

4.3.2.3.2 Plates with Bolted and Welded Features

The plates with bolted and welded features experienced similar, more slightly greater, amounts of coating loss and rusting as the flat plates. Specifically, the average

percent coating loss for the plates with bolted and welded features was 31% compared to 24% for the flat plates. The average percent of the surface area that was rusted on the plates with bolted and welded features was 1.3% compared to 0.6% for the flat plates. This is consistent with the visual observations in Section 4.2.4, where it was noticed that the deterioration on the 1-coat IOZ specimens with bolted and welded features was most severe on the bolts.

4.3.2.4 3-Coat OZ Paint System Specimens

As for the 1-Coat IOZ specimens, the results for the 3-coat OZ specimens are in terms of percent coating loss and percent rust, as shown in Figure 4-21. These metrics cannot be directly compared to mass loss, but similarly measure the effectiveness of the corrosion protection. The process for determining these values is described in Section 3.3.6.5. The percent coating loss values for all 3-coat OZ specimens were relatively low, remaining near zero for the first 20 cycles and below 4% throughout the entire 80 cycles of accelerated corrosion testing. The average percent coating loss of the specimens was 0.15% at 10 cycles, 0.09% at 20 cycles, 1.0% at 40 cycles, and 2.7% at 80 cycles. At 10, 20, and 40 cycles, each of the three data points at a given cycle had similar values and are therefore sometimes overlapping in the figure. The percent of the surface area rusted was low for all specimens and at or near zero for up through the first 40 cycles. At 80 cycles, the percent of the surface area that was rusted was 1%, and was concentrated primarily on the corners and edges of the specimens (as shown in Section 4.2.5).

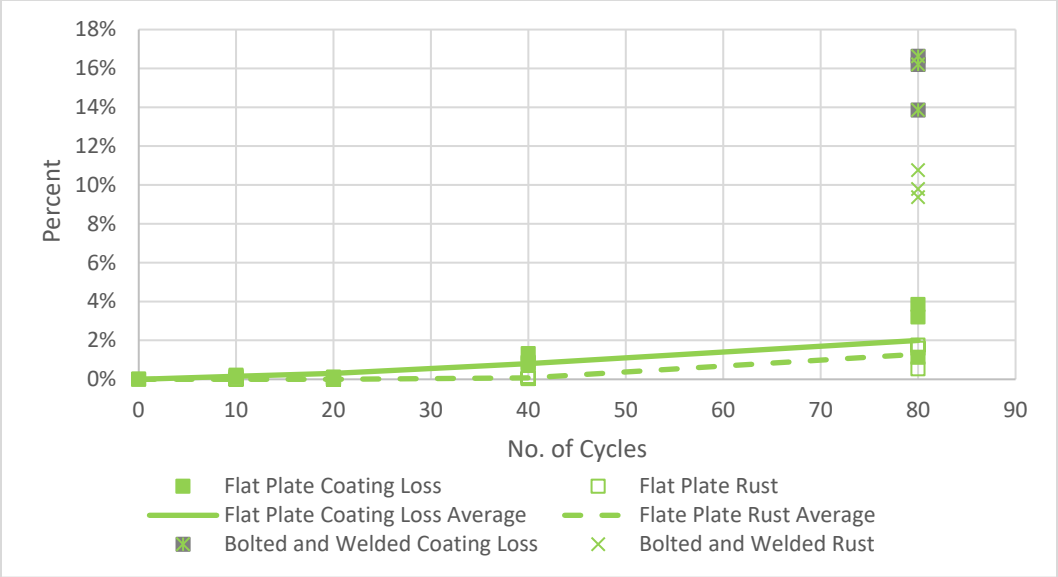

Figure 4-21. 3-Coat OZ Percent Coating Loss Due to Accelerated Corrosion Testing

4.3.2.4.1 **Plates with Bolted and Welded Features**

The plates with bolted and welded features performed considerably worse than the flat plates in terms of percent coating loss and rust development. Specifically, the maximum percent coating lost for the flat plate was 3.8% compared to the maximum percent rusted of the plates with bolted and welded connections was 16.6%. Similarly, the maximum percent rusted of the flat plate was 1.8%, while the maximum percent rusted of the plate with bolted and welded connections was 10.8%. This is consistent with the visual observations in Section 4.2.5, where it was noticed that most of the deterioration on the 3-coat OZ specimens was concentrated on the bolts.

4.3.2.5 UWS Specimens

4.3.2.5.1 **Flat Plates**

The mechanism of corrosion protection for UWS specimens is through a patina and works such that there is no sacrificial layer, meaning that all mass loss

experienced by UWS specimens is bare steel loss. The average mass loss as a percent loss of the original masses of the specimens can be seen in Figure 4-22 as 1.80% at 10 cycles, 4.19% at 20 cycles, 8.54% at 40 cycles, and 17.08% at 80 cycles. Figure 4-22 also shows the (bare steel) mass loss of each of the UWS specimens. The graph shows an increasing trend between cycles 0 and 20 then shows a corrosion rate slightly decreasing with time between cycles 20 and 80. The slope between Cycle 0 and 10 is 0.18%; the slope between Cycle 10 and 20 is 0.24%; the slope between Cycle 20 and 40 is 0.22%; and the slope between Cycle 40 and 80 is 0.21%.

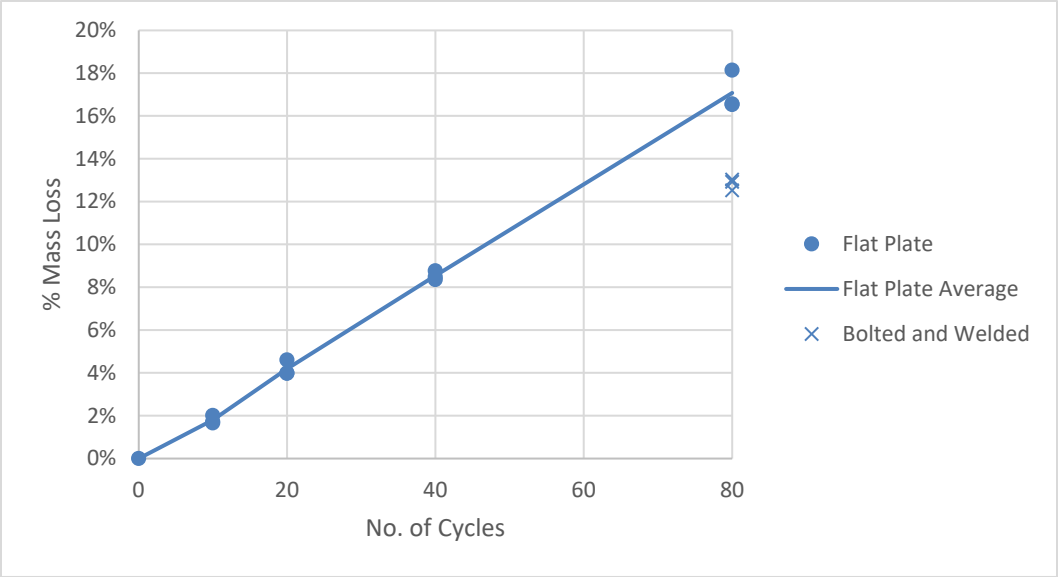

Figure 4-22. UWS Mass Loss Due to Accelerated Corrosion Testing

4.3.2.5.2 **Plates with Bolted and Welded Features**

The data points from the plates with bolted and welded features, which were all removed from testing at 80 cycles, are also shown, indicated by the "x" points in Figure 4-22. The values of percent mass loss at 80 cycles are lower for the plates with bolted and welded features than for the flat plates. The mass loss values in grams help make sense of this trend. The flat plates removed from testing at 80 cycles lost

between 184 and 202 grams, while the plates with bolted and welded features lost between 221 and 231 grams. The plates with bolted and welded features were typically had an initial mass around 600 grams heavier than the flat plates. So, while the plates with bolted and welded features did lose more mass in grams than the flat plates, this trend did not equate to percent mass loss since the plates with bolted and welded features had more initial mass. It is logical that the plates with bolted and welded features did not lose the same percentage of mass because it was the surface area of the specimens corroding, and the surface areas between the flat plates and the plates with bolted and welded features were similar, but the initial mass of the plates with bolted and welded features was significantly higher. This trend is suspected to be different from the coated specimens because the coating on the bolts was observed to be the location of most corrosion on the coated specimens, but the uncoated specimens experience more uniform corrosion on both the plates and the bolts.

4.3.2.6 Comparison of Corrosion Protection Systems

The results for the galvanized, metallized, and UWS flat plate specimens were plotted on one graph (Figure 4-23), while the results for the 1-coat IOZ and 3-coat OZ painted flat plate specimens were plotted on another (Figure 4-24). These groupings are based on combining the corrosion protection systems that are evaluated based on the same metrics into the same graphs (i.e., percent mass loss in Figure 4-23 and percent coating loss and rusting in Figure 4-24). Note that in Figure 4-23 the percent mass loss values are the total mass loss, including coating loss of the galvanized and metalized specimens. For the galvanized specimens, the steel loss was zero throughout the testing. For the metalized specimens, additional discussion of the relative amounts of steel and coating loss can be found in Section 4.3.2.2.

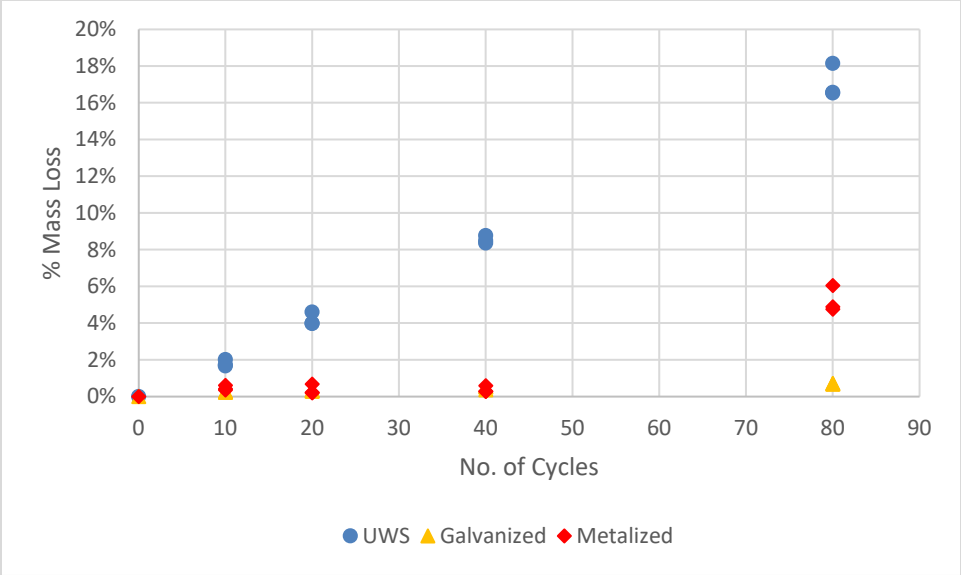

Figure 4-23. Galvanized, Metallized, and UWS Total Mass Loss Due to Accelerated Corrosion Testing

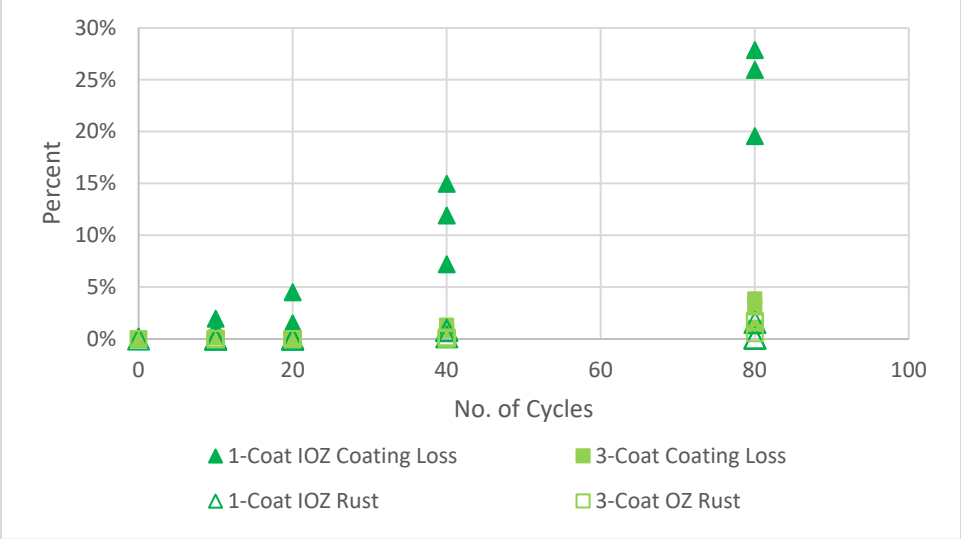

Figure 4-24. 1-Coat IOZ and 3-Coat OZ Percent Coating Loss and Surface Rust Due to Accelerated Corrosion Testing

The total mass loss results show that the galvanized specimens are consistently the lowest throughout all cycles at 0%. The UWS values are the highest. The metallized values are similar to the galvanized specimens for the first 40 cycles and fall between the galvanized and UWS results at 80 cycles. The relative ranking of the corrosion protection systems in order of best to worst performance based on mass loss is therefore: galvanizing, metallizing, then UWS, although this ranking may be affected by the superior fabrication of the galvanized relative to metallized specimens.

The comparison of the painted specimens shows that while the 1-coat IOZ specimens experienced more coating loss, the percent of the surface area that was rusted was similar. Specifically, the percent coating loss results show that the 1-coat IOZ specimens experience 10 times the coating loss, on average. However, at 80 cycles of testing the percent of the surface rusted was, on average, greater for the 3-coat OZ specimens while the ranges overlap for the percent rusted of 1-coat IOZ and 3-coat OZ specimens. The percent of the surface area rusted for all specimens remained below 2%.

4.3.3 XRD Analysis

The XRD values acquired from laboratory testing at 10, 20, 40, and 80 cycles are shown for UWS specimens compared to the targeted benchmarks from field work in Table 4-1. The benchmark values were obtained from field work done on UWS bridges. Similarities in the iron compound composition between laboratory testing results and field test results help to assure that the laboratory corrosion mechanism is consistent with that of field corrosion. The percent of each iron compound in the table that is within the range of the measured field test benchmark values are highlighted in green. Based on the results, all UWS XRD values are within range of the measured field test values at Cycle 80.

Table 4-1 XRD Benchmarks and Measured Values

		UWS			
Compound	**Measured Field Test Range**	**Cycle 10**	**Cycle 20**	**Cycle 40**	**Cycle 80**
Lepidocrocite	0 - 21%	25%	30%	24%	18%
Goethite	0 - 52%	14%	11%	34%	12%
Akaganeite	4 - 56%	1%	5%	5%	32%
Hematite	0 - 22%	0%	7%	0%	0%
Maghemite/ Magnetite	0 - 51%	60%	29%	35%	35%
Ferrihydrite	0 - 34%	0%	15%	0%	0%
Ferric Sulfate	0 - 19%	0%	4%	2%	3%
Schwermanite	0 - 20%	0%	0%	0%	0%

Lepidocrocite, goethite, and akageneite are isomers of ferric oxy-hydroxide (FeOOH), meaning that they all have the same chemical formula but have a different arrangement of atoms from each other. Some isomers of FeOOH have been demonstrated as forming a protective patina. Lepidocrocite is the first iteration of FeOOH, meaning it is expected to appear first in the formation of the patina. Then, atoms begin to rearrange and convert to goethite and/or akageneite. Formation of goethite is preferred in a patina, as it has more tightly spaced atoms which provide better protection. Akageneite, oppositely, provides weaker protection. The UWS XRD results show that at first the patina was mostly comprised of lepidocrocite, as expected. After that, there is variability in the patterns of the XRD composition with increased cycling.

4.4 Scaling Relationship between Accelerated Corrosion Testing Results and Field Results

The results obtained were a function of number of accelerated corrosion testing cycles. In order to contextualize these results in terms of real-world situations, a

relationship between number of cycles and number of years in the field was determined. As previously discussed, thickness loss values were compared to those from prior field work (Rupp 2020) and work from Albrecht et al. (1989). Albrecht et al. provided ranges of expected thickness losses per year for five qualitative "corrosivity categories" ("very low," "low," "medium," "high," or "very high").

Figure 4-25 shows the upper bound of the four most severe of these ranges (with solid lines) along with the averages from field work data from bridges in high deicing and coastal environments (dashed lines) and the accelerated corrosion testing thickness loss averages using the UWS data from Method 5 and from the final phase of testing (solid black data points). This plot equates one cycle to one year. Figure 4-26 shows the same plot but with a scaling equating two cycles equals to one year. This plot was created to explore scaling the thickness loss values from laboratory accelerated corrosion testing to the values obtained in the field from bridges in a relatively severe deicing environment. Similarly, Figure 4-27 recreates this plot with a scaling of one cycle equals 0.75 years, which results in scaling the laboratory accelerated corrosion testing thickness loss values to the values obtained in the field from bridges in a coastal environment.

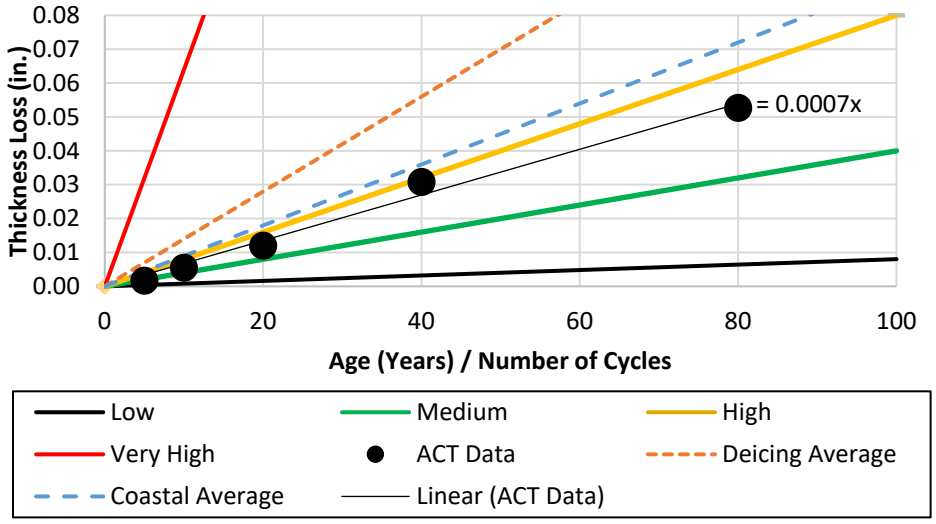

Figure 4-25. UWS Thickness Loss Scaled Such that 1 Cycle = 1 Year

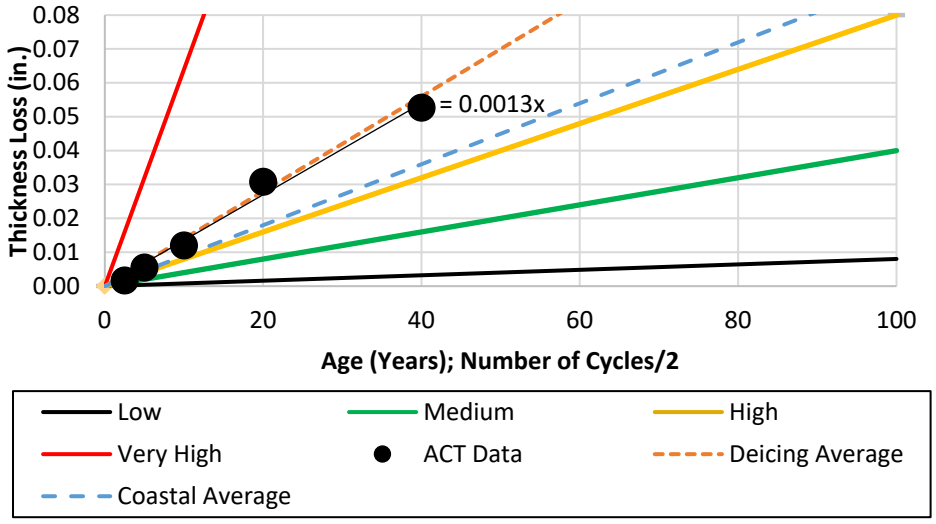

Figure 4-26. UWS Thickness Loss Scaled Such that 2 Cycles = 1 Year

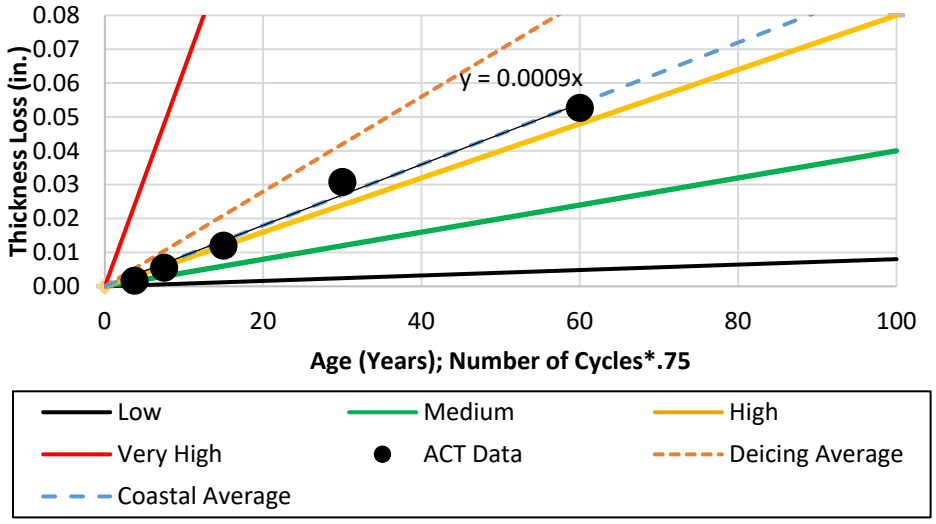

Figure 4-27. UWS Thickness Loss Scaled Such that 1 Cycles = 0.75 Years

Based on the scaling shown in Figure 4-25 where one cycle equals one year, the thickness loss values obtained from laboratory testing fall into the "high" category, which is desired for matching the intention of this work of mimicking bridges in relatively severe environments. The "very high" category is not desired, as that category describes an environment that is extremely severe where uncoated bridges should not be built. Although it is possible to individually scale the data to each environment, as shown in Figures 4-29 and 4-30, the field-measured data of both environments contains data from bridges that had poor performance and were built in environments where UWS bridges are not advised to be built. Scaling the laboratory thickness loss values to this data, therefore, may be overcomplicating the situation in an attempt to provide more accuracy than is possible. Therefore, it was determined that the scaling of one cycle equals one year is the best scaling approach to evaluate performance of a relatively severe coastal or deicing environment.

4.5 Longevity Estimates and Comparison of Corrosion Protection Systems

Based on the results obtained from laboratory accelerated corrosion testing on each of the five corrosion protection systems, longevity estimates were calculated to determine how long each corrosion protection system would be expected to last in a relatively severe coastal or deicing environment. These estimates were based on the scaling described above in Section 4.4, where one cycle of laboratory testing equals one year in the field. Each corrosion protection system was evaluated based on realistic benchmarks, as described below. Longevity estimates were calculated using the linear equations obtained from the data resulting from laboratory testing over 80 cycles, which were then equated to the limiting benchmark to find the number of years it would take to reach the limit. The results of this process are shown in Table 4-2. When these calculations resulted in longevity estimates greater than 100 years a specific value is not reported to avoid inaccurate extrapolations of the data given that 100 years modestly exceeds the timeframe represented by the laboratory testing.

The trendlines used in determining the Table 4-2 values are shown in Figures 4-31 – 4-35. (Note that the scale of each of these figures varies to clearly show the fit of the trendline to the data points; relative performance can be seen in Table 4-2 and Figures 4-23 and 4-24.) Figures 4-31 – 4-35 show that a linear fit to the laboratory data generally provides a reasonable approximation of the data, with the possible exception of the metallized data. The metallized data is better described by a bilinear curve fit, but a linear curve fit of all data was adopted for simplicity and consistency. While this may under represent the corrosion of the metallized specimens, this can be viewed as somewhat compensating for the omission of proper edge preparation of these specimens (described in Section 3.2.1).

The longevity estimates for UWS was based on the number of years it would take to reach 1/16 inch of section loss in the through-thickness direction, i.e., 1/16 inch

of thickness loss. This dimension is the greatest concern because it represents the dimension with the greatest percent change (i.e., relative to plate widths) and therefore the greatest concern for diminished structural capacity. It is also the dimension that has been observed as being most effected by corrosion in field observations. Using thickness loss as a metric also has the advantages that it can be easily measured in the field and could also represent a value of sacrificial thickness that could be specified in the design of uncoated members. Since the laboratory-measured values for mass were more accurate than those for thickness loss due to the uneven nature of the specimens after corroding, the 1/16-inch thickness loss value was converted to a percent mass loss value. Using a density of 129 g/in^3 for UWS, an initial mass was calculated for a 4" x 6" x 0.375" steel plate for both UWS. A mass after 1/16" of thickness loss was then calculated using the same densities but a volume calculated using a 4" x 6" x 0.3125" plate to account for the 1/16" of thickness loss. This equaled 17% mass loss.

Various benchmarks were used for the galvanized, metallized, and painted longevity estimates because different state Departments of Transportation (DOTs) have different criteria for determining maintenance requirements. The galvanized and metallized longevity estimates were planned to be based on the number of years it would take to reach 1%, 3% 5%, 10%, and 20% bare steel mass loss, with the 20% bare steel mass loss being most analogous to the UWS performance benchmark. However, given the lack of a reliable method for distinguishing coating loss from mass loss, these same percentages of total mass loss were used instead. This results in the values presented in Table 4-2 as being conservative values for the longevity of metallized and galvanized specimens. A mass loss of 20% corresponded to a longevity estimate greater than 100 years in all cases, and is thus not included in the data summary presented in Table 4-2. Thus, of the three corrosion protection systems that can be directly compared in terms of mass loss, the relative ranking from best to

worst is galvanized, followed by metallizing, and then UWS for these specimens. However, the edge preparation of the galvanized specimens relative to the metallized specimens may have affected this ranking.

Longevity estimates for the painted specimens are given based on the following thresholds: 5%, 10%, and 20% coating loss as well as 5% surface rusting. These thresholds for coating loss are analogous to partial coating failure while the surface rusting threshold is analogous to complete coating failure. Based on these metrics the 3-coat OZ paint system was expected to provide a 100-year service life. The 1-coat OZ specimens indicated a longevity estimate of 34 – 69 years based on the typical benchmarks of 10 – 20% coating loss; however, the 1-coat IOZ corrosion protection system generally prevented rusting even when there was significant coating loss. The results indicate more than a 100-year service life before 5% surface rusting would occur for both paint types.

The specimens used to achieve these results underwent good quality control (meaning they were not scribed and did not have any cuts or nicks in the coatings before testing) and proper handling (meaning no damage was introduced after fabrication). These were deliberate choices in order to test samples according to modern best practices. These situations may or may not occur in the field. Additionally, the testing methodology did not account for UV rays that are harmful to paint and cause a breakdown of paint. For that reason, the longevity estimates for painted specimens provided by this research may not be conservative.

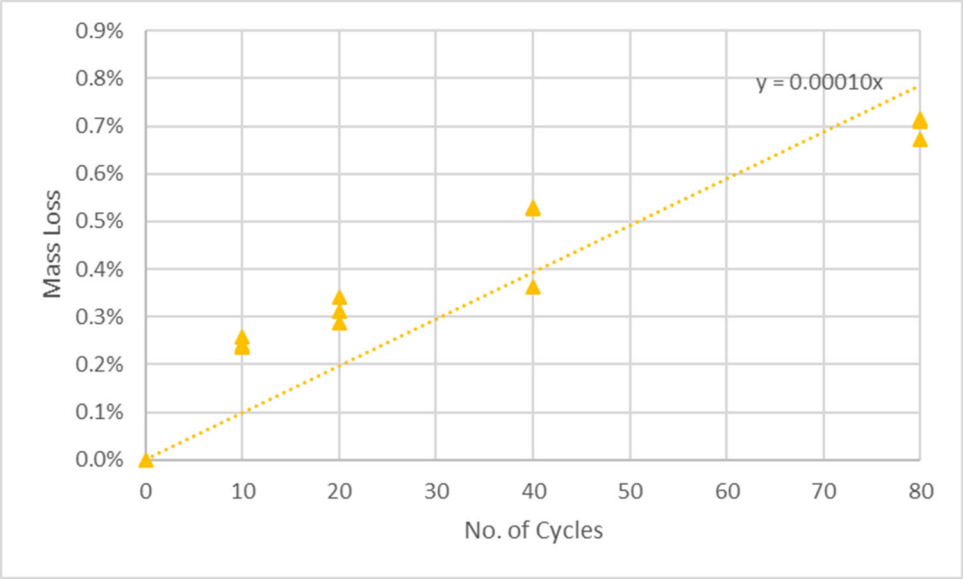

Figure 4-28. Galvanized Percent Total Mass Loss Linear Trendline Used to Determine Longevity

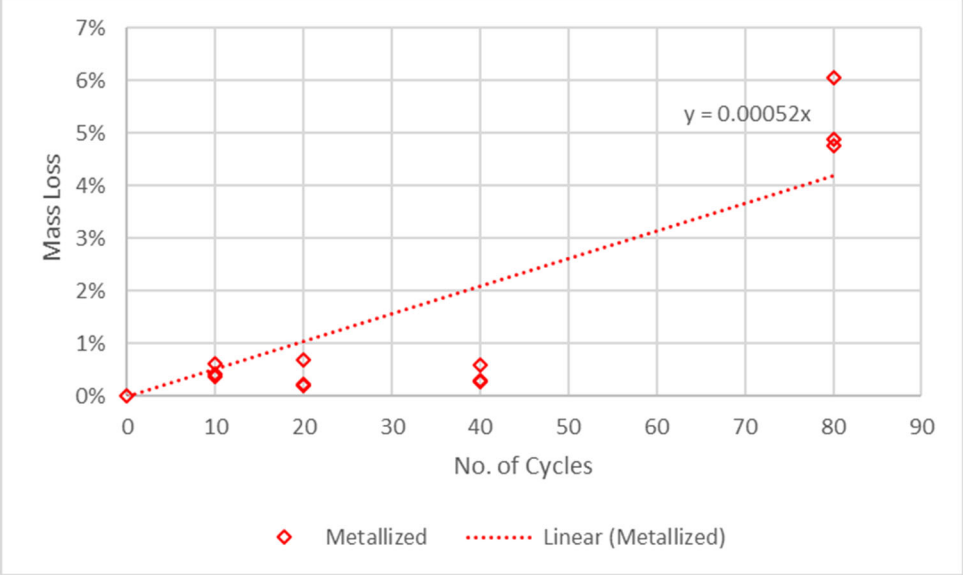

Figure 4-29. Metallized Percent Total Mass Loss Linear Trendline Used to Determine Longevity

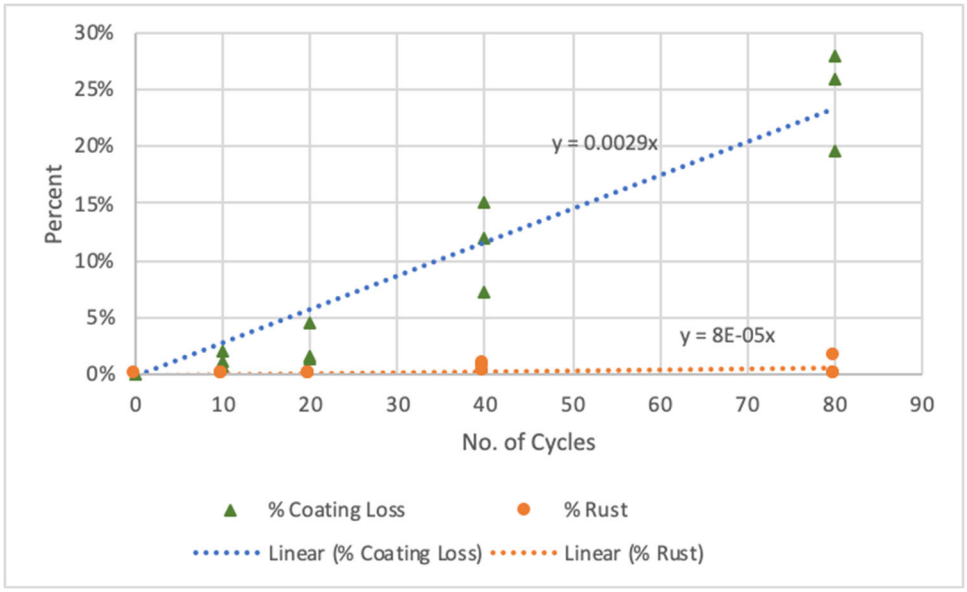

Figure 4-30. 1-Coat (IOZ) Paint Percent Rusted Linear Trendline with Percent Coating Loss Linear Trendline Used to Determine Longevity

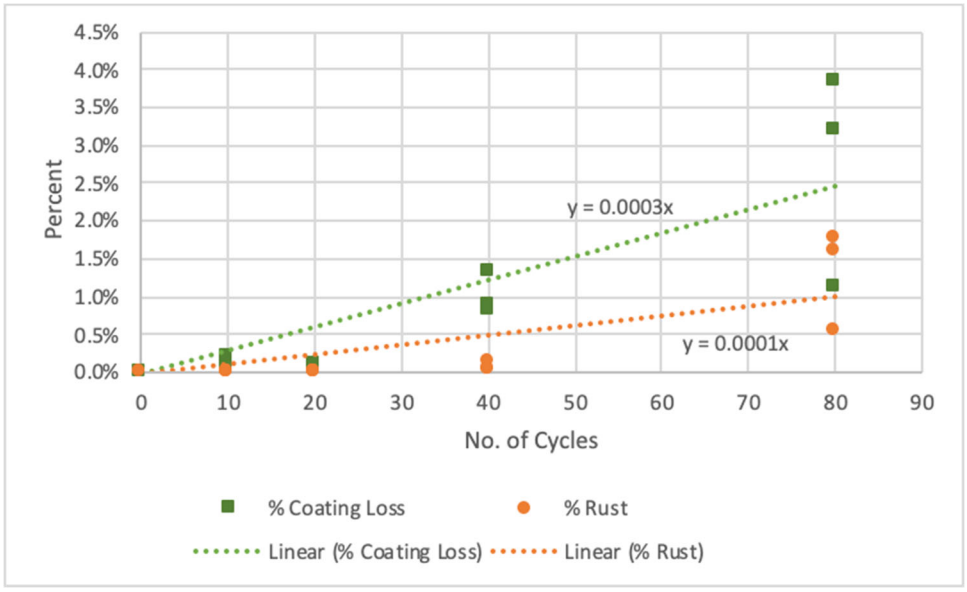

Figure 4-31. 3-Coat (OZ) Paint Percent Rusted Linear Trendline Used to Determine Longevity

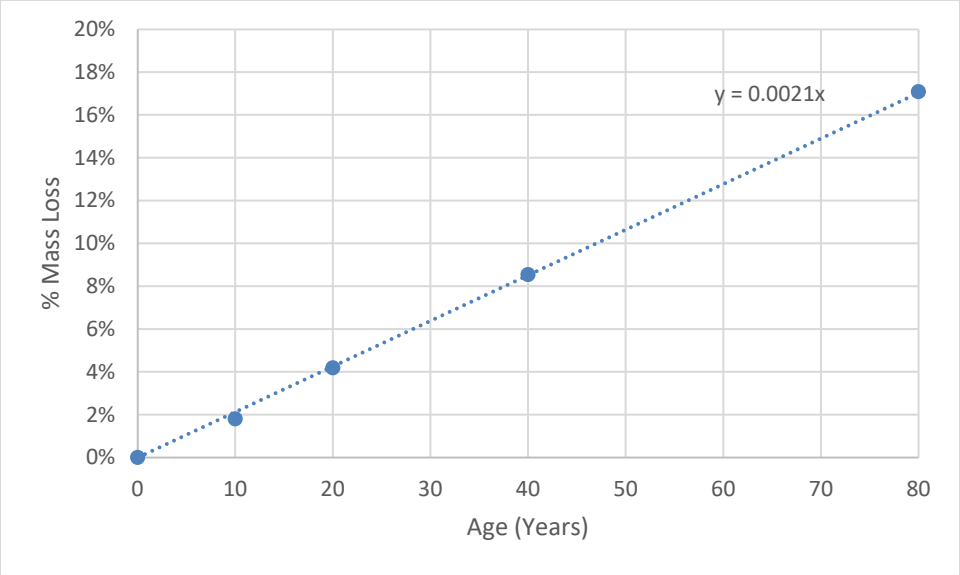

Figure 4-32. UWS Percent Mass Loss Linear Trendline Used to Determine Longevity

Table 4-2 Longevity Estimates for Each Corrosion Protection System Based on Laboratory Accelerated Corrosion Testing

Corrosion Protection System	Limiting Benchmark	Longevity Estimate (Years)
Galvanized	1% Total Mass Loss	100
	3% Total Mass Loss	*
	5% Total Mass Loss	*
	10% Total Mass Loss	*
Metallized[+]	1% Total Mass Loss	19
	3% Total Mass Loss	58
	5% Total Mass Loss	96
	10% Total Mass Loss	*
1-Coat (IOZ) Paint	5% Coating Loss	17
	10% Coating Loss	34
	20% Coating Loss	69
	5% Rust	*
3-Coat (OZ) Paint System	5% Coating Loss	*
	10% Coating Loss	*
	20% Coating Loss	*
	5% Rust	*
UWS	1/16" Thickness Loss (=17% Mass Loss)	81

***** *= > 100 years*

[+] *Note: These specimens lacked proper edge preparation and are therefore conservative.*

Chapter 5

CONCLUSIONS

5.1 Summary

The research conducted consisted of three main parts: 1) a statistical analysis of the performance of corrosion protection systems based on SCR, 2) laboratory testing of modifications to existing accelerated corrosion testing procedures to better resemble corrosion rates and mechanisms observed in the field in relatively severe environments, and 3) implementation of the improved accelerated corrosion testing procedures to evaluate and compare performance of five corrosion protection systems. The corrosion protection systems used were UWS, 1-coat IOZ paint, 3-coat OZ paint, galvanizing, and metallizing.

5.2 Key Findings

5.2.1 Statistical Analysis of NBI Data

The statistical analysis used data from 11,865 highway bridges throughout the United States. A one-way ANOVA and Games-Howell post hoc test of SCR values for UWS, paint, galvanized, and metallized highway bridges found that all corrosion protection systems have statistically significant differences in performance when compared with each other except when any group is compared to metallized bridges. Using the same data, a scatter plot of SCR vs. age was created for each corrosion protection system, which was used to find a linear trendline of performance. A relative ranking of corrosion protection systems was determined from this analysis, finding that galvanized consistently had the highest SCR while paint consistently had the lowest SCR. UWS was intermediate to galvanized and paint. The metallized SCR data had a different slope than all of the other corrosion protection systems, so its

placement in the relative ranking changed throughout the 50-year time period analyzed. Splitting paint into “old” paint and “new” paint for bridges built before and after 1998 (respectively) did not make a difference in the relative ranking, although newer paint was found to perform better than older paint.

5.2.2 Accelerated Corrosion Testing Methodology Modifications

Five modifications were made to the accelerated corrosion testing procedures described by Fletcher et al. (2003) and were tested using UWS and carbon steel specimens. These modifications included changes in salt concentration during the salt application stage, duration of the humid stage, adding a rinse stage, and changing temperature. The UWS results of each iteration were benchmarked based on mass loss rate over time, thickness loss, and XRD analysis to determine which iteration best matched real-world corrosion.

It was found that Method 5, in which the salt concentration during the salt application stage was reduced from 5% to 2% and the temperature was increased during the humid stage from 50° C to 60° C provided results that best resembled field corrosion of UWS bridges in severe environments. This improvement of methodology was indicated primarily based on the mass loss rate over time, which stabilized and had a decreasing rate with time as is seen in the field. Method 5 specimens also had iron compound compositions similar to those found in the field, which was determined through XRD analysis. UWS thickness loss values from Method 5 were categorized as “high” based on Albrecht et al. (1989) corrosivity categories if scaled such that one cycle equals one year, meaning that these values accurately reflect a relatively severe environment.

5.2.3 Laboratory Accelerated Corrosion Testing

The final phase of testing implemented the accelerated corrosion testing procedures from Method 5 for 80 cycles using all five corrosion protection systems. For the painted and metallized specimens, most corrosion began at the edges and / or corners. The galvanized specimens did not experience any visible coating loss throughout all 80 cycles, meaning that any mass loss was coating loss only, as no bare steel was exposed. Based on these visual observations and the longevity estimates given in Table 4-2, galvanizing was judged to provide the best performance of all corrosion protection systems evaluated in this work. Metallizing performed similar to galvanizing up through 40 cycles of testing, but then experienced an increase in corrosion at 80 cycles. The metallizing data also failed to produce a consistently increasing relationship, which may be attributed to the unequal levels of coating loss between specimens removed at the same cycle and the reduced quality control in the fabrication of these specimens (see Section 3.2.1). Paint was analyzed separately, as it was evaluated in terms of percent rusted instead of in terms of mass loss. The comparison of the painted specimens showed that while the 1-coat IOZ specimens experienced more coating loss, the percent of the surface area that was rusted was similar. The percent of the surface area rusted for all painted specimens remained below 2%.

Longevity estimates were calculated using the laboratory-obtained data for each corrosion protection system. Estimates resemble the longevity of a given corrosion protection system in a relatively severe environment based on realistic limiting criteria. UWS was found to last 81 years based on a limiting value of 1/16 inch of thickness loss. Since DOTs have different criteria for determining maintenance requirements, the paint longevity estimate was calculated based on, 5%, 10%, and 20% coating loss and 5% surface rusting. The 1-coat IOZ was estimated to last 34

years based on a 10% coating loss criterion, which is among the more stringent criteria implemented by owners for a repainting schedule, and up to more than 100 years based on a 5% surface area rusted criterion. The 3-coat IOZ system was estimated to last more than 100 years based on all listed criteria. It is noted that the accelerated corrosion testing method used in this work did not include UV exposure, which may lead to different degradation rates for paint. Galvanizing and metallizing were similarly evaluated for 1%, 3% 5%, 10%, and 20% mass loss. Galvanizing has the potential to provide more than 100 years of service life for all of the service life benchmarks considered. Metallizing was estimated to last approximately 20 years based on a stringent 1% mass loss criterion and nearly 100 years or more based on a mass loss criterion of 5% or above. It should be noted, however, that any estimates above 80 years (for any corrosion protection system) go beyond the range of the accelerated corrosion testing performed in this research.

5.2.4 Comparison of NBI and Accelerated Corrosion Testing Data

In Section 2.3.1.2, a plot was made showing SCR vs. age (Figure 2-7) for the corrosion protection systems based on trendlines created for each corrosion protection system through the collection of a database of 11,865 bridges linked to NBI data. Figure 2-7 shows a relative ranking of the corrosion protection systems in descending order of performance as: galvanizing, UWS, then paint (and newer paint out performing older paint), with metallizing having variable performance over different age ranges.

These results generally match what is found for the longevity estimates in Table 4-2. Galvanizing has among the longest estimated service life, with a longevity estimate of 100 years or more no matter which percent mass loss criteria is chosen. The 3-coat OZ paint system has produced a longevity estimate of more than 100 years.

However, these specimens were ideally fabricated and were not subjected to UV conditioning; so, these results may be unconservative for typical field conditions. The order after that is dependent on the percentages considered. But if lower percent rusted or percent mass loss is considered, meaning either 1% or 3%, then UWS provide the next longest service life. After that, the metallized specimens provided the longest service life, followed by the 1-coat IOZ. The relative ranking of metallizing may be also be affected by the differing fabrication of these specimens, which lacked edge preparation. Furthermore, the differing metrics used to evaluate paint (% coating loss or surface rusting) and the other corrosion protection systems (mass loss) is also acknowledged as introducing some level of subjectivity into these rankings. The fact that structures can be repainted should also be considered when interpreting these longevity estimates and using this data for performing life cycle cost analyses.

There is significant variability in the data used to develop the average SCR trendlines shown in Figure 2-7 (see Figures 2-3 – 2-6), clearly revealing the importance of good design, detailing, and maintenance practices. However, the average SCR of all corrosion protections systems shown in Figure 2-7 is between 5 and 7 at 50 years. According to the Long Term Bridge Performance Committee, SCR of 7 or more describe "good" condition and SCR of 5 or 6 are describe "fair" condition, while ratings of 4 or less describe "poor" condition. Assuming that repair or reconstruction are not required for "good" and "fair" condition bridges, , the statistical analysis showed that all corrosion protection systems should provide a service life of at least 50 years, with no appreciable section loss to the base material, in average conditions (i.e., the conditions producing the average performance for the groups of bridges in this dataset). Attention to proper design, detailing, and maintenance is known to extend this service life. These service life estimates were consistent with the findings from the laboratory accelerated corrosion testing simulating severe

environments, which show the ability of all corrosion protection systems to provide a service life of 50 years or more, depending on the performance benchmark chosen.

5.3 Future Work

The longevity estimates obtained in this work can be combined with cost data to provide a data driven approach for the selection of corrosion protection systems in severe environments from a life cycle cost perspective. Such work would ideally consider scenarios with differing maintenance types and schedules to further optimize the life cycle cost and performance of steel corrosion protection systems. The research results could also be directly applied into practice by directly using the results in Table 4-2 for longevity estimates. However, any direct use of these estimates should clearly recognize the assumptions on which these estimates are based, most significant of which are: relatively severe environments, high quality fabrication, high quality material handling, and negligible effect of UV exposure.

This research used five corrosion protection systems, but additional research could be performed using different corrosion protection systems that have not previously been evaluated. The laboratory testing performed for this research was meant to simulate a relatively severe environment. Future testing could be done benchmarked to less severe or different environments. The nature of this work leaves the possibility to perform future laboratory testing to evaluate repairs. Any of the specimens that have corroded can be repaired as would be done in the field and then put through additional corrosion testing to evaluate the effectiveness of the repair. Finally, the problems found at the edges and corners of the specimens in this research lead to the possibility of evaluating the pros and cons of using edge epoxy or any other special edge treatment in future testing.

REFERENCES

2019. *Analysis Toolpak*. Microsoft.

2021. *DIFFRAC.EVA*. Bruker.

2021. *Matlab*. MathWorks.

2021. *MicroStation*. Bentley.Agbelie, B. R., Labi, S., Fricker, J., Qiao, Y., Zhang, Z., and Sinha, K. C. (2017). "Lifecycle Decision Framework for Steel Bridge Painting." *Journal of Bridge Engineering*, 22(11), 06017004–1-06017004–6.

AASHTO/NSBA. (2016). "Steel Bridge Fabrication Guide Specification", S2.1-2016, AASHTO/NSBA.

ASTM. (1968). "Corrosiveness of Various Atmospheric Test Sites as Measured by Specimens of Steel and Zinc", Metal Corrosion in the Atmosphere, ASTM STP 435, American Society for Testing and Materials, pp. 360-391.

Albrecht, P., Coburn, S., Wattar, F., and Tinklenberg, G. (1989). "Guidelines for the Use of Weathering Steel in Bridges", *NCHRP Report 314*, Washington, DC.

ASTM Standard D1193 (2018). "Standard Specification for Reagent Water," ASTM International, West Conshohocken, PA, 2018, DOI: 10.1520/D1193-06R18, www.astm.org

ASTM Standard G1. (2017). "Standard Practice for Preparing, Cleaning, and Evaluating Corrosion Test Specimens," ASTM International, West Conshohocken, PA, 2017, DOI: 10,1420/G0001-03R17E01, www.astm.org

Bai, T. (2022). *Quantification of Suitable Environments for Unpainted Weathering Steel Bridges.* Doctoral Dissertation, University of Delaware, Newark, DE, Pending publication.

Davidson, D., Thompson, L. Lutze, F., Tiburcio, B., Smith, K., Meade, C., Mackie, T., McCune, D., Townsend, H. and Tuszynski, R. (2003). "Perforation Corrosion Performance of Autobody Steel Sheet in On-Vehicle and Accelerated Tests" *Advances in Coatings and Corrosion Prevention*, SP-1770, Society of Automotive Engineers, Warrendale, PA.

FHWA (1995). "Recording and Coding Guide for the Structure Inventory and Appraisal of the Nation's Bridges", Report No. FHWA-PD-96-001, FHWA, Office of Engineering, Bridge Division, Bridge Management Branch, Washington, DC.

Fletcher, F.B., Townsend, H.E., and Wilson, A.D. (2003). “Corrosion Performance of Improved Weathering Steels for Bridges”, *Proc. World Steel Bridge Symposium*, Nov. 19-20, Orlando, FL.

Fletcher, F.B. (2011). “Improved Corrosion Resistant Steel for Highway Bridge Construction”, *Report FHWA-HRT-11-062*, Federal Highway Administration, McLean, VA

Garbade, Dr. Michael J. (2018). “Understanding K-Means Clustering in Machine Learning.” Medium. September 12, 2018. https://towardsdatascience.com/understanding-k-means-clustering-in-machine-learning-6a6e67336aa1.

Géron, Aurélien. (2019). *Hands-On Machine Learning with Scikit-Learn and TensorFlow*. Second edition. O’Reilly Media, Inc.

Guftman, H. (1968). "Effects of Atmospheric Corrosion of Rolled Zinc." Metal Corrosion in the Atmosphere, ASTM STP 435, American Society for Testing and Materials, pp.223-239.

ISO (1991). ISO 9223: Corrosion of Metals and Alloys. Classification of Corrosivity of Atmospheres, International Standard Organization, Geneva, 1991.

James, G., Witten, D., Hastie, T., and Tibshirani, R. (2017). “An introduction to statistical learning with applications in R”. Springer, New York, NY.

Kluyver, T., Ragan-Kelley, B., Pérez, F., Granger, B.E., Bussonnier, M., Frederic, J., Kelley, K., Hamrick, J.B., Grout, J., Corlay, S. and Ivanov, P. (2016). “Jupyter Notebooks-a publishing format for reproducible computational workflows”, in Loizides, F. and Schmidt, B. (Eds.), *Positioning and Power in Academic Publishing: Players, Agents and Agendas*, 87–90.

Laerd Statistics. 2018. *One-Way ANOVA*. [online] Available at: <https://statistics.laerd.com/statistical-guides/one-way-anova-statistical-guide-4.php> [Accessed October 2020].

McConnell, J.; Shenton, H.; Mertz, D.; and Kaur, D. (2014a). “Performance of Uncoated Weathering Steel Highway Bridges Throughout the United States”, *Transportation Research Record*, Issue 2406, 61-67.

McConnell, J.; Shenton, H.; Mertz, D.; and Kaur, D. (2014b). “National Review on Use and Performance of Uncoated Weathering Steel Highway Bridges”, *ASCE Journal of Bridge Engineering*, 19(5), p.01014009-1 1014009-11.

McConnell, J.; Shenton, H.; and Mertz, D. (2016). "Performance of Uncoated Weathering Steel Bridge Inventories: Methodology and Gulf Coast Region Evaluation", *ASCE Journal of Bridge Engineering*, 21(12).

Real Python. (2019). "K-Means Clustering in Python: A Practical Guide – Real Python." 2019. https://realpython.com/k-means-clustering-python/.

SAE (2016). "SAE J2334 Laboratory Cyclic Corrosion Test", SAE International, Warrendale, PA.

APPDENDIX A – SPECIMEN MATERIAL PROPERTIES

Table A-1. 1-Coat (IOZ) Paint Properties

Metric	**Value**
Product	Carbozinc 11 HS
Generic Type	Solvent Based Inorganic Zinc
Dry Temperature Resistance	Continuous: 400° C
	Non-Continuous: 427° C
Dry Film Thickness	2-3 mils
Total Zinc Dust in Dry Film	84% (By Weight)
Solids Content	75% +/- 2% (By Volume)

Table A-2. 3-Coat (OZ) Paint System Properties

Coat	**Metric**	**Value**
Coat 1: OZ	Product	Carbozinc 859
	Generic Type	Organic Zinc-Rich Epoxy
	Dry Temperature Resistance	Continuous: 204° C
		Non-Continuous: 218° C
	Dry Film Thickness	3-5 mils
	Total Zinc Dust in Dry Film	81% (By Weight)
	Solids Content	66% +/- 2% (By Volume)
Coat 2: Epoxy	Product	Carboguard 893
	Generic Type	Cycloaliphatic Amine Epoxy
	Dry Temperature Resistance	Continuous: 93° C
		Non-Continuous: 121° C
	Dry Film Thickness	3-6 mils for mild environments and as an intermediate coat over zinc rich primers
		4-6 mils for more severe environments
	Solids Content	77% +/- 2% (By Volume)
Coat 3: Urethane	Product	Carbothane 133 LV
	Generic Type	Aliphatic Acrylic-Polyester Polyurethane
	Dry Temperature Resistance	Continuous: 149° C
	Dry Film Thickness	3-5 mils per coat
	Solids Content	72% +/- 2% (By Volume)

Table A-3.Steel Material Chemistry

Metric	Uncoated Carbon Steel Specimens	Uncoated 50W Specimens	Coated Specimens (50/50W Dual Certified)
Carbon	0.19%	0.15%	0.14%
Sulfur	0.006%	0.003%	0.007%
Manganese	0.84%	1.04%	1.10%
Phosphorus	0.006%	0.010%	0.010%
Silicon	0.03%	0.34%	0.37%
Columbium	-	<0.001%	0.002%
Vanadium	0.003%	0.024%	0.038%
Nickel	0.004%	0.22%	0.18%
Chromium	<0.0006%	0.46%	0.58%
Copper	0.03%	0.31%	0.27%
Molybdenum	0.002%	-	0.007%
Aluminum	0.03%	-	0.035%
Boron	-	-	0.0002%
Titanium	0.002%	-	-
Cobalt	0.002%	-	-
Arsenic	0.006%	-	-

Table A-4. Metalized Material Properties as Determined by XRF Analysis After Accelerated Corrosion Testing

Element	Percent Mass
Zn	66.8
Al	30.5
Fe	0.4
All Other	2.3

Table A-5. Galvanized Face Material Properties as Determined by XRF Analysis After Accelerated Corrosion Testing

Element	Percent Mass
Zn	92.2
Fe	6.2
All Others	1.6

APPDENDIX B – ACCELERATED CORROSION TESTING SOLUTION CHEMISTRY

Table B-1. Amount of Salt Used in Salt Bath for Varying Concentrations

NaCl Concentration (% by Weight)	Method(s) Used	Grams of NaCl in Big Bin (100 L Water)	Grams of NaCl in Small Bin (50 L Water)
1	4	1,000	500
2	1, 5 (and Final Phase Testing)	2,000	1,000
5	2, 3	5,000	2,500

Table B-2. Rinse Water Bath Chemical Composition to Match Targeted Ion Concentration

Ion	**Target Concentration (mg/L)**	**Salt of Ion**	**Molecular Weight of Ion (g/mol)**	**Molecular Weight of Salt (g/mol)**	**Amount of Ion Needed for 1 50 L Bath (g)**	**Amount of Salt Needed for 1 50 L Bath (g)**	**Amount of Ion Needed for 1 100 L Bath (g)**	**Amount of Salt Needed for 1 100 L Bath (g)**
Chloride (Cl^-)	7	Sodium Chloride (NaCl)	35.45	58.44	0.35	0.58	0.70	1.15
Nitrate (NO_3^-)	23	Sodium Nitrate ($NaNO_3$)	62.00	84.99	1.15	1.58	2.30	3.15
Sulfate (SO_4^{2-})	6	Sodium Sulfate (Na_2SO_4)	96.06	142.04	0.30	0.44	0.60	0.89

Calculations to Determine Values in Table A8:

g ion needed = target concentration (g/L) * L of water in bath

g salt needed = g ion needed * (1/molecular weight of ion (g/mol)) * molecular weight salt (g/mol)

For example:

g Cl Needed for 1 50 L bath = (7 mg/L * 1 g/1000 mg) * 50 L = 0.35 g Cl

g NaCl Needed for 1 50 L bath = (0.35 g) * (1/35.34 g/mol) * 58.44 g/mol = 0.58 g NaCl

g Cl Needed for 1 100 L bath = (7 mg/L * 1 g/1000 mg) * 100 L = 0.70 g Cl

g NaCl Needed for 1 100 L bath = (0.70 g) * (1/35.34 g/mol) * 58.44 g/mol =1.15 g NaCl

Table B-3. Rinse Water Bath $NaHCO_3$ Composition to Match Targeted Alkalinity

Salt	**Alkalinity (meq/L)**	**Molecular Weight of Salt (g/mol)**	**Target Concentration (mg/L)**	**Amount Required for 1 50 L Bath (g)**	**Amount Required for 1 100 L Bath (g)**
Sodium Bicarbonate ($NaHCO_3$)	0.5069	84.01	42.60	2.13	4.26

Calculations to Determine Values in Table A8:

g salt needed = alkalinity (meq/L) * molecular weight of salt (g/mol) * L of water in bath

For example:

g $NaHCO_3$ Needed for 1 50 L bath = 0.5069 meq/L * 84.01 mg/mmol * (1/1000 g/mg) * 50 L = 2.13 g $NaHCO_3$

g $NaHCO_3$ Needed for 1 100 L bath = 0.5069 meq/L * 84.01 mg/mmol * (1/1000 g/mg) * 100 L = 4.26 g $NaHCO_3$

APPDENDIX C – ENVIRONMENTAL CHAMBER PROGRAMMING

This appendix first lists the steps for programming the environmental chamber. The numerical inputs corresponding to the testing performed in this work is then summarized by Tables C-1 – C-3.

1. Click the "Program Editor" tab at the bottom of the screen.
2. Click the "New Program" button.
3. Press "Add" to add a new step.
4. Choose "Ramp."
5. Set the duration to 20 minutes, the temperature to 60° C, and the humidity to 95% RH.
6. Press "Add" to add a new step.
7. Choose "Soak."
8. Set the duration to 5 hours and 40 minutes, the temperature to 60° C, and the humidity to 95% RH.
9. Press "Add" to add a new step.
10. Choose "Ramp."
11. Set the duration to 50 minutes, the temperature to 60° C, and the humidity to 50% RH.
12. Choose "Soak."
13. Set the duration to 17 hours and 10 minutes, the temperature to 60° C, and the humidity to 50% RH.

If taking a break on weekends:

14. Copy the "Ramp" and "Soak" steps you created by selecting them and then clicking "Copy" such that there are 5 24-hour cycles of ramp, soak, ramp, soak. Each step must be copied individually but can be manually

moved in order once copied. Make sure they have been copied in the correct order.

15. Press “Add” to add a new step.

16. Choose “Ramp.”

17. Set the duration to 20 minutes, the temperature to 60° C, and the humidity to 50% RH.

18. Press “Add” to add a new step.

19. Choose “Soak.”

20. Set the duration to 47 hours and 40 minutes, the temperature to 60° C, and the humidity to 50% RH.

21. Press “Add” to add a new step.

22. Choose “Jump” and select step 1 to jump to. Set the number of loops to equal the number of weeks of testing (ie, for 80 cycles choose 15 loops).

If no break on weekends:

14. Press “Add” to add a new step.

15. Choose “Jump” and select step 1 to jump to. Set the number of loops to equal the number of 24-hour testing cycles (i.e., for 80 cycles choose 80 loops).

Table C-1. Environmental Chamber Programming for Methods 1, 3, and 4

Initial Ramp (From Machine Turned Off)			
Step	**Time (mins)**	**Temperature (°C)**	**Relative Humidity (%)**
Ramp	20	50	95
Daily Weekday Cycle			
Step	**Time (mins)**	**Temperature (°C)**	**Relative Humidity (%)**
Ramp	20	50	95
Soak	5:40	50	95
Ramp	50	60	50
Soak	17:10	60	50
Weekend/Holiday Cycle			
Step	**Time (mins)**	**Temperature (°C)**	**Relative Humidity (%)**
Ramp	20	60	50
Soak	47:40	60	50

Table C-2. Environmental Chamber Programming for Method 2

Initial Ramp (From Machine Turned Off)			
Step	**Time (mins)**	**Temperature (°C)**	**Relative Humidity (%)**
Ramp	20	50	95
Daily Weekday Cycle			
Step	**Time (mins)**	**Temperature (°C)**	**Relative Humidity (%)**
Ramp	20	50	95
Soak	2:40	50	95
Ramp	50	60	50
Soak	20:10	60	50
Weekend Cycle			
Step	**Time (mins)**	**Temperature (°C)**	**Relative Humidity (%)**
Ramp	20	60	50
Soak	47:40	60	50

Table C-3. Environmental Chamber Programming for Method 5 (and Final Phase Testing)

Initial Ramp (From Machine Turned Off)			
Step	**Time (mins)**	**Temperature (°C)**	**Relative Humidity (%)**
Ramp	20	60	95
Daily Weekday Cycle			
Step	**Time (mins)**	**Temperature (°C)**	**Relative Humidity (%)**
Ramp	20	60	95
Soak	5:40	60	95
Ramp	50	60	50
Soak	17:10	60	50
Weekend Cycle			
Step	**Time (mins)**	**Temperature (°C)**	**Relative Humidity (%)**
Ramp	20	60	50
Soak	47:40	60	50

APPDENDIX D – pH AND CONDUCTIVITY READINGS

This appendix includes the pH and conductivity readings from trial methods 1-5 as well as the final phase of testing including all corrosion protection systems. The readings were taken in the salt bath after the salt application stage, with the exception of Tables D-3 and D-4. Those tables detail the readings taken from Method 3, which used both a salt bath and a rinse bath simulating rainwater. In Table D-3, odd cycle numbers indicate measurements taken in the salt bath, while even cycle numbers indicate measurements taken in the rinse bath. For Method 3, it was important that the rinse bath chemistry matched the chemistry of the field-collected rainwater as the specimens were soaking in the bath, so the pH was measured before the specimens were submerged in the bath and adjusted to be within +/- 0.5 of the targeted pH of 6.76. The pH values adjusted to meet this target are shown in Table D-4.

Table D-1. Method 1 Salt Bath pH and Conductivity Readings

Cycle	pH		Conductivity (mS/cm)	
	Big Container	**Small Container**	**Big Container**	**Small Container**
1	9.00	9.06	27.8	27.9
2	8.77	8.81	27.5	27.8
3	7.58	8.12	27.3	28.0
4	7.47	7.86	27.4	28.5
5	7.12	7.52	27.7	28.5
6	8.30	8.23	28.2	27.8
7	7.39	7.07	27.8	28.2
8	7.82	7.07	27.8	28.0
9	7.28	7.01	28.6	27.7
10	8.04	7.01	28.5	27.9
11	8.84	7.97	28.5	27.6
12	8.69	7.79	27.9	27.1
13	8.11	7.49	28.6	27.5
14	7.70	7.28	28.6	27.3
15	7.73	7.20	28.6	27.0
16	8.73	7.75	28.0	26.8
17	8.54	7.54	27.7	27.1
18	8.62	7.7	27.7	27.1
19	7.70	7.32	27.9	27.6
20	7.94	7.20	27.7	25.6

Note: The big container held the flat plate specimens, while the small container held the plates with bolted and welded features

Table D-2. Method 2 Salt Bath pH and Conductivity Readings

Cycle	pH		Conductivity (mS/cm)	
	Big Container	**Small Container**	**Big Container**	**Small Container**
1	8.96	8.41	62.1	62.0
2	8.43	8.37	62.3	61.6
3	7.79	7.90	61.8	60.4
4	7.70	7.63	61.8	61.9
5	7.63	7.52	60.5	60.9
6	7.42	7.37	61.8	61.5
7	7.42	7.28	61.5	59.8
8	7.19	7.06	61.9	61.5
9	7.31	7.00	62.5	62.4
10	7.19	6.96	62.4	62.6
11	7.03	6.09	60.1	59.6
12	6.87	6.99	59.3	59.3
13	6.85	6.76	61.4	59.8
14	6.95	6.76	62.2	61.3
15	6.83	6.76	61.6	60.8
16	6.65	6.59	61.8	60.8
17	6.65	6.59	62.2	61.0
18	7.01	6.54	62.0	60.8
19	7.10	6.50	63.2	61.7
20	7.11	6.50	60.5	60.4

Note: The big container held the flat plate specimens, while the small container held the plates with bolted and welded features

Table D-3. Method 3 Salt Bath and Rinse Bath[1] pH and Conductivity Readings (Measured AFTER Salt Application/Rinse Bath Stage)

Cycle	pH		Conductivity (mS/cm)	
	Big Container	**Small Container**	**Big Container**	**Small Container**
1	6.76	8.04	62.4	60.8
2[1]	7.05	6.41	0.29	0.47
3	6.50	8.23	72.6	71.7
4[1]	8.64	6.93	0.60	0.60
5	6.34	7.95	58.3	59.2
6[1]	8.10	7.18	0.37	0.30
7	6.90	7.50	59.8	57.6
8[1]	7.07	6.93	0.46	0.38
9	7.28	7.36	57.9	68.9
10[1]	6.97	7.30	0.49	0.40
11	7.45	7.17	57.7	57.2
12[1]	6.76	6.97	0.25	0.23
13	7.74	7.22	72.0	57.9
14[1]	6.97	6.96	0.25	0.29
15	7.49	7.00	71.3	71.1
16[1]	7.0	7.03	0.35	0.28
17	7.71	7.19	71.5	71.6
18[1]	6.76	6.81	0.40	0.37
19	7.21	7.08	70.6	72.9
20[1]	6.51	6.58	0.47	0.38

[1] Indicates a rinse cycle, meaning that the rinse bath was used instead of the salt bath

Note: The big containers held the flat plate specimens, while the small containers held the plates with bolted and welded features

Table D-4. Method 3 Rinse Bath pH and Conductivity Readings (Measured BEFORE Specimens Were Soaked in the Rinse Baths to Ensure Targeted pH)

Cycle	pH	
	Big Container	**Small Container**
2	6.40	6.22
4	*	*
6	6.92	6.76
8	6.70	6.84
10	6.76	6.94
12	6.51	6.76
14	6.81	6.81
16	6.94	6.90
18	6.84	6.82
20	6.60	6.76

* Indicates a missing reading due to the unavailability of the pH meter on that day

Note: The big container held the flat plate specimens, while the small container held the plates with bolted and welded features

Table D-5. Method 4 Salt Bath pH and Conductivity Readings

Cycle	pH		Conductivity (mS/cm)	
	Big Container	**Small Container**	**Big Container**	**Small Container**
1	7.13	8.17	15.82	16.26
2	7.24	7.48	16.86	16.19
3	7.30	7.30	16.76	17.42
4	7.29	7.23	17.02	17.01
5	7.34	7.22	17.13	17.10
6	7.41	7.40	17.10	15.8
7	7.51	7.24	14.54	13.47
8	7.52	7.33	17.34	16.73
9	7.58	7.35	17.82	16.70
10	7.60	7.22	18.05	17.04
11	7.85	7.74	16.83	16.92
12	7.70	7.63	16.95	17.30
13	7.77	7.59	17.50	17.51
14	8.48	8.10	17.82	17.54
15	7.65	7.46	17.30	17.82
16	7.36	7.43	17.79	17.89
17	7.24	7.40	17.47	17.53
18	7.73	7.65	17.52	17.55
19	7.86	7.72	17.87	17.91
20	7.53	7.49	17.62	17.37

Note: The big container held the flat plate specimens, while the small container held the plates with bolted and welded features

Table D-6. Method 5 Salt Bath pH and Conductivity Readings

Cycle	pH		Conductivity (mS/cm)	
	Big Container	**Small Container**	**Big Container**	**Small Container**
1	7.25	7.64	*	*
2	7.35	7.45	*	*
3	7.31	7.40	*	*
4	7.31	7.24	*	*
5	7.48	7.18	*	*
6	7.56	7.29	*	*
7	7.61	7.60	*	*
8	7.89	7.84	*	*
9	8.46	8.25	*	*
10	9.09	7.92	*	*
11	7.11	7.62	*	*
12	7.35	7.49	*	*
13	7.67	7.77	*	*
14	8.38	8.22	*	*
15	8.51	8.30	*	*
16	*	*	*	*
17	*	*	*	*
18	8.20	7.38	*	*
19	8.40	7.31	*	*
20	8.31	7.20	*	*

* Indicates a missing reading due to the unavailability of the pH or conductivity meter on that day.

Note: The big container held the flat plate specimens, while the small container held the plates with bolted and welded features

Table D-7. Final Phase Testing Salt Bath pH and Conductivity Readings

Cycle	pH				Conductivity (mS/cm)			
	Big Container 1	**Big Container 2**	**Small Container 1**	**Small Container 2**	**Big Container 1**	**Big Container 2**	**Small Container 1**	**Small Container 2**
1	6.96	6.86	7.01	7.07	33.2	34.1	34.3	33.5
2	7.26	6.98	7.64	7.15	33.1	33.8	33.9	33.2
3	7.82	7.17	8.25	7.25	33.3	34.4	33.6	33.5
4	7.97	7.29	7.94	7.25	33.3	35.0	33.5	33.1
5	8.16	7.41	7.99	7.49	33.7	35.1	34.2	34.0
6	8.44	7.58	7.8	7.44	33.4	33.0	32.8	32.8
7	8.33	7.82	8.07	7.62	33.6	33.5	32.0	33.7
8	8.74	8.24	8.10	7.77	33.8	34.7	33.5	33.7
9	8.76	8.41	8.09	7.79	33.8	32.7	33.4	32.5
10	8.80	8.45	8.31	8.09	33.5	34.6	33.0	33.5
11	8.71	8.42	8.26	8.08	32.9	33.3	33.2	33.0
12	8.74	8.64	8.49	8.30	33.3	34.4	33.9	33.2
13	8.65	8.58	8.47	8.26	33.3	33.8	33.4	32.9
14	8.65	8.58	8.36	8.17	34.1	34.1	33.1	32.9
15	8.60	8.50	8.38	8.22	34.0	33.4	34.3	33.5
16	8.80	8.27	8.25	8.07	32.8	33.9	32.8	32.8
17	*	*	*	*	*	*	*	*
18	8.88	8.33	8.35	8.12	32.8	32.4	32.7	32.2
19	8.88	8.35	8.39	8.17	32.6	33.4	33.5	32.9
20	8.83	8.27	8.30	8.30	33.2	34.2	34.0	32.0

21 (S1)	8.28	7.74	8.34	8.24	32.1	33.9	33.5	32.7
22 (S2)	8.28	7.85	8.17	7.92	33.3	34.5	33.1	32.0
23 (S3)	8.12	7.67	8.12	7.84	33.5	34.6	32.9	32.4
24 (S4)	8.22	7.85	8.09	7.78	33.1	34.0	33.1	33.1
25 (S5)	8.18	7.68	8.10	7.72	33.4	34.9	34.2	33.0
26 (S6)	7.68	7.47	7.66	7.40	34.6	33.5	34.2	33.0
27 (S7)	7.81	7.52	7.72	7.52	33.0	33.7	33.8	32.4
28 (S8)	7.68	7.48	7.60	7.33	34.7	33.7	32.5	32.7
29 (S9)	7.59	7.41	7.52	7.27	34.3	34.0	33.0	32.4
30 (S10)	7.86	7.55	7.58	7.32	34.8	33.7	33.6	33.0
31 (S11)	7.26	7.18	7.13	7.09	33.3	33.3	33.0	32.2
32 (S12)	7.97	7.56	7.52	7.34	33.4	33.8	33.0	31.8
33 (S13)	7.64	7.55	7.65	7.44	32.8	34.2	33.2	33.0
34 (S14)	7.59	7.46	7.54	7.30	33.6	34.0	33.7	32.6
35 (S15)	7.47	7.41	7.54	7.24	33.4	34.3	33.4	32.4
36 (S16)	7.46	7.30	7.42	7.28	33.7	33.2	33.1	32.5
37 (S17)	7.22	7.07	7.51	7.32	33.6	33.7	33.6	33.1
38 (S18)	7.28	7.25	7.56	7.21	33.6	33.5	33.7	32.7
39 (S19)	7.24	7.24	7.38	7.16	34.0	33.1	33.7	32.8
40 (S20)	7.29	7.24	7.25	7.15	33.9	34.1	33.6	30.1
41 (S21)	6.99	7.06	7.07	6.98	28.6	30.3	29.9	28.8
42 (S22)	7.00	6.96	7.02	6.97	32.7	30.1	30.0	29.6
43 (S23)	7.02	6.99	7.03	6.95	30.5	30.1	28.2	29.0
44 (S24)	7.03	6.98	7.05	6.96	31.4	32.5	32.0	30.0
45 (S25)	7.00	7.00	7.12	7.02	32.3	33.0	31.4	29.3
46 (S26)	6.98	6.95	7.06	6.95	33.0	32.0	30.6	29.9
47 (S27)	7.01	6.90	7.16	6.86	33.4	34.0	33.3	31.5
48 (S28)	7.08	6.86	7.16	6.91	34.0	34.1	33.0	30.3
49 (S29)	7.07	7.06	7.19	6.94	33.8	34.3	33.1	30.0

50 (S30)	7.06	6.99	7.19	6.91	34.1	34.9	33.8	33.6
51 (S31)	7.02	-	7.10	6.97	33.1	-	34.3	31.9
52 (S32)	7.24	-	7.42	7.17	31.3	-	33.6	31.7
53 (S33)	7.18	-	7.34	7.18	33.3	-	34.2	32.6
54 (S34)	7.06	-	7.02	6.89	32.8	-	33.5	31.9
55 (S35)	6.99	-	7.15	6.92	29.7	-	30.3	28.5
56 (S36)	7.07	-	7.05	6.89	32.9	-	32.4	28.6
57 (S37)	7.11	-	7.14	6.97	33.4	-	30.7	28.2
58 (S38)	7.14	-	7.13	7.05	30.4	-	30.3	29.2
59 (S39)	7.01	-	7.02	6.88	33.3	-	32.8	31.5
60 (S40)	7.17	-	7.16	6.94	33.9	-	33.6	32.8
61 (S41)	7.08	-	7.20	7.05	32.2	-	33.6	32.0
62 (S42)	7.27	-	7.24	7.11	32.0	-	33.1	31.8
63 (S43)	7.40	-	7.45	7.16	31.9	-	32.6	31.2
64 (S44)	7.60	-	7.55	726	32.8	-	33.8	32.0
65 (S45)	7.55	-	7.58	7.26	32.7	-	33.6	31.8
66 (S46)	7.12	-	7.31	7.08	32.8	-	33.1	32.7
67 (S47)	7.36	-	7.52	7.24	33.0	-	34.0	33.1
68 (S48)	7.07	-	7.08	6.91	32.8	-	33.5	32.6
69 (S49)	7.09	-	7.14	7.02	33.0	-	33.0	32.2
70 (S50)	7.14	-	7.21	6.96	32.4	-	33.1	32.4
71 (S51)	6.90	-	7.03	6.85	30.7	-	30.7	30.2
72 (S52)	7.07	-	7.39	7.09	32.8	-	32.4	31.6
73 (S53)	6.97	-	7.09	6.95	33.3	-	32.8	32.3
74 (S54)	7.05	-	7.33	6.90	32.4	-	33.0	32.6
75 (S55)	7.01	-	7.22	6.97	32.9	-	33.1	32.7
76 (S56)	7.62	-	7.58	7.43	33.0	-	32.6	32.4
77 (S57)	7.17	-	7.44	7.09	33.2	-	33.4	32.5
78 (S58)	7.16	-	7.45	7.15	32.9	-	33.5	32.3

79 (S59)	7.08	-	7.31	7.11	33.0	-	32.9	32.4
80 (S60)	6.98	-	7.16	6.95	33.5	-	32.8	32.3
(S61)	6.70	-	-	-	31.7	-	-	-
(S62)	6.62	-	-	-	31.4	-	-	-
(S63)	6.58	-	-	-	31.9	-	-	-
(S64)	6.55	-	-	-	31.4	-	-	-
(S65)	6.26	-	-	-	33.3	-	-	-
(S66)	6.62	-	-	-	33.5	-	-	-
(S67)	6.45	-	-	-	33.7	-	-	-
(S68)	6.38	-	-	-	33.8	-	-	-
(S69)	6.29	-	-	-	33.1	-	-	-
(S70)	6.32	-	-	-	33.7	-	-	-
(S71)	6.57	-	-	-	34,0	-	-	-
(S72)	6.40	-	-	-	33.8	-	-	-
(S73)	6.42	-	-	-	34.1	-	-	-
(S74)	6.28	-	-	-	31.5	-	-	-
(S75)	6.17	-	-	-	32.3	-	-	-
(S76)	6.41	-	-	-	32.7	-	-	-
(S77)	6.44	-	-	-	33.6	-	-	-
(S78)	6.45	-	-	-	34.1	-	-	-
(S79)	6.34	-	-	-	33.8	-	-	-
(S80)	6.42	-	-	-	33.4	-	-	-

* Indicates a missing reading due to the unavailability of the pH or conductivity meter on that day.

- Indicates a bin that was no longer in use from consolidation of the bins after specimen removal

Note:
“Big Container 1” held:

- galvanized, metallized, and 1-coat (IOZ) flat plates for Cycles 1-20
- galvanized, metallized, and 1-coat (IOZ flat plates for Cycles 21-50
- galvanized, metallized, 1-coat (IOZ), 3-coat (OZ), and UWS flat plates for Cycles 51-80

“Big Container 2” held:

- 3-coat (OZ) and UWS flat plates for Cycles 1-20 and 31-50
- 3-coat (OZ), and UWS flat plates for Cycles 21-30

“Small Container 1” held:

- galvanized, metallized, and 1-coat (IOZ) plates with bolted and welded features for Cycles 1-80

“Small Container 2” held

- 3-coat (OZ) and UWS plates with bolted and welded features for Cycles 1-20
- 3-coat (OZ), and UWS plates with bolted and welded features for Cycles 21-80

APPDENDIX E – GALVANIZED AND METALLIZED SPECIMEN CLEANING DATA

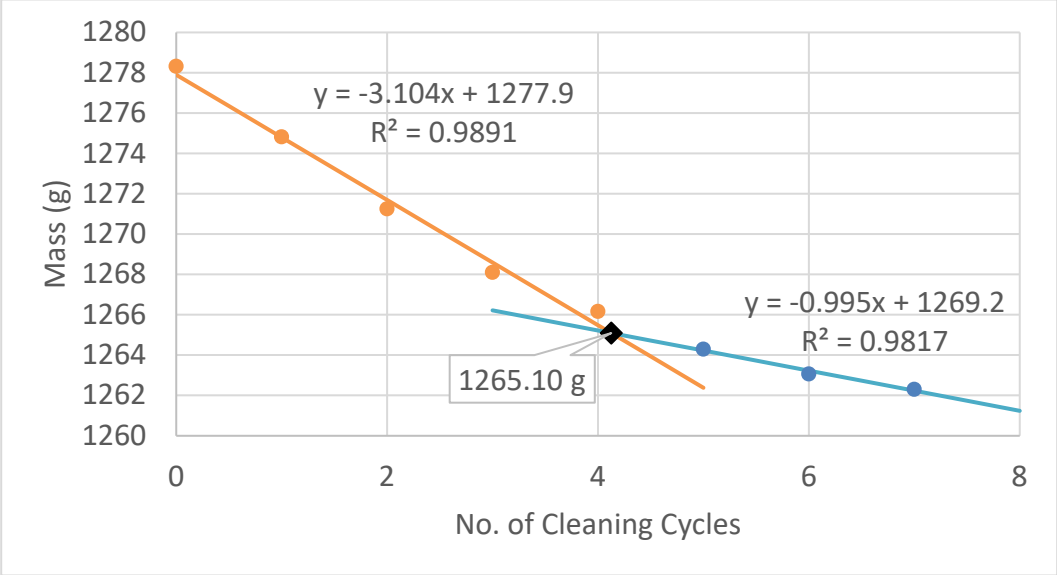

Figure E-1. Cleaning Data for G1 (Removed after 80 Cycles of Testing)

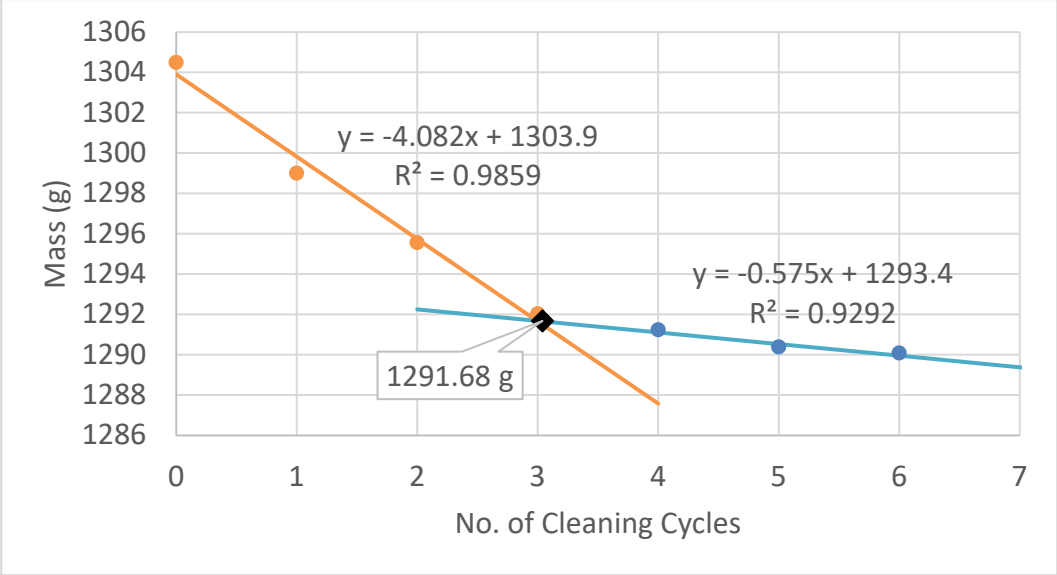

Figure E-2. Cleaning Data for G2 (Removed after 80 Cycles of Testing)

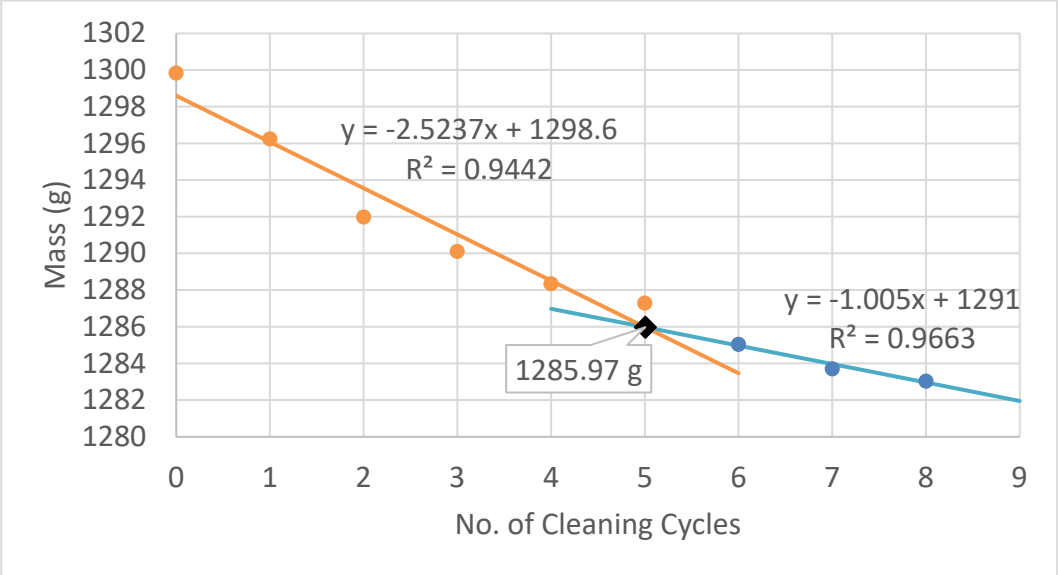

Figure E-3. Cleaning Data for G3 (Removed after 80 Cycles of Testing)

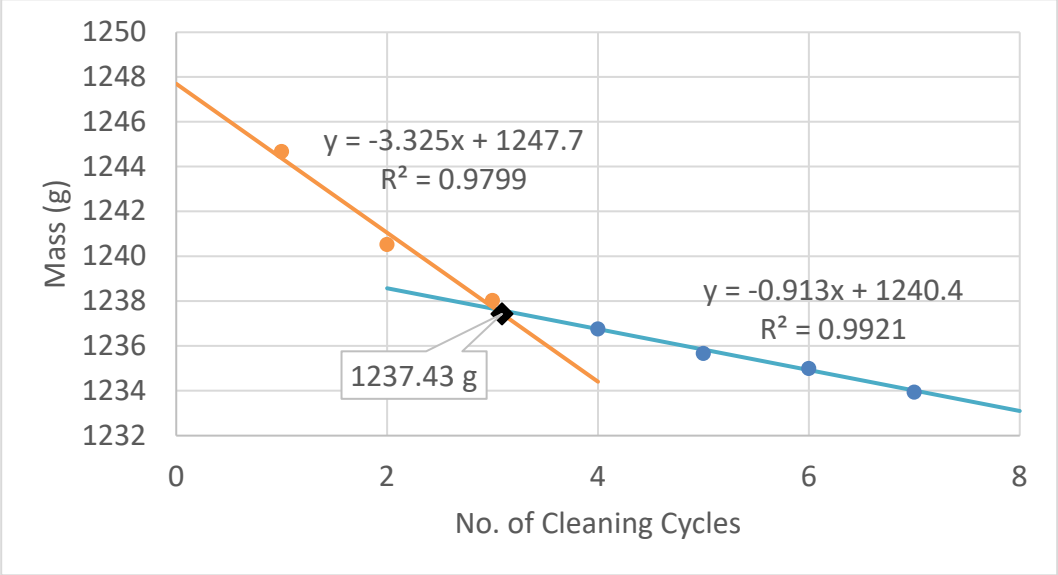

Figure E-4. Cleaning Data for G4 (Removed after 40 Cycles of Testing)

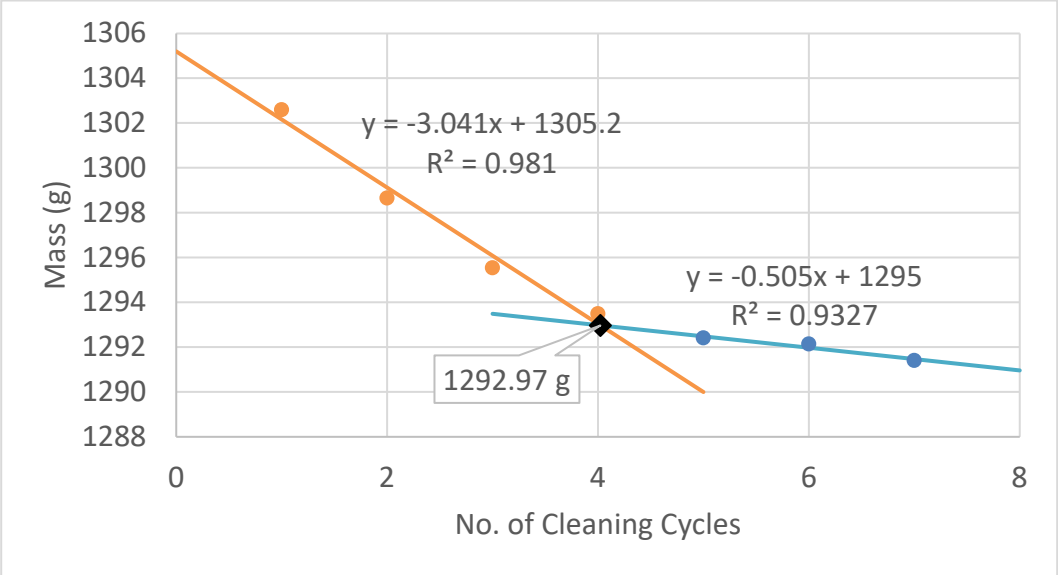

Figure E-5. Cleaning Data for G5 (Removed after 40 Cycles of Testing)

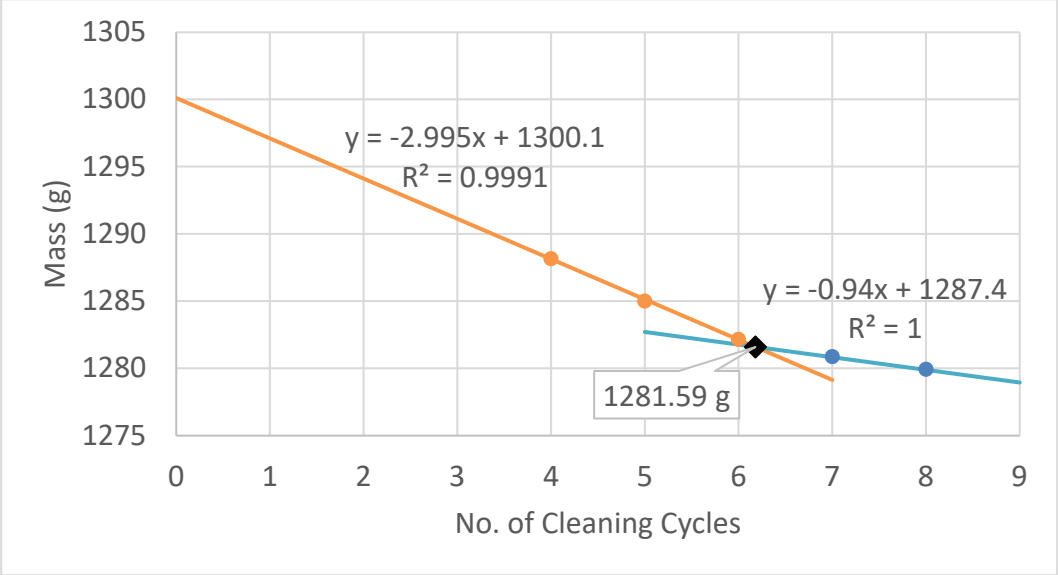

Figure E-6. Cleaning Data for G6 (Removed after 40 Cycles of Testing)

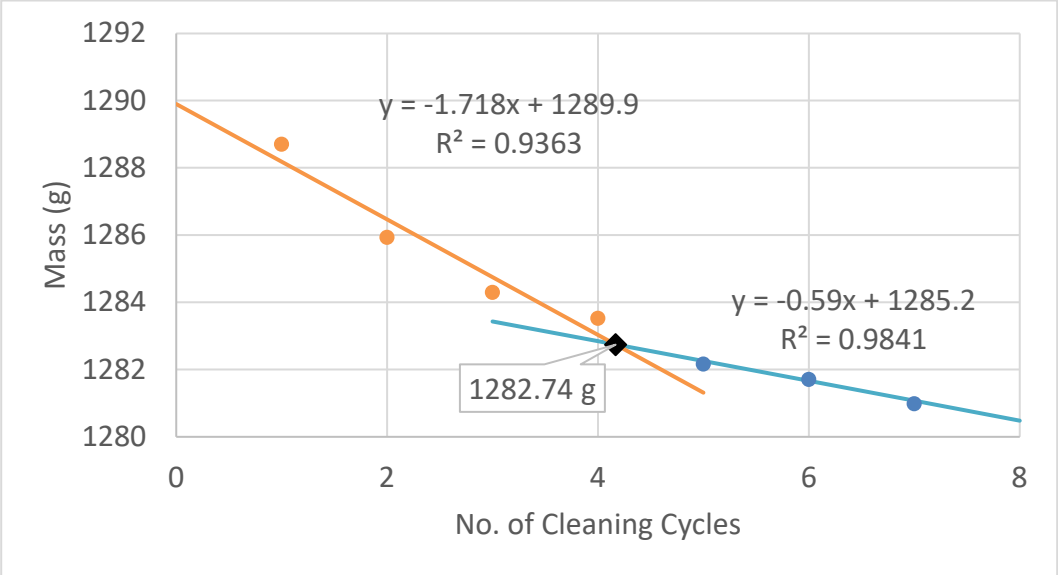

Figure E-7. Cleaning Data for G7 (Removed after 20 Cycles of Testing)

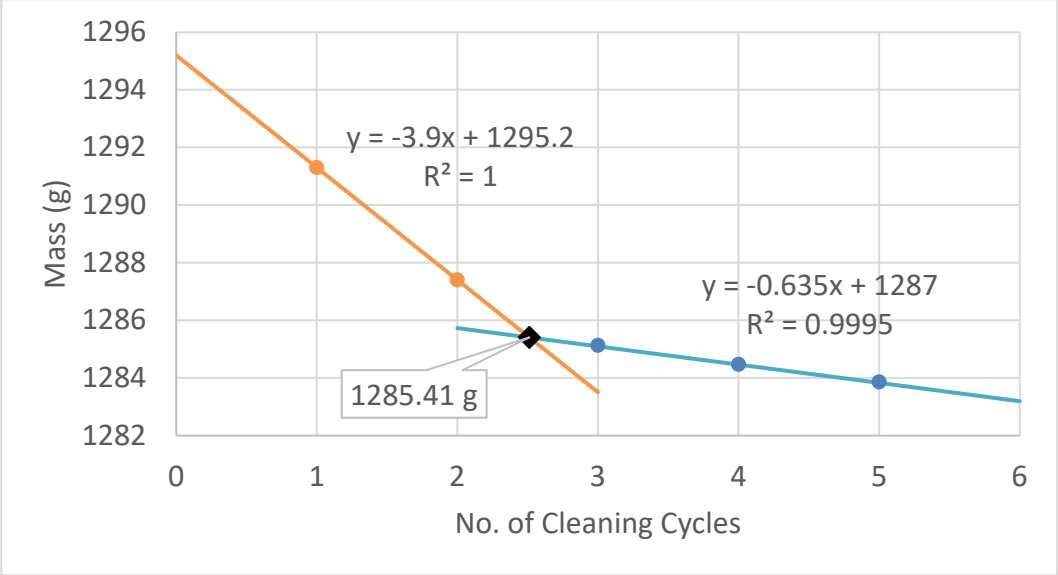

Figure E-8. Cleaning Data for G8 (Removed after 20 Cycles of Testing)

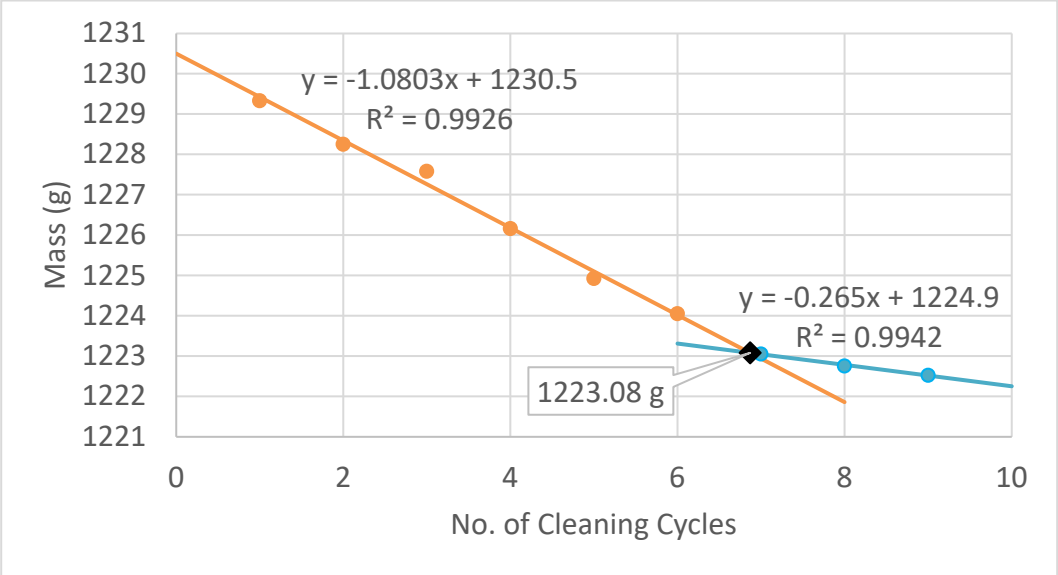

Figure E-9. Cleaning Data for G9 (Removed after 20 Cycles of Testing)

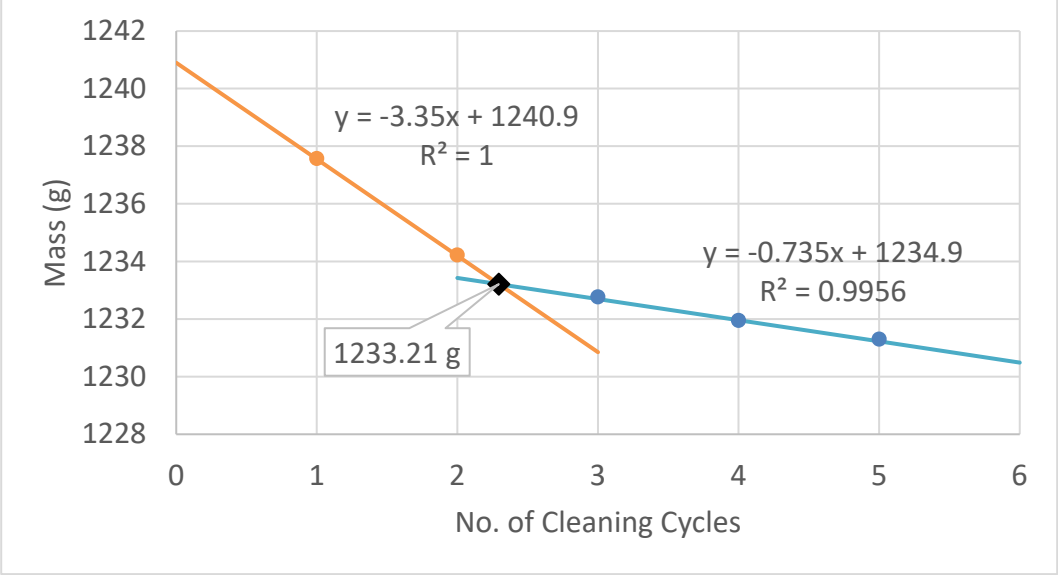

Figure E-10. Cleaning Data for G10 (Removed after 10 Cycles of Testing)

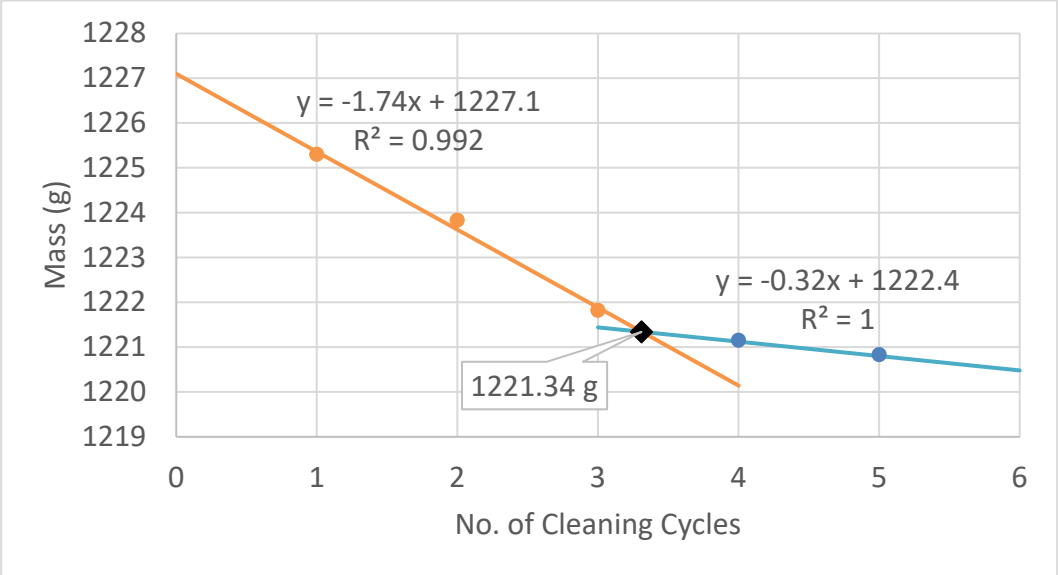

Figure E-11. Cleaning Data for G11 (Removed after 10 Cycles of Testing)

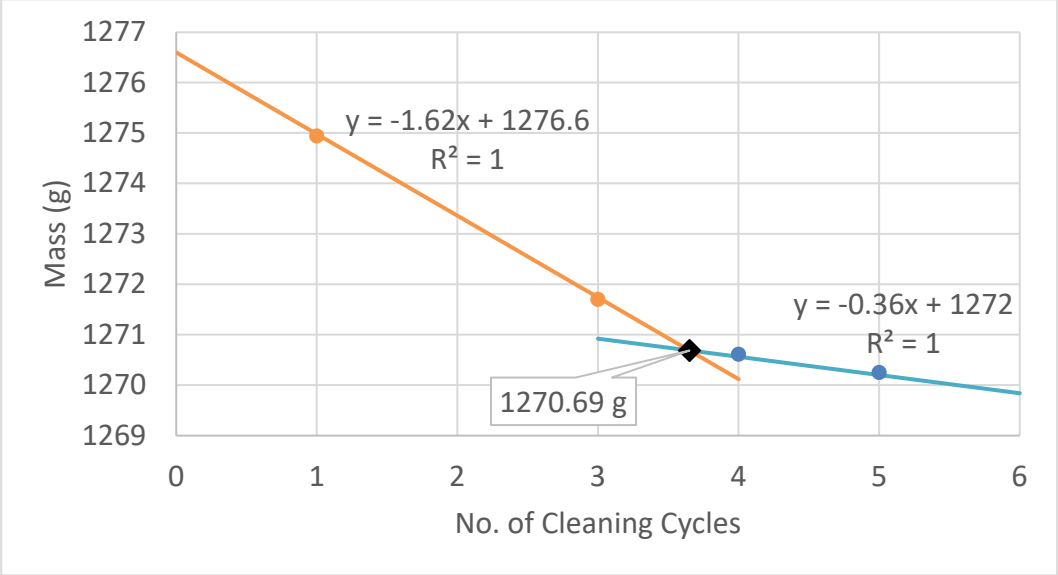

Figure E-12. Cleaning Data for G12 (Removed after 10 Cycles of Testing)

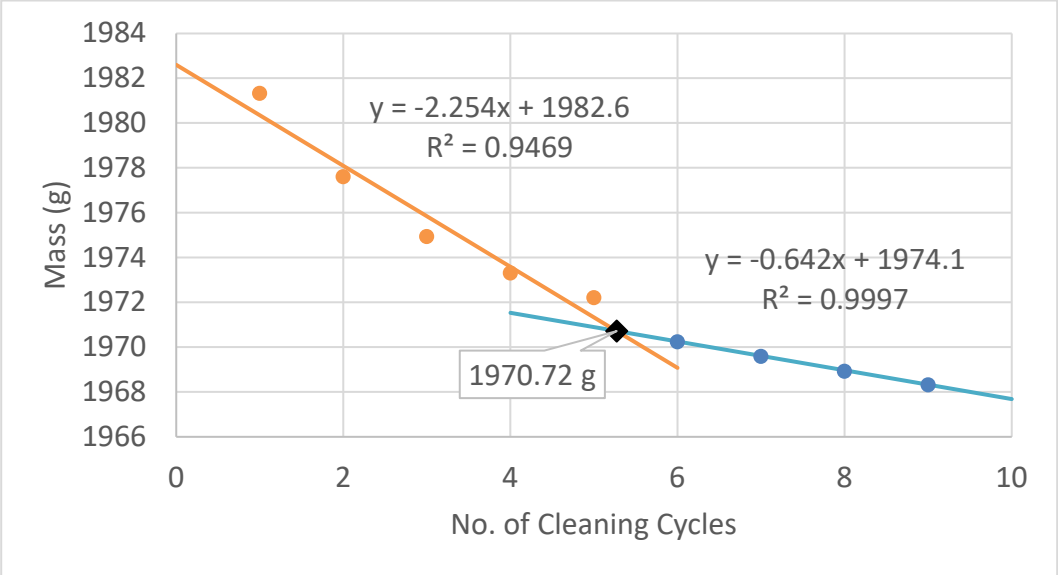

Figure E-13. Cleaning Data for GB-1 (Removed after 80 Cycles of Testing)

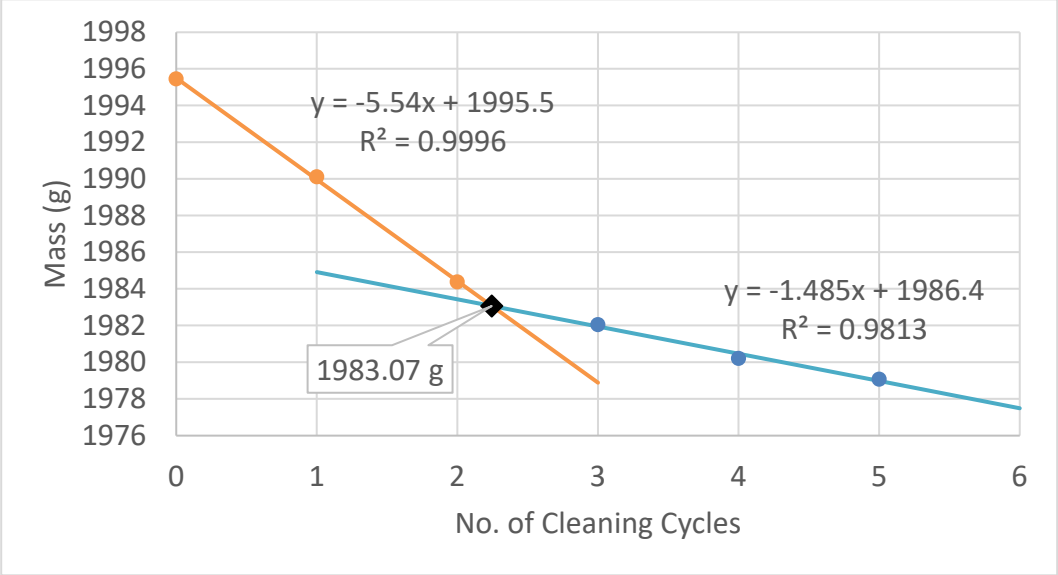

Figure E-14. Cleaning Data for GB-2 (Removed after 80 Cycles of Testing)

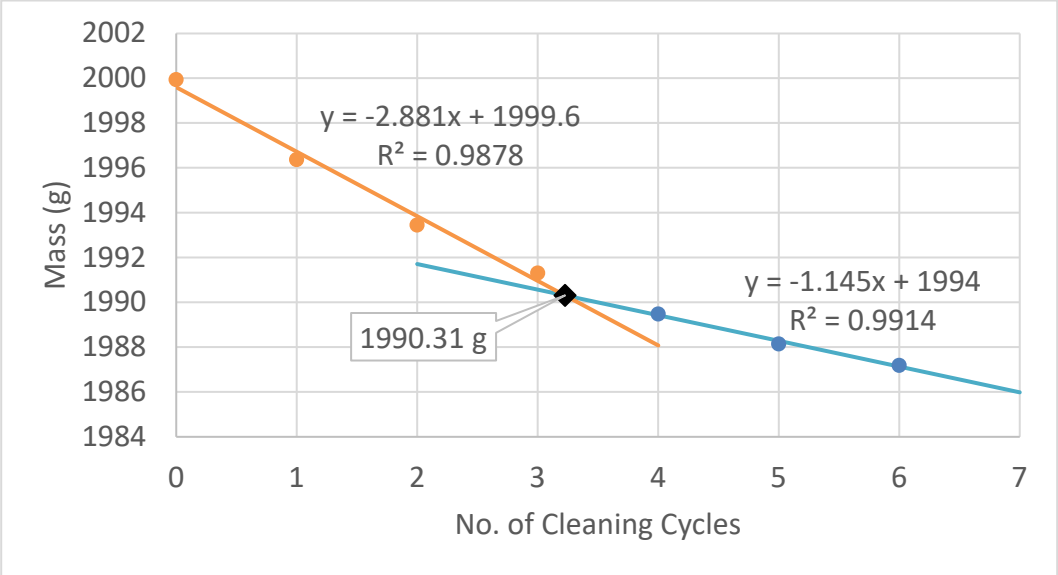

Figure E-15. Cleaning Data for GB-3 (Removed after 80 Cycles of Testing)

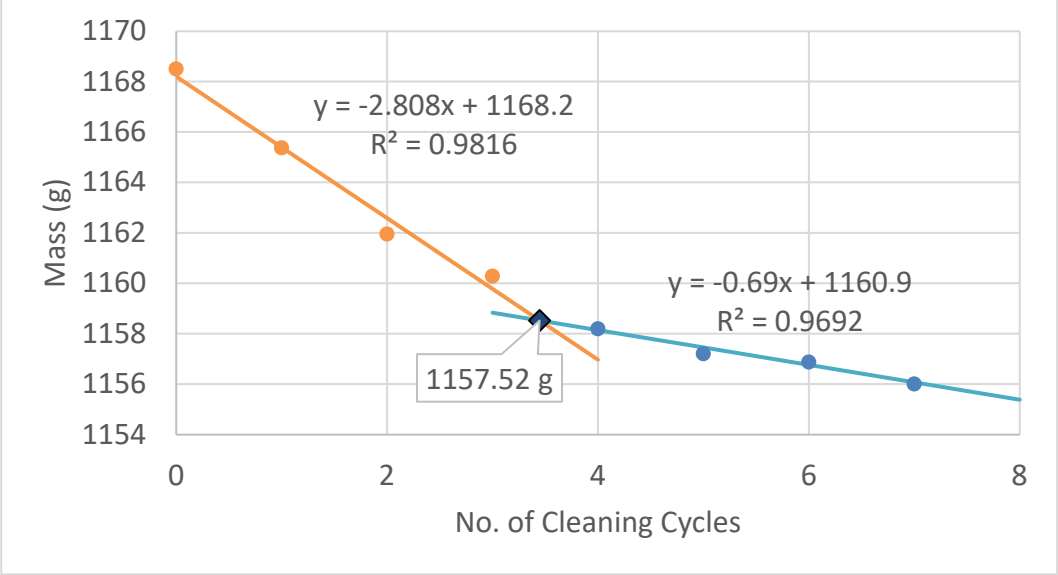

Figure E-16. Cleaning Data for M1 (Removed after 80 Cycles of Testing)

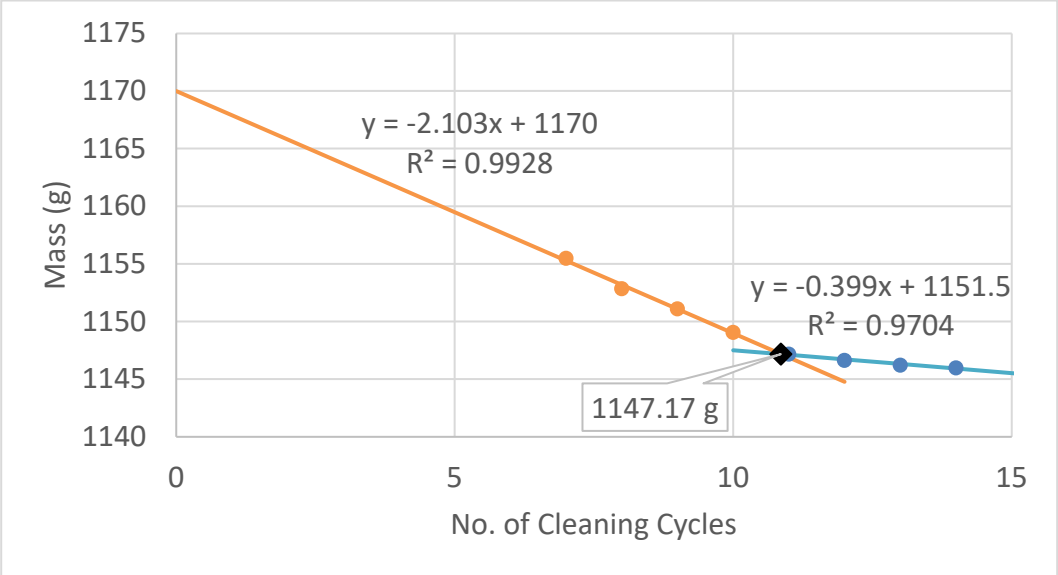

Figure E-17. Cleaning Data for M2 (Removed after 80 Cycles of Testing)

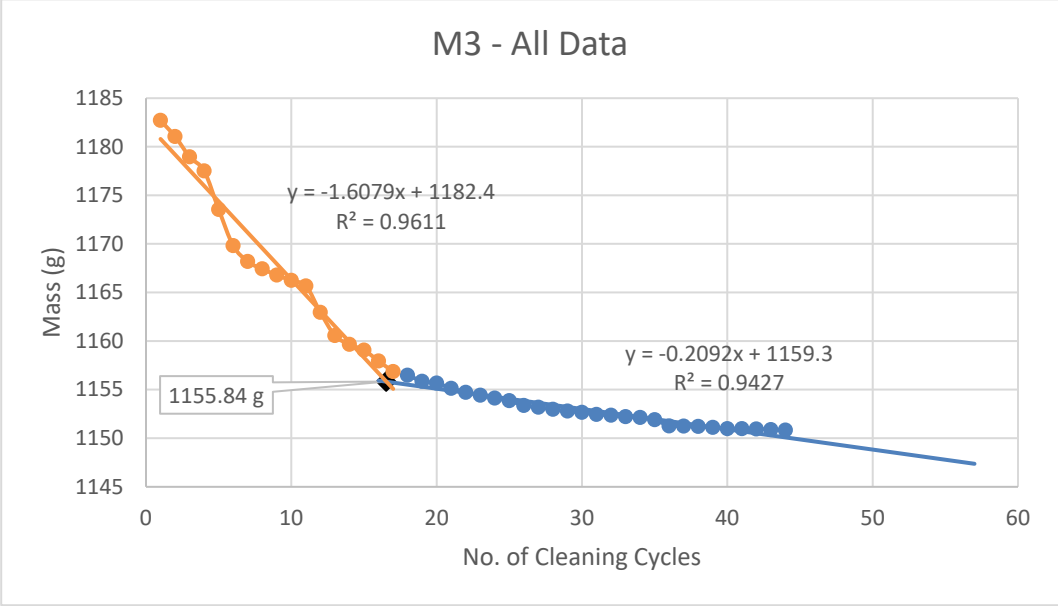

Figure E-18. Cleaning Data for M3 (Removed after 80 Cycles of Testing)

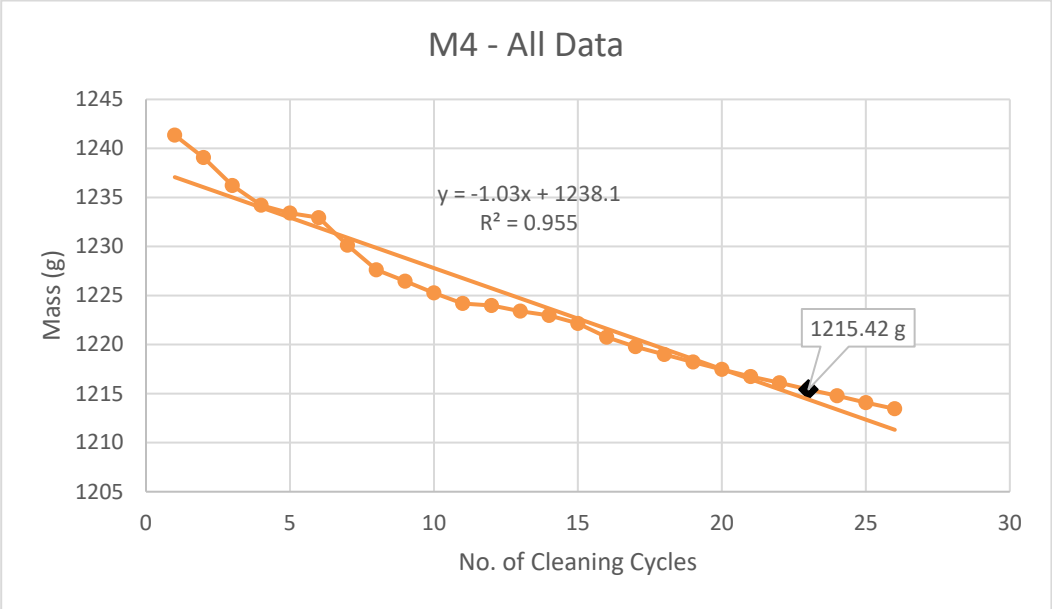

Figure E-19. Cleaning Data for M4 (Removed after 40 Cycles of Testing)

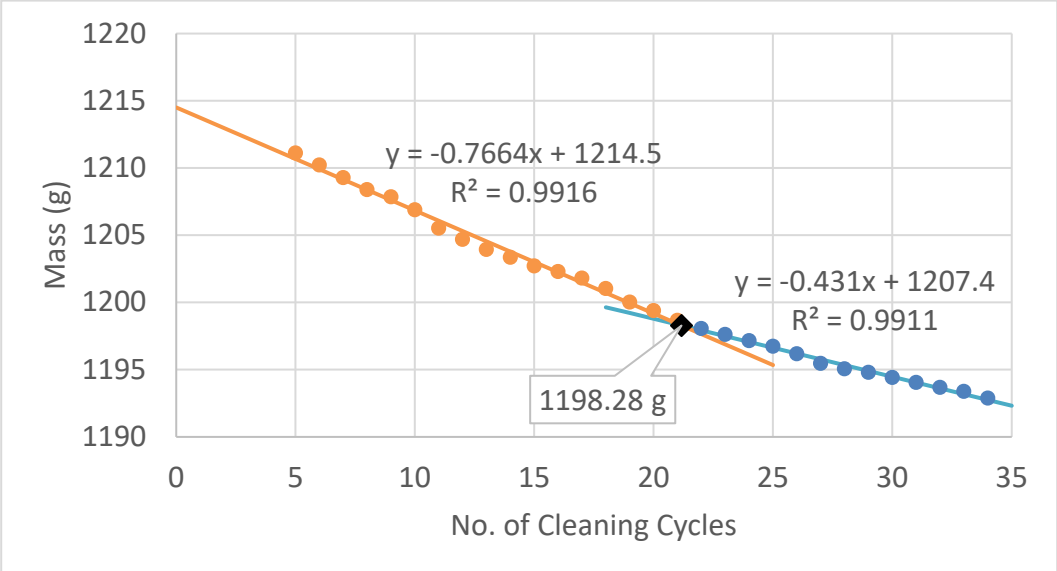

Figure E-20. Cleaning Data for M5 (Removed after 40 Cycles of Testing)

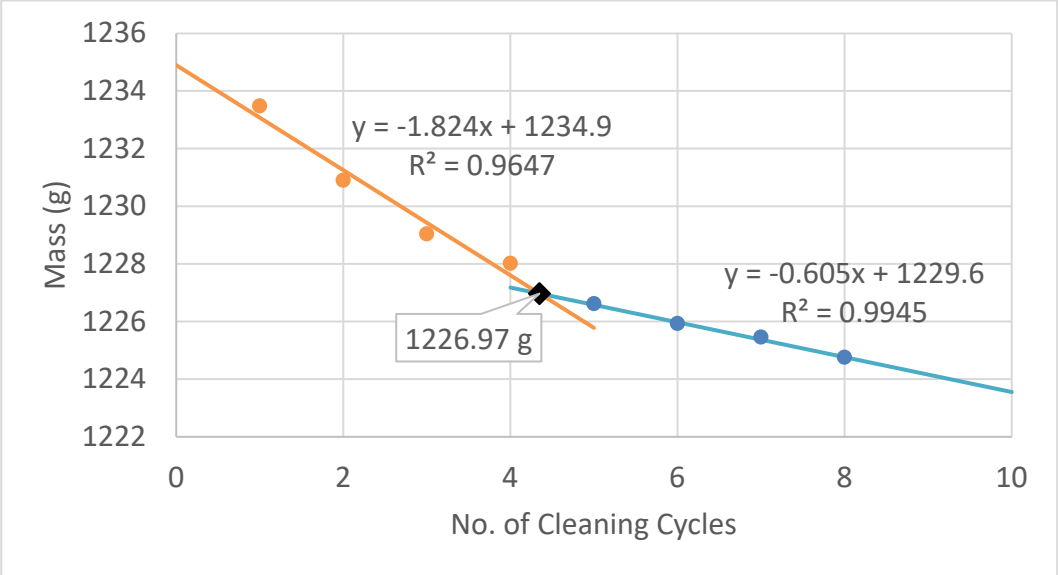

Figure E-21. Cleaning Data for M6 (Removed after 40 Cycles of Testing)

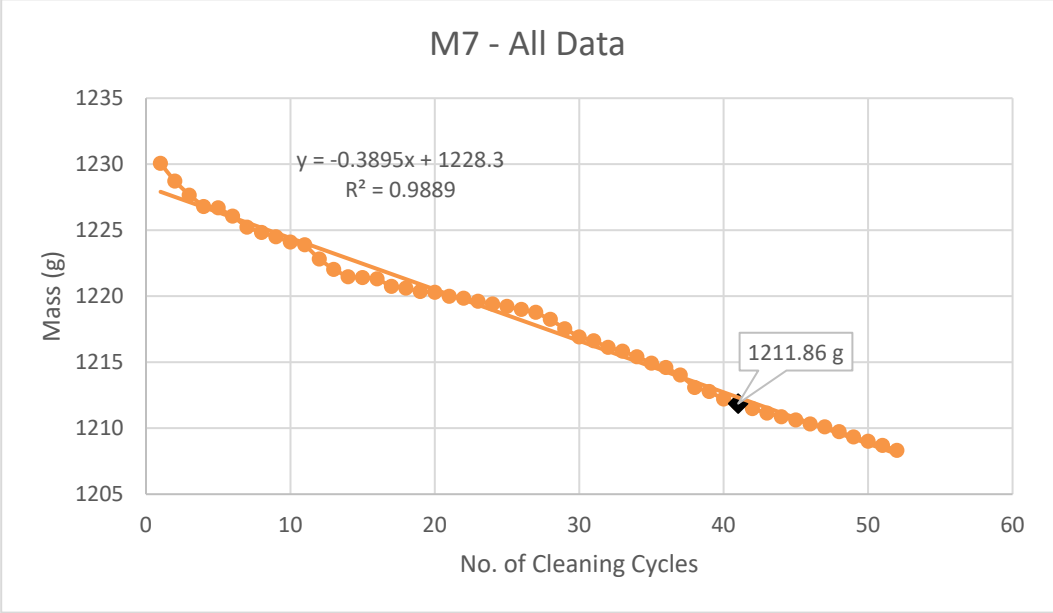

Figure E-22. Cleaning Data for M7 (Removed after 20 Cycles of Testing)

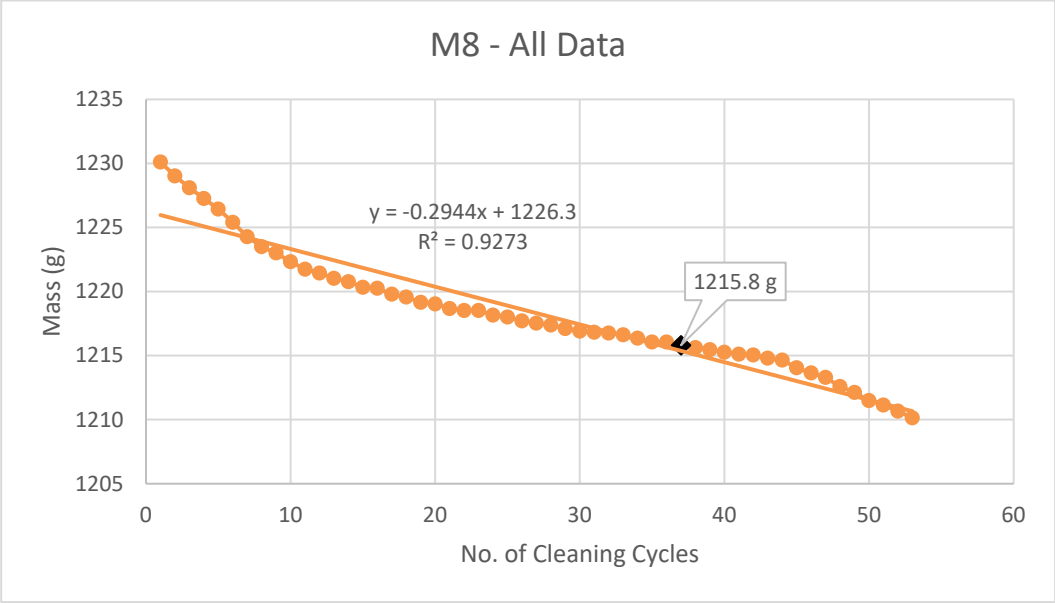

Figure E-23. Cleaning Data for M8 (Removed after 20 Cycles of Testing)

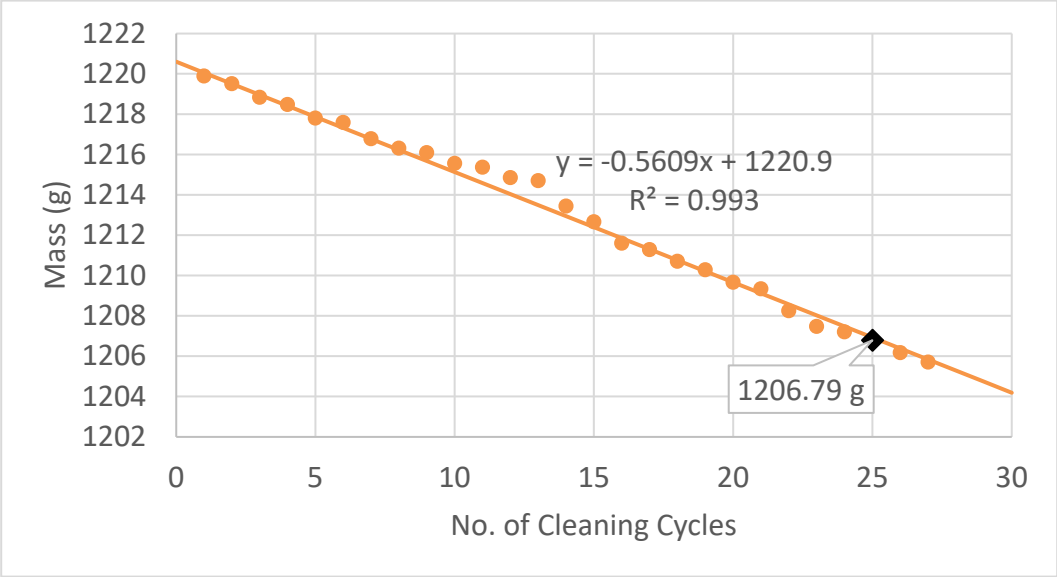

Figure E-24. Cleaning Data for M9 (Removed after 20 Cycles of Testing)

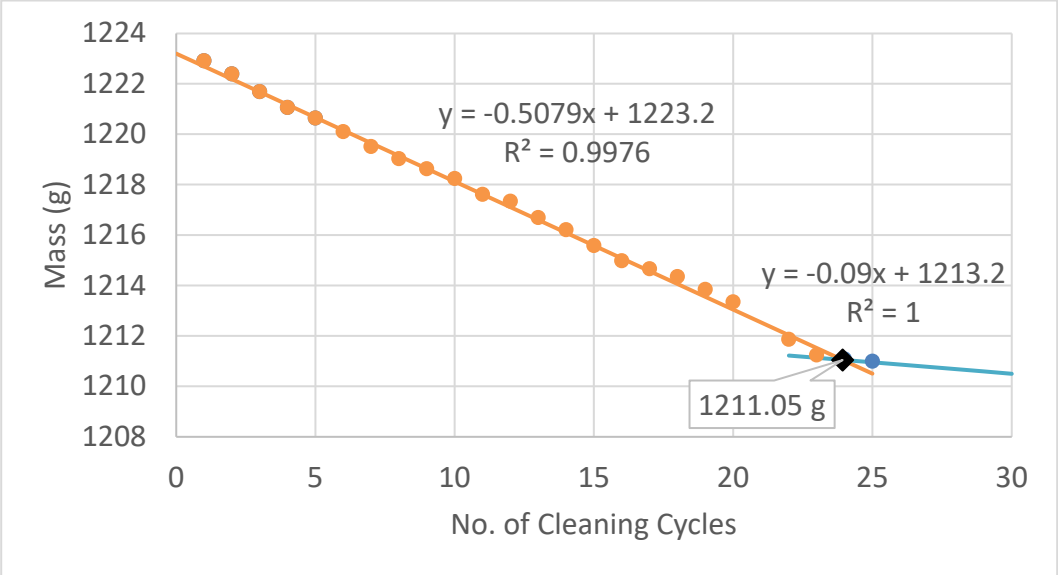

Figure E-25. Cleaning Data for M10 (Removed after 10 Cycles of Testing)

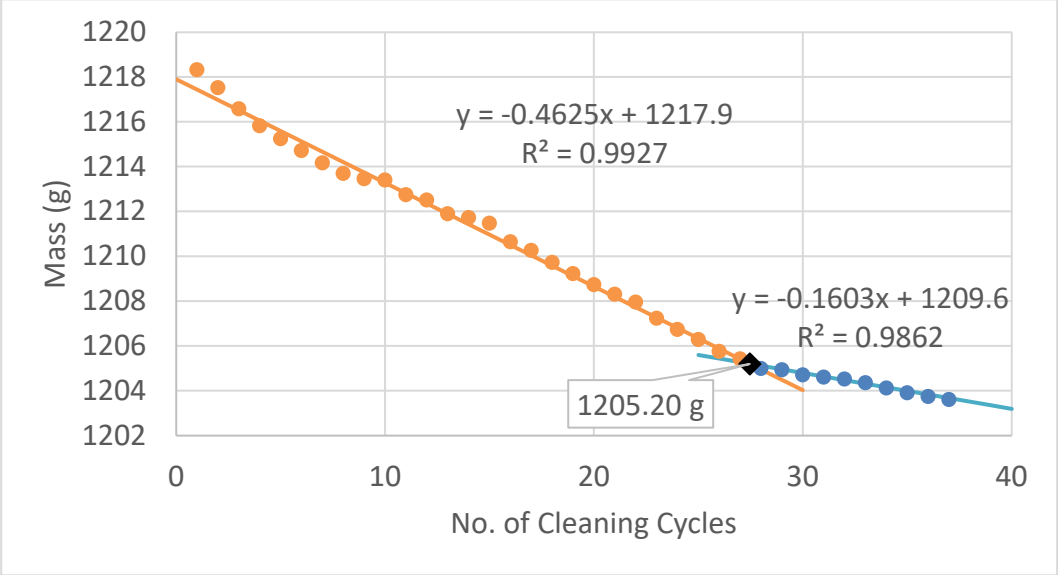

Figure E-26. Cleaning Data for M11 (Removed after 10 Cycles of Testing)

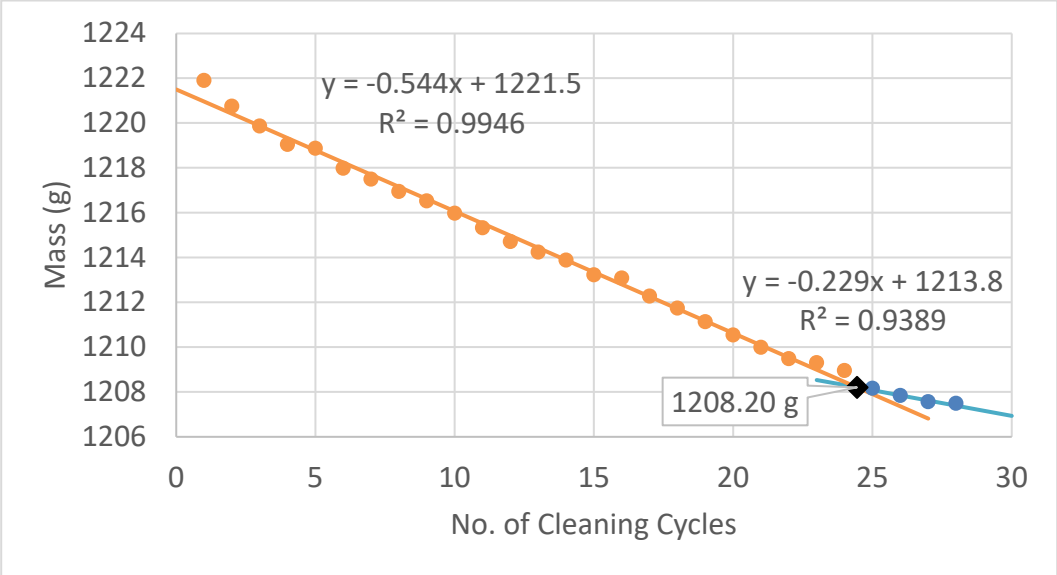

Figure E-27. Cleaning Data for M12 (Removed after 10 Cycles of Testing)

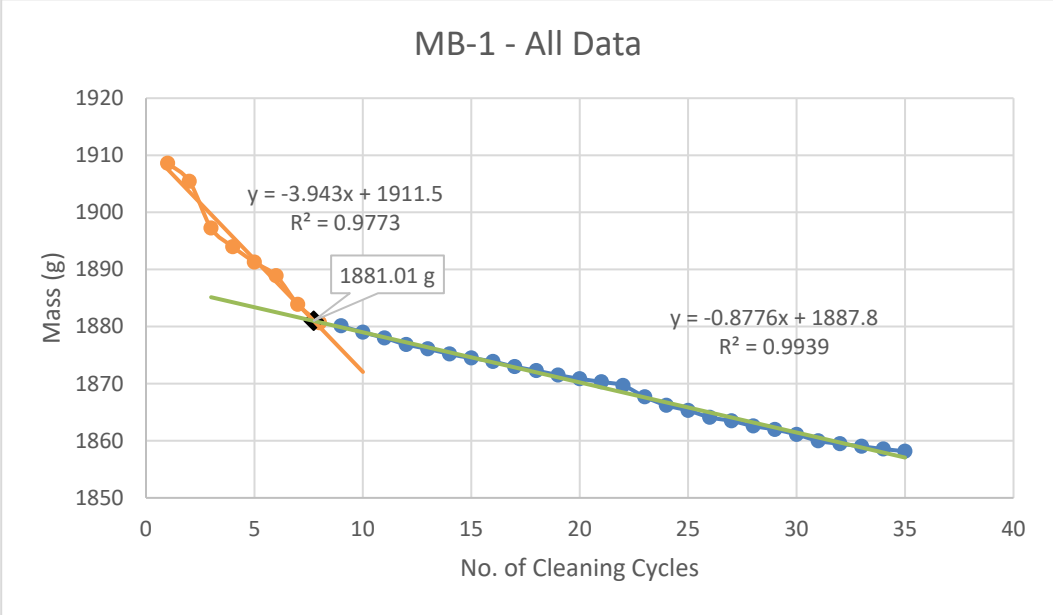

Figure E-28. Cleaning Data for MB-1 (Removed after 80 Cycles of Testing)

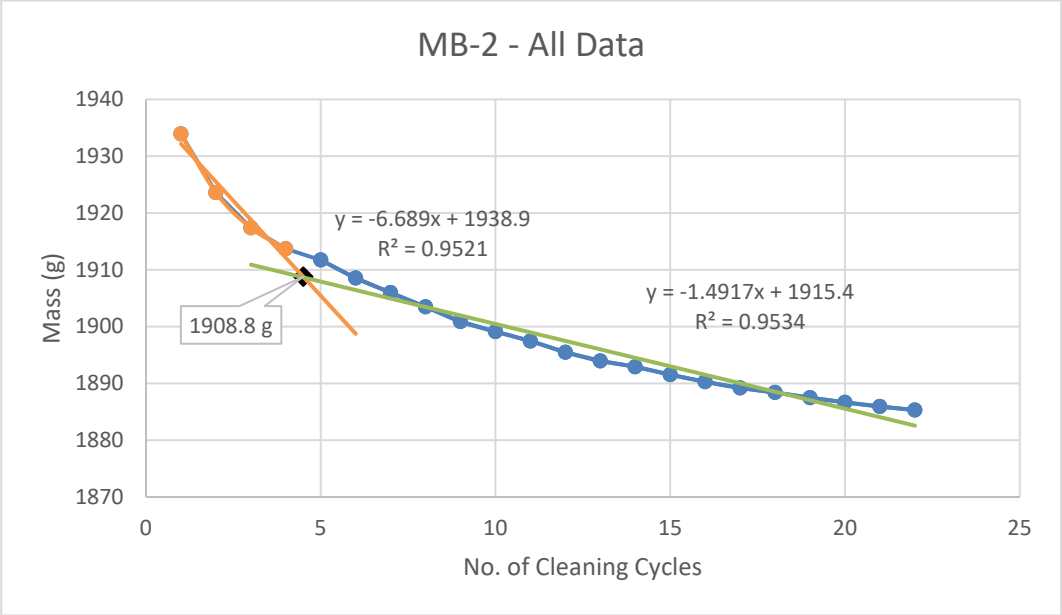

Figure E-29. Cleaning Data for MB-2 (Removed after 80 Cycles of Testing)

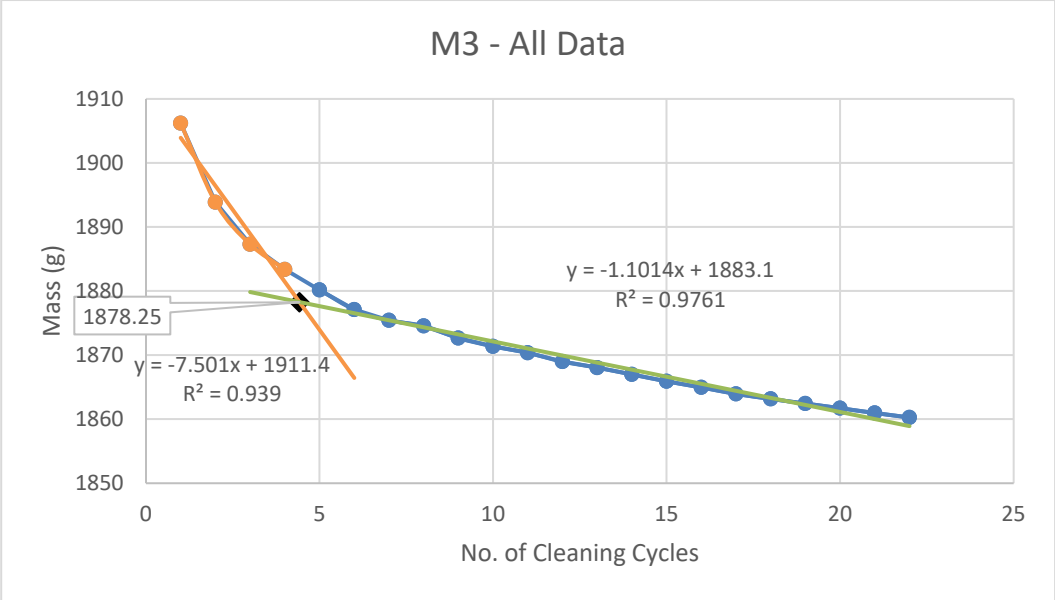

Figure E-30. Cleaning Data for MB-2 (Removed after 80 Cycles of Testing